

DTIC FILE COPY

7057-16

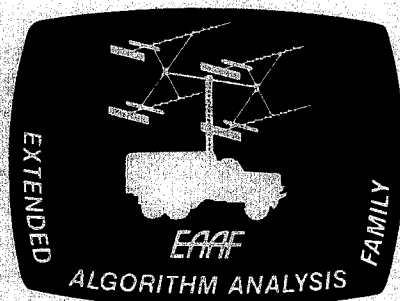
AD-A189 361

**U.S. Army Intelligence Center and School
Software Analysis and Management System**

BRAGG-CELL Receiver Study

Technical Memorandum No. 19

Lonnie A. Wilson



**DTIC
ELECTE
DEC 30 1987**

10 April 1987

DISTRIBUTION STATEMENT A

**Approved for public release
Distribution Unlimited**

**National Aeronautics and
Space Administration**

JPL

**Jet Propulsion Laboratory
California Institute of Technology
Pasadena, California**

JPL D-4307
ALGO_PUB_0033

87 12 22 032





SECURITY CLASSIFICATION OF THIS PAGE (When Data Entered)

REPORT DOCUMENTATION PAGE		READ INSTRUCTIONS BEFORE COMPLETING FORM
1. REPORT NUMBER ALGO-PUB-0033	2. GOVT ACCESSION NO.	3. RECIPIENT'S CATALOG NUMBER
4. TITLE (and Subtitle) Technical Memo 19, "Bragg-Cell Receiver Study"		5. TYPE OF REPORT & PERIOD COVERED FINAL
		6. PERFORMING ORG. REPORT NUMBER D-4307
7. AUTHOR(s) Dr. L. Wilson		8. CONTRACT OR GRANT NUMBER(s) NAS7-918
9. PERFORMING ORGANIZATION NAME AND ADDRESS Jet Propulsion Laboratory ATTN: 171-209 California Institute of Technology 4800 Oak Grove, Pasadena, CA 91109		10. PROGRAM ELEMENT, PROJECT, TASK AREA & WORK UNIT NUMBERS RE 182 AMEND #187
11. CONTROLLING OFFICE NAME AND ADDRESS Commander, USAICS ATTN: ATSI-CD-SF Ft. Huachuca, AZ 85613-7000		12. REPORT DATE 10 Apr 87
		13. NUMBER OF PAGES 81
14. MONITORING AGENCY NAME & ADDRESS (if different from Controlling Office) Jet Propulsion Laboratory, ATTN: 171-209 California Institute of Technology 4800 Oak Grove, Pasadena, CA 91109		15. SECURITY CLASS. (of this report) UNCLASSIFIED
		15a. DECLASSIFICATION/DOWNGRADING SCHEDULE NONE
16. DISTRIBUTION STATEMENT (of this Report) Approved for Public Dissemination		
17. DISTRIBUTION STATEMENT (of the abstract entered in Block 20, if different from Report) Prepared by Jet Propulsion Laboratory for the US Army Intelligence Center and School's Combat Developer's Support Facility.		
18. SUPPLEMENTARY NOTES		
19. KEY WORDS (Continue on reverse side if necessary and identify by block number) Bragg-Cell, Acoustic Signal, Transducer Non-linearity, Computer simulation, computer code, Instantaneous Frequency Measurement		
20. ABSTRACT (Continue on reverse side if necessary and identify by block number) A software implementation of a model of the Bragg-cell radar receiver is the product of this memo. Initially, the ideal Bragg-cell is described mathematically. The first-order AG transducer non-linearities are then introduced. This model is then tested with either constant or Gaussian input and constant or Gaussian first-order non-linearity (distortion signal). This model still required validation against actual Bragg-cell data. The model code is included in the appendix.		

U.S. ARMY INTELLIGENCE CENTER AND SCHOOL
Software Analysis and Management System

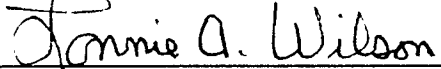
BRAGG-CELL RECEIVER STUDY

EAAF

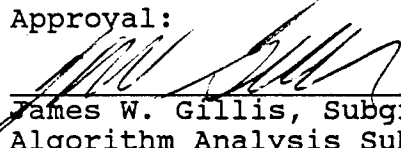
Technical Memorandum No. 19

10 April 1987

Author:



Lonnie A. Wilson, Consultant
SigPro Systems Incorporated


Approval:


James W. Gillis, Subgroup Leader
Algorithm Analysis Subgroup


Edward J. Records, Supervisor
USAMS Task

Concur:


A. F. Ellman, Manager
Ground Data Systems Section


Fred Vote, Manager
Advanced Tactical Systems

JET PROPULSION LABORATORY
California Institute of Technology
Pasadena, California



PREFACE

The work described in this publication was sponsored by the United States Army Intelligence Center and School. The writing and publication of this paper was supported by the Jet Propulsion Laboratory, California Institute of Technology, under a contract with the National Aeronautics and Space Administration, NAS 7-918, RE 182, A187.

EXECUTIVE SUMMARY

This Technical Memorandum was prepared originally as part of the Generic ELINT/COMINT Sensor Report (FY-86) which was eliminated under the FY-87 statement of work (SOW #2), undated (delivered to JPL 19 November 1986).

The purpose of the Generic ELINT/COMINT Sensor Report, of which this paper was intended (in its final form) to become part of, was to establish a basic superhetrodyne receiver based sensor model and perform simulations with it to determine the shaping or coloring of the statistical distributions of the radar free-space signal parametrics by a typical sensor prior to reaching the self-correlation processes. It was also intended for incorporation into the algorithm test bed so algorithms could be tested with realistic distorted data rather than unrealistic stastically pure data.

This work was originated in support of unanswered questions from previous self-correlation studies. The modeling and simulation approach was used because "live date" could not be obtained.

This paper is being published because it was completed in FY-86 with FY-86 funds and still serves a useful function.

Several significant results were noted while performing simulations on this model. The first order math model is developed for the Bragg-cell receiver. Whether the input distributions were uniform or Gaussian, the output distributions were found to be shaped so as to append a staircased triangular distribution.



SigPro Systems

I N C O R P O R A T E D

BRAGG-CELL RECEIVER STUDY

FINAL REPORT

MARCH 1987

JPL CONTRACT NO. 957474 MOD. NO. 1

This work was performed for the Jet Propulsion Laboratory, California Institute of Technology, sponsored by the National Aeronautics and Space Administration.

Reference herein to any specific commercial product, process, or service by trade name, trademark, manufacturer, or otherwise, does not constitute or imply its endorsement by the United States Government, SigPro Systems, Inc., or the Jet Propulsion Laboratory, California Institute of Technology.

Post Office Box 4452, Salinas, CA 93912-4452
Telephone 408-443-6555



ABSTRACT

Bragg-cell receivers are employed in specialized Electronic Warfare (EW) applications for the measurement of frequency. Bragg-cell receiver characteristics are fully characterized for simple RF emitter conditions, but less understood for complex and wideband RF emitter signals. This receiver is early in its development cycle when compared to the IFM receiver.

Functional mathematical models are derived and presented in this report for the Bragg-cell receiver. Theoretical analysis is presented and digital computer signal processing results are presented for the Bragg-cell receiver. Probability density function analysis are performed for output frequency.

Probability density function distributions are observed to depart from assumed distributions for wideband and complex RF signals. This analysis is significant for high resolution and fine grain EW Bragg-cell receiver systems.

NEW TECHNOLOGY

None

TABLE OF CONTENTS

EXECUTIVE SUMMARY	
ABSTRACT	1
NEW TECHNOLOGY	2
TABLE OF CONTENTS	3
INTRODUCTION	4
BRAGG-CELL RECEIVER.	5
Introduction	5
Ideal Bragg-cell Receiver Characterization	5
Practical Bragg-cell Receivers	13
PROBABILITY DENSITY FUNCTION ANALYSIS- Bragg-cell Receiver .	19
SIGNAL PROCESSING ANALYSIS	26
Introduction	26
Bragg-cell Receiver Model Results	26
CONCLUSIONS & RECOMMENDATIONS	100
REFERENCES.	101
APPENDIX A	102

INTRODUCTION

The development effort is for theoretical analysis, software algorithms implementations, signal processing analysis, and test analysis for probability density function characterization of a Bragg-cell receiver system. SigPro Systems Inc. is performing this work under JPL Contract No. 957474, Mod. No. 1.

This final report describes the completed study on the Bragg-cell receiver. A functional mathematical model is derived for the receiver. This math model is implemented into digital computer software and signal processing analyses are performed.

Theoretical analysis is developed for the Bragg-cell receiver. Ideal and practical subsystem implementations are presented and analyzed. The key ELINT parameter of interest is frequency, hence, the theoretical analysis presents the basic analysis approach for frequency. Probability density function analysis is presented for first-order subsystem model.

The theoretical model for the Bragg-cell is developed into a digital computer program. All computer programs are listed in Appendix A.

Signal processing analysis is performed using the derived first-order model. The pdf characteristics of the Bragg-cell receiver's output frequency are determined for assumed input frequency pdf (constant and Gaussian) characteristics.

BRAGG CELL RECEIVER

INTRODUCTION

A Bragg-cell receiver is used to measure frequencies of input RF radar pulses, with wide frequency coverage, large dynamic ranges and simultaneous or time coincident signals. The ideal Bragg-cell receiver will measure the frequency parameter on a single pulse basis with no distortion. Practical Bragg-cell receivers will distort the frequency characteristic of a radar emitter because the ideal Bragg-cell receiver characteristics are difficult to approximate in real life.

The radar's frequency parameter can be characterized using a random variable. The random variable may be quantified by the probability density function (pdf), mean value, variance and other moments. As a radar signal passes through the Bragg-cell receiver the random signal description is modified or distorted by the receiver's nonlinear transfer function characteristic. Bragg-cell receiver characterization of RF frequency will differ from actual radar emitter characterization by multifaceted distortion effects.

This section presents a functional description of the Bragg-cell receiver with potential distortion sources and mechanisms and a first-order Bragg-cell receiver model is developed. This Bragg-cell receiver model is used to analyze the distortion of the frequency's pdf. The first-order Bragg-cell receiver model is limited to key distortion effects.

IDEAL BRAGG-CELL RECEIVER CHARACTERIZATION

A functional block diagram of a Bragg-cell receiver is shown in Figure 1. The basic receiver includes an RF-to-IF downconverter, Bragg-cell with AO transducer, laser source, beam expander optics, beam focusing optics, detector array and processing electronics.

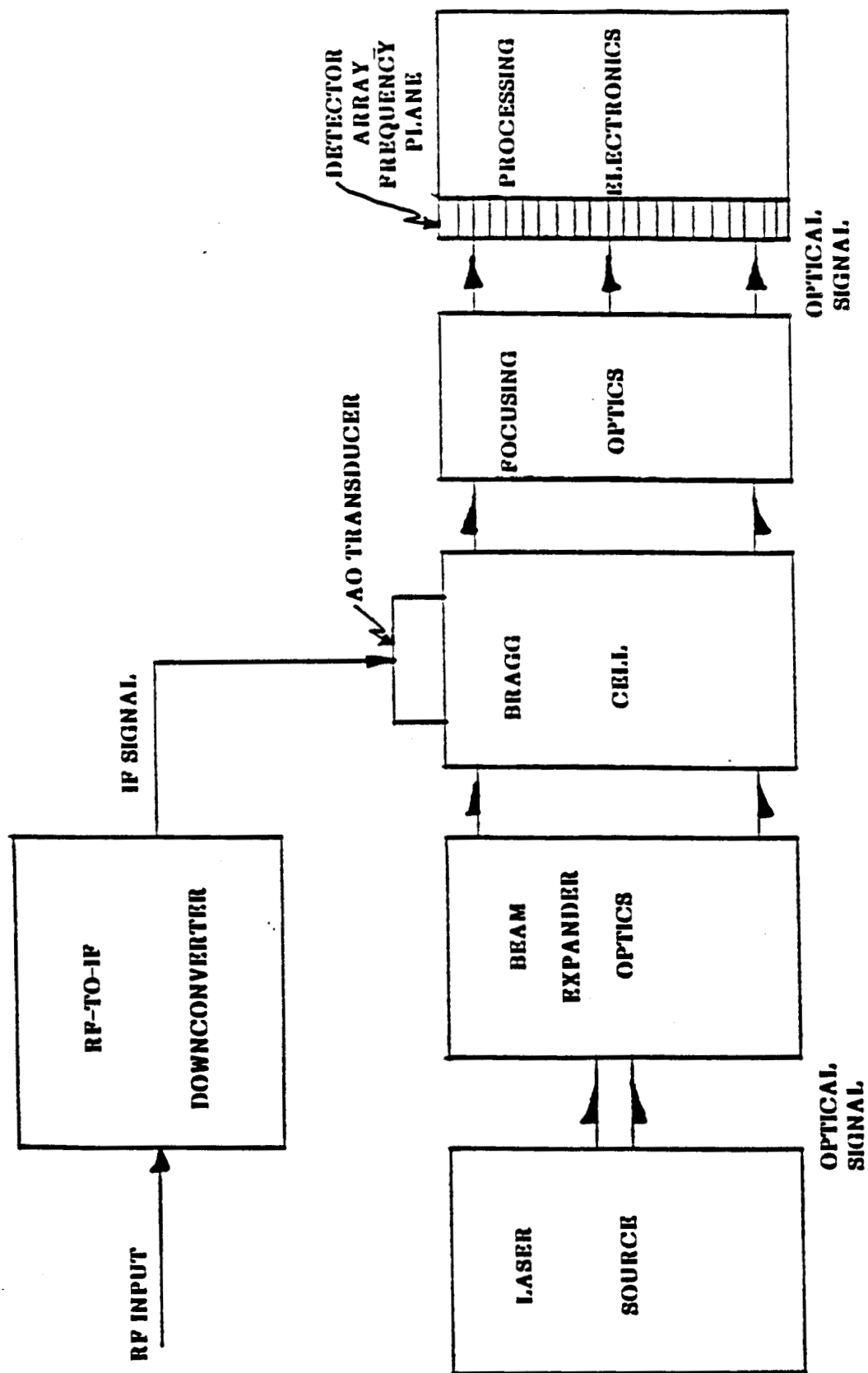


FIGURE 1. Functional Block Diagram of a Bragg-Cell Receiver.

The RF input signal is characterized by

$$x(t) = X(t) \cos[\omega_c t + \phi(t)] \quad \text{Eq. 1}$$

where

- $x(t)$ = Pulsed or CW signal,
- $X(t)$ = amplitude modulation function,
- ω_c = fixed angular carrier frequency,
- $\phi(t)$ = phase deviation function.

The RF-to-IF downconverter is described in Reference 1. The ideal downconverter is composed of an ideal local oscillator which is a perfect CW signal, a perfect product mixer, and an ideal bandpass filter. The ideal IF signal output from the downconverter is described quantitatively by:

$$y(t) = X(t) \cos[\omega_{IF} t + \phi(t)] \quad \text{Eq. 2}$$

Equation 2 is identical to Equation 1 with the fixed angular frequency being changed from ω_c to ω_{IF} . The IF center frequency is chosen to match the center frequency of the Bragg-cell and AO transducer. Ideally the IF signal replicates the input RF signal. The RF-to-IF downconverter is described and characterized in Reference 1. RF-to-IF downconverter analysis will not be presented in this report.

The IF signal drives the AO transducer which launches an acoustic signal through the Bragg-cell. Specifically, the IF electronic signal is converted into an acoustic wave (slow wave replication of the IF signal) which propagates

through the optically transparent Bragg-cell. Through the elasto-optic effect, the acoustic wave produces a spatial modulation of the refractive index in the Bragg-cell (Reference 2.)

The laser source is expanded by the beam expander optics and illuminates the Bragg-cell. As the laser light passes through the Bragg-cell, the refractive index variations produced by the acoustics wave (which is a slow form replica of the IF signal) are impressed onto the optical signal as a spatial phase modulation.

Focusing optics are used to equivalently Fourier transform the modulated optical beam. Resultant optical Fourier transform signal is focused onto the detector array or frequency focal plane (see Figure 1.) The photodiode detector array is used to capture and convert the optical signal to an electronic signal representation. The detector array is a linear photodiode array which is functionally used to detect and measure light intensity versus frequency of the transformed optical signal. The detector array is electronically read by the processing electronics, which also provides follow-on signal processing functions.

The Bragg-cell modulator is depicted in Figure 2. The incident laser light interacts with the acoustic signal in the cell to produce a diffracted light information signal along with undeflected laser light signal. The diffracted laser signal is also frequency shifted by the acoustic signal frequency. The incident laser light hits the Bragg-cell at an angle θ_i with respect to the z axis. The IF electronic signal is sent to the AO transducer to convert the IF signal to a replica acoustic signal. The acoustic wave of frequency f_1 propagates with velocity v_s along the x - axis in the Bragg-cell.

The diffracted laser light signal results from the AO interaction effects between the incident laser beam and the acoustic information bearing signal

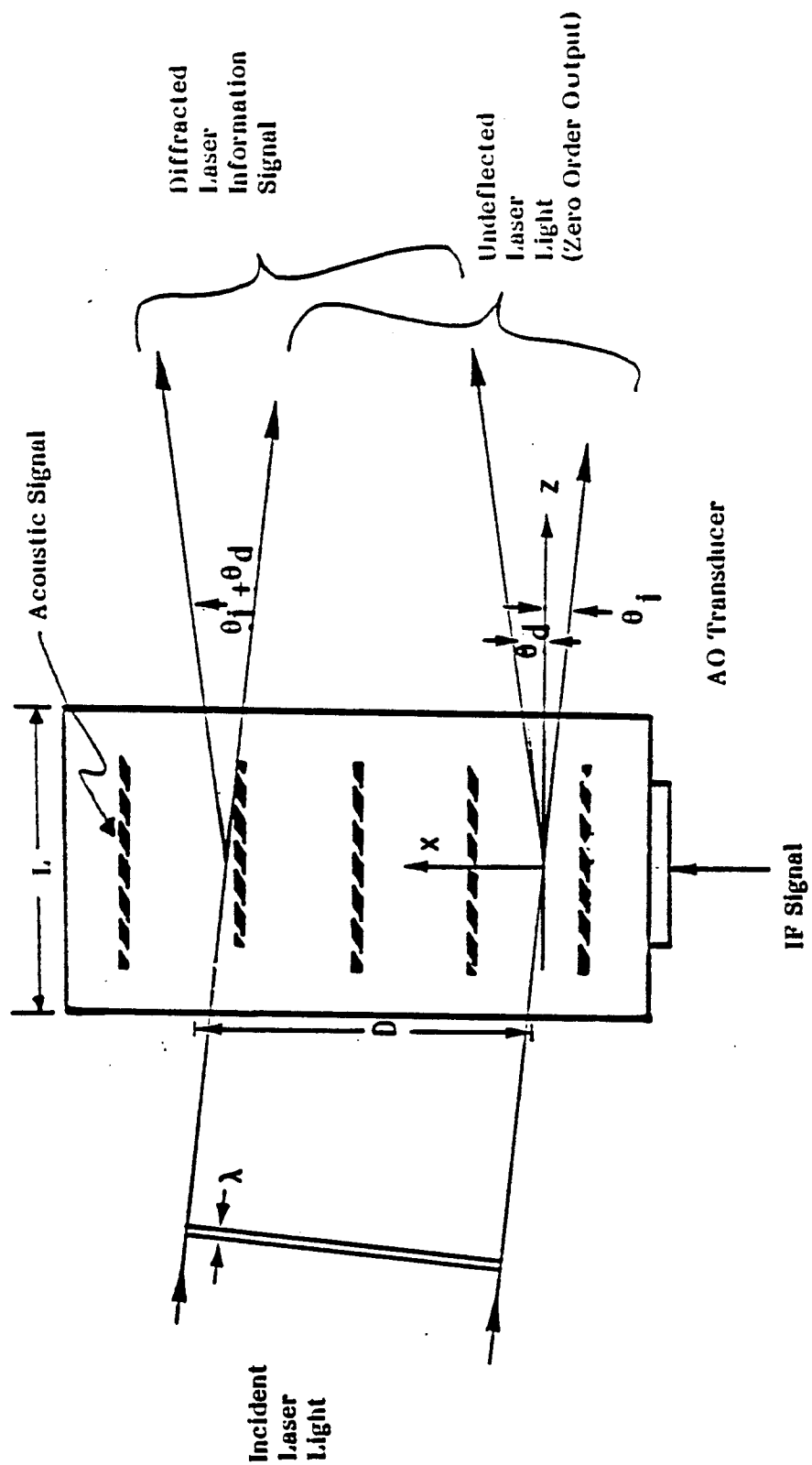


Figure 2. Bragg-Cell Modulator

in the Bragg-cell. Maximum diffracted laser light energy occurs in the first order beam when (Reference 2):

$$\theta_i = \sin^{-1} \left[\frac{\lambda f_1}{2 V_s} \right] \quad \text{Eq. 3.}$$

and

$$\theta_d = \theta_i \quad \text{Eq. 4}$$

where

- λ = Wavelength of laser light
- f_1 = Frequency of acoustic wave
- V_s = Velocity of acoustic wave in Bragg-cell along the x-axis.
- θ_i = Effective angle of incident laser light.
- θ_d = Effective angle of first order diffracted laser light information signal.

Detailed Bragg-cell analysis would require AO cell refractive index variations analysis for precise quantification. This first order Bragg-cell model does not require this detailed analysis. Functionally the Bragg-cell model is accurate and conceptually clear for the external angles θ_i and θ_d .

Bragg-cell processors are, in general, configured so that $\theta_i \ll 0.1$ radian, hence, Equation 3 can be readily and accurately simplified to:

$$\theta_i = \frac{\lambda f_i}{2 V_s} \quad \text{Eq. 5.}$$

Using Equation 4 and 5, the following equation for the effective angle of the first order diffracted laser light information signal is:

$$\theta_d = \frac{\lambda f_i}{2 V_s} \quad \text{Eq. 6}$$

Equation 6 reveals that θ_d varies directly with the acoustic wave frequency. As stated earlier, the IF signal frequency is related to the acoustic wave frequency by: (Reference 2)

$$f_{IF} = K f_i \quad \text{Eq. 7.}$$

where K is a constant.

Equation 8 results by combining Equations 6 and 7,

$$\theta_d = \frac{\lambda f_{IF}}{2 K V_s} \quad \text{Eq. 8.}$$

Equation 8 shows that θ_d varies directly with the IF signal carrier frequency.

The actual displacement of the diffracted laser information signal from the undeflected laser light (see Figure 2) is given by (Reference 2.)

$$d = \frac{F \lambda f_{IF}}{K V_s} \quad \text{Eq. 9.}$$

where F is the focal length of the focusing optics.

A fixed Bragg-cell receiver will result in Equation 9 reducing to:

$$d = K_1 f_{IF} \quad \text{Eq. 10}$$

The actual displacement, d , of the diffracted laser beam relative to the undeflected laser light passing through the Bragg-cell is directly proportional to the IF frequency of the input IF electronic signal. The diffracted laser beam will hit the linear detector array at a specific location which corresponds to one IF frequency. The Bragg-cell receiver is calibrated by varying the IF frequency of the input IF signal over the entire operating bandwidth and capturing and analyzing the electrical output signal from the linear detector array. Detector array element signal versus IF frequency characteristic is used to quantify the Bragg-cell receiver's frequency measurement performance.

The undeflected laser light is (the zero-order output from the Bragg-cell) described by:

$$\mathcal{L}_o(t) = L_o(t) \cos[2\pi f_s t + \gamma(t)] \quad \text{Eq. 11.}$$

where

- $\mathcal{L}_o(t) =$ undeflected laser light signal.
- $L_o(t) =$ amplitude or intensity of undeflected laser light signal.
- $f_s =$ laser light frequency
- $\gamma(t) =$ phase variations on laser light signal.

The diffracted laser information signal is quantified mathematically as:

$$Q_1(t) = L_1(t) \cos \left[2\pi(f_2 + f_1)t + \delta(t) \right] \quad \text{Eq. 12.}$$

where

$Q_1(t)$ = Diffracted laser information signal.

$L_1(t)$ = Amplitude or intensity of diffracted laser information signal.

$f_2 + f_1$ = Frequency of information signal.

$\delta(t)$ = Phase variations of information signal.

Equation 12 reveals that the diffracted laser output signal is frequency shifted. The frequency shift is produced by the laser light signal and acoustic signal interaction in the Bragg-cell.

The Bragg-cell receiver is conceptually a parallel, multi-channel spectrum analyzer, which determines the Fourier magnitude spectrum of the input IF signal. The electronic circuit model for the Bragg-cell receiver is depicted in Figure 3. The IF signal input is applied to a parallel narrowband filter bank with an associated diode detector and filter bank. Each output signal is a power or energy indicator of the IF signal spectral content in each selected narrowband filter.

PRACTICAL BRAGG-CELL RECEIVERS

The ideal Bragg-cell receiver is characterized in the previous section, with the measured frequency being derived from Equations 9, 10, and 12. This section will identify and briefly present some key differences between practical Bragg-cell receivers and the ideal Bragg-cell receiver. The Bragg-cell receiver, shown in Figure 1, is a reference for this discussion.

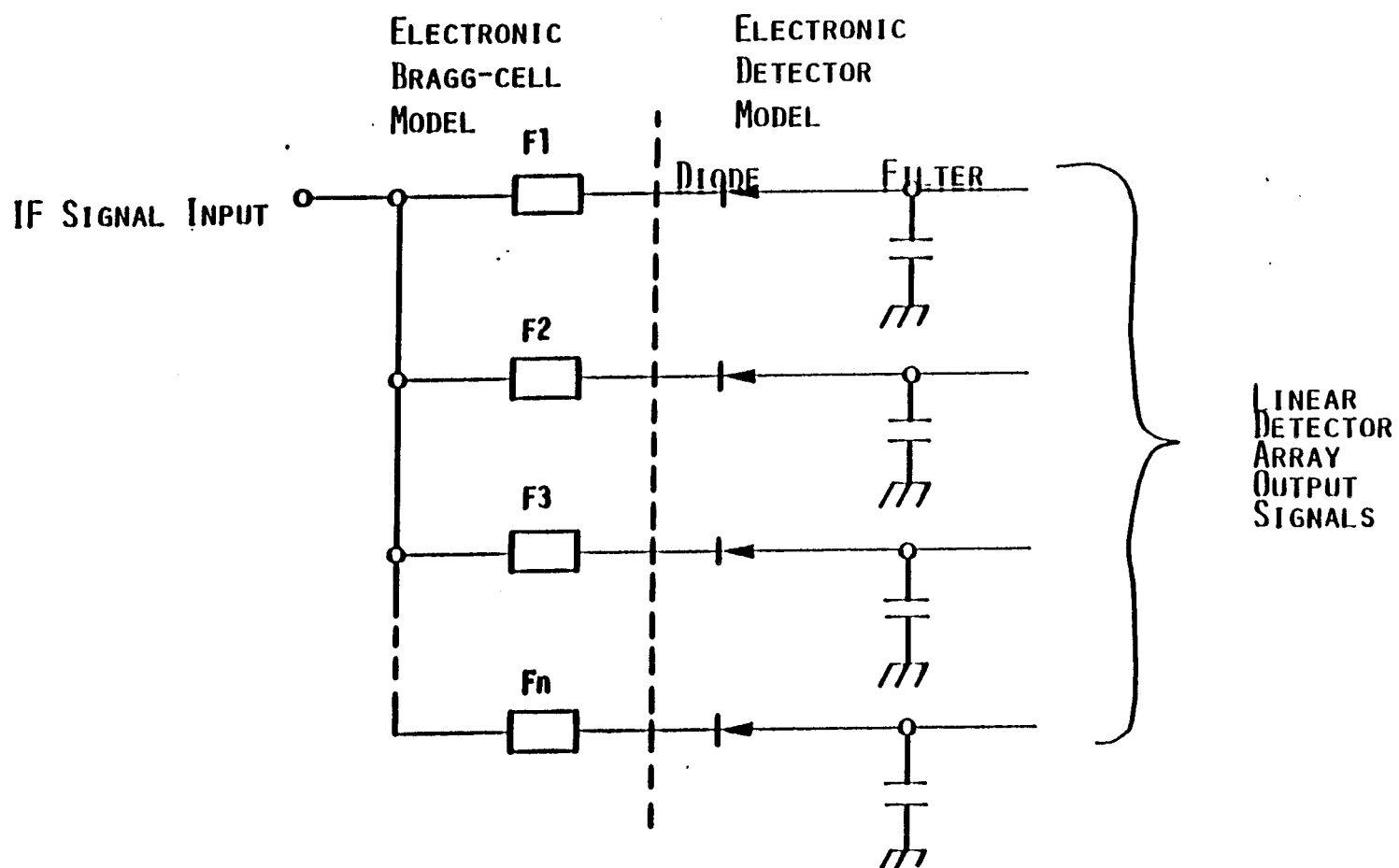


FIGURE 3. ELECTRONIC CIRCUIT MODEL FOR BRAGG-CELL RECEIVER

BRAGG CELL

The ideal Bragg-cell is assumed to have an undistorted acoustic signal replica (at acoustic frequency) of the IF input signal propagating through the cell. The AO transducer provides this electronic IF signal to acoustic signal conversion. The AO transducer has transfer function nonlinearities, which produces unwanted and added acoustic signal components. Simple sinusoidal electronic signals are subject to minor variations, while complex and wideband signals may be significantly distorted by the nonlinear transducer action.

The ideal Bragg-cell is assumed to provide a perfect acoustic signal termination, at the far end of the cell. In general, the acoustic signal termination is not perfect, which cause low level acoustic signal reflections and distortion generated signal components to propagate back through the cell. These reflected acoustic signals are considered as additional distortion sources, hence, variations in the diffracted laser information signal can be expected.

Actual distortion effects are determined by AO transducer nonlinearities, reflected acoustic signal levels, total acoustic signal parameter descriptors and Bragg-cell properties. The complete acoustic signal's instantaneous frequency is determined by amplitudes, frequencies, and phases of desired acoustic signal, undesired reflected acoustic signals and nonlinearly generated and unwanted acoustic signals. Frequency variations produced by instantaneous frequency changes will produce angle variations in the diffracted laser information signal; thus, frequency measurement errors in the Bragg-cell receiver.

LASER SOURCE

The laser light source is ideally assumed to be constant amplitude and fixed frequency signal. Actual laser sources can have some minor frequency shifts. Minor frequency shifts will results in small angle variations in the diffracted laser information signal. (See Equation 3.)

Frequency variations will widen the effective spotsize and change the angle of the diffracted laser beam, which means the light energy may be spread over more detector elements in the linear detector array.

The laser light signal does not have a constant intensity or amplitude. The amplitude is quantified by deterministic and random signal components. These amplitude variations will result in diffracted laser information signal intensity level variations at the detector plane.

OPTICS

Beam expander optics and diffraction signal focusing optics are fundamental modules in the Bragg-cell receiver. Beam expander optics shape the coherent laser beam to illuminate one entire side of the Bragg-cell. This beam expansion provides a long path interaction between the acoustic signal and laser light within the Bragg-cell. Beam expander optics and laser source are positioned so that the laser light strikes the cell at the Bragg angle. Nonlinearities, positional variations, and rotational variations in the beam expander optics can produce amplitude and angle variations in the diffracted laser information signal. These errors are usually very small for well-designed optics.

Focusing optics are used as the so-called Fourier transform lens. The Bragg-cell is positioned in the front focal plane of the lens. The photodetector

array is positioned at the back focal plane of the lense. (Reference 3.) Again, nonlinearities and location variations in the focusing optics variations can produce intensity and angle variations in the diffracted laser information signal. These errors are also very small in well-designed optics.

DETECTOR ARRAY

The ideal detector array is assumed to be a long linear array with high frequency resolution and sensitivity. Practical Bragg-cell receivers use long linear photodiode arrays, where typically 512 or 1024 photodiodes are closely spaced along the array length.

Figure 4 presents an illustration of two diffracted laser information signals striking the photodetector array at two different diodes (two different frequencies.) In actual practice, the light spotsize for each beam is larger than the area of one photodiode; hence, the light spills onto the area between detectors and also onto adjacent detectors.

Diffracted laser information signal angle variations (frequency variations) produce energy spread over several or many photodiode cells. Each photodiode cell is used to determine the signal energy in resolved and calibrated frequency space. The photodetector array is electronically readout to determine frequency and amplitude information for each diffracted laser light information signal. The photodetector array is functionally and practically described as a frequency sampling unit, with 512 to 1024 frequency bins. Each photodiode determines the elemental frequency resolution.

Bragg-cell receivers can accurately measure frequencies of time coincident or time overlapped signals, which is a big advantage over other receivers, such as the IFM receiver. These receivers are available with bandwidths to approximately 1 GHz, and frequency resolutions of 100 KHz to 10 MHz. The

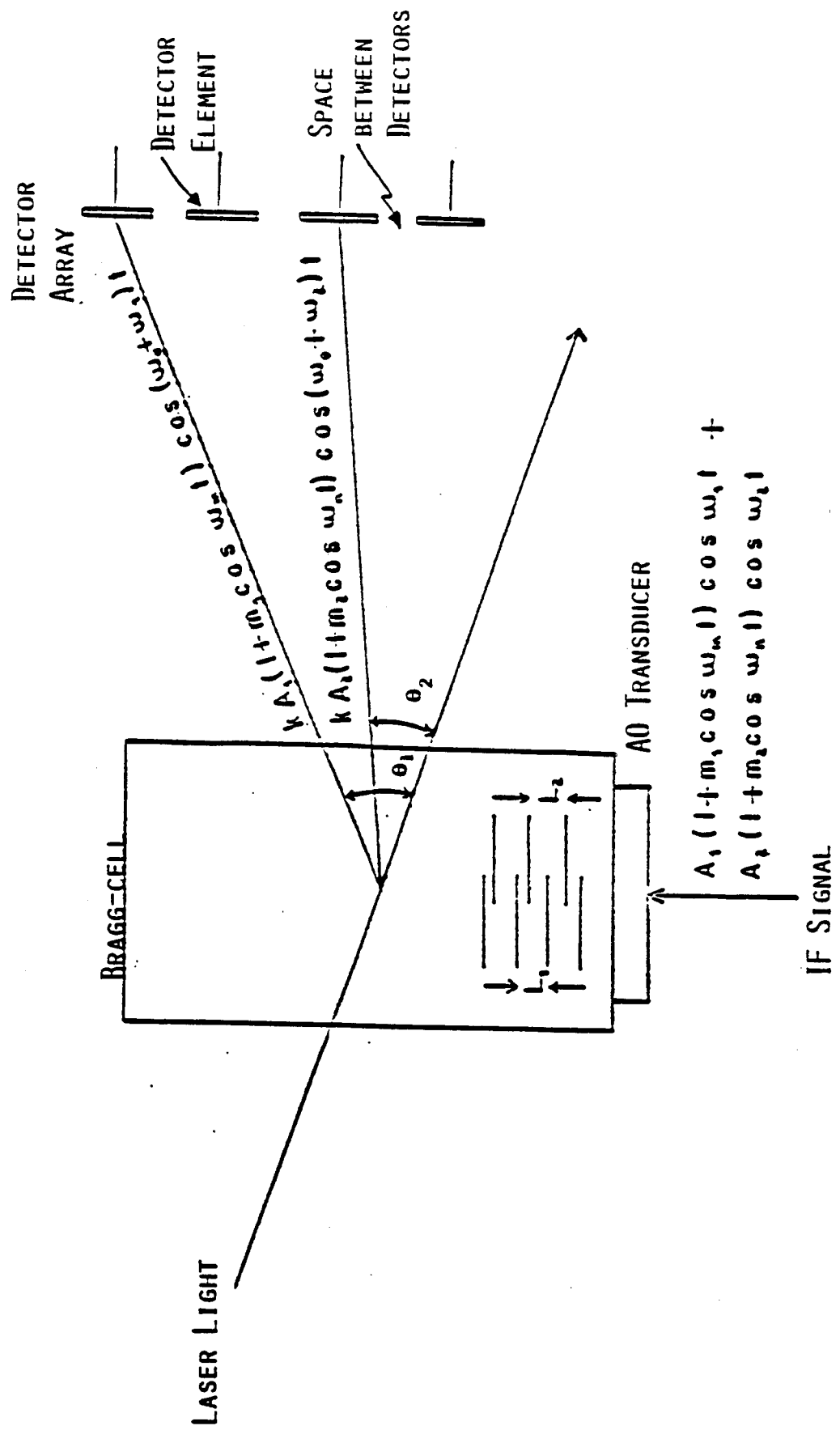


FIGURE 4. SIMPLIFIED DIAGRAM OF BRAGG-CELL RECEIVER WITH TWO INPUT SIGNALS.

Bragg-cell receiver's dynamic range is approximately 30 to 40 db. with the photodetector array's dynamic range being the critical limiting factor.

PROBABILITY DENSITY FUNCTION ANALYSIS

BRAGG-CELL RECEIVER

The probability density function (pdf) of the Bragg-cell receiver's measured frequency parameter is considered in this section. The pdf characteristic is developed for a first order Bragg-cell receiver model under high signal-to-noise ratio conditions. The IF signal's frequency characteristic is assumed to have a constant pdf or a Gaussian pdf.

Ideal and practical Bragg-cell receivers are discussed earlier in this report, and characteristics equations are provided for the ideal receiver. The Bragg-cell and AO transducer are key producers of first-order distortion effects. Distortion effects include AO transducer nonlinearities and reflected acoustic signals returning from the far end of the Bragg-cell. This analysis assumed that acoustic signals generated by AO transducer nonlinearities are significantly larger than reflected acoustic signals.

The ideal Bragg-cell receiver contains a single acoustic signal

$$z(t) = Z(t) \cos[2\pi f_1 t + d_1(t)] \quad \text{Eq. 13.}$$

which results in the diffracted laser information signal given in Equation 12. f_1 is the frequency of the acoustic signal, which is directly related to the frequency of the input IF signal. (See Equation 7.)

AO transducer nonlinearities are producing undesired acoustic signals

in the Bragg-cell. Undesired or unwanted acoustic signals are described as a cosinusoidal series of N components (harmonics and intermodulation components at a significant energy level) which are characterized as:

$$u(t) = \sum_{m=2}^N U_m(t) \cos[2\pi f_m t + d_m(t)] \quad \text{Eq. 14.}$$

where

$u(t)$ = Total unwanted acoustic signals in Bragg-cell. The AO transducer will generate harmonics of f_1 and other intermodulation frequency components.

$U_m(t)$ = Amplitude of n th. unwanted acoustic signal component.

f_m = Frequency of n th. unwanted acoustic signal component. Harmonics of f_1 and intermodulation frequency components are present.

$d_m(t)$ = Phase variations of n th. unwanted acoustic signal component.

The total acoustic signal in the Bragg-cell is found by summing Equations 13 and 14:

$$w(t) = z(t) + u(t) \quad \text{Eq. 15.}$$

Equation 15 can be rewritten, with a lot of work, as:

$$w(t) = z(t) A(t) \cos[2\pi f_1 t + d_1(t) + \beta(t)] \quad \text{Eq. 16.}$$

where

$$A(t) = \sqrt{\left[\sum_{n=2}^N S_n(t) \right]^2 + \left[1 + \sum_{n=2}^N C_n(t) \right]^2}$$

$$\beta(t) = \tan^{-1} \left[\frac{\sum_{n=2}^N S_n(t)}{1 + \sum_{n=2}^N C_n(t)} \right]$$

$$S_n(t) = K_n \sin(2\pi \Delta f_n t + \Delta \theta_n)$$

$$C_n(t) = K_n \cos(2\pi \Delta f_n t + \Delta \theta_n)$$

$$K_n = \frac{U_n(t)}{Z(t)}$$

$$\Delta f_n = f_n - f_1$$

$$\Delta \theta_n = \phi_n(t) - \phi_1(t)$$

The instantaneous frequency variation, resulting from $\beta(t)$ phase variations in Equation 16, is

$$\Delta f_i(t) = \frac{\left[\sum_{m=2}^N S_m(t) \right] \left[\sum_{m=2}^N \Delta \omega_m S_m(t) \right] + \left[1 + \sum_{m=2}^N C_m(t) \right] \left[\sum_{m=2}^N \Delta \omega_m C_m(t) \right]}{2 \pi A^2(t)} \quad \text{Eq. 17.}$$

The instantaneous frequency variation is a very complex function of amplitudes, frequencies, and phases of all unwanted acoustic signal components in the Bragg-cell. Equation 17 can be rewritten using the Fourier series expansion as a fixed frequency plus a series of harmonically related frequency components. A first-order approximation is the reduction of Equation 17 to a fixed frequency,

$$\Delta f_i(t) \doteq f_2 \quad \text{Eq. 18.}$$

f_2 is used to approximate the resultant frequency component, which is produced by unwanted acoustic signal components propagating in the Bragg-cell.

Resultant phase variations are approximated as:

$$\beta(t) \doteq 2 \pi f_2 t \quad \text{Eq. 19.}$$

The total acoustic signal (Eq. 16) can be approximated as:

$$w(t) \doteq Z(t) A(t) \cos[2\pi f_1 t + 2\pi f_2 t + \alpha_1(t)] \quad \text{Eq. 20.}$$

The total instantaneous frequency of $w(t)$ (Equation 20) is:

$$f_i(t) \doteq f_1 + f_2 \quad \text{Eq. 21.}$$

Equation 12 can be easily changed to approximate unwanted acoustic signals. The modified Equation 12 results in the following equation:

$$L_1(t) = L'_1(t) \cos[2\pi(f_2 + f_1 + f_2)t + \delta'(t)]. \quad \text{Eq. 22.}$$

The actual displacement of the diffracted laser information signal (Equation 22) relative to the undeflected laser light is

$$d = \frac{F\lambda(f_1 + f_2)}{V_s}. \quad \text{Eq. 23.}$$

Equation 23 reveals that d is a random variable since it is a summation of two random variables f_1 and f_2 . Conceptually, the spot size of the diffracted laser information signal is increased by the unwanted acoustic signal components. The actual displacement d is directly calibrated to a photodiode

cell in the linear detector array, which corresponds to a specified frequency bin.

f_1 and f_2 are assumed to be independent random variables for this analysis. Pdf characteristics of f_1 and f_2 are assumed to be either constant or Gaussian. The pdf characteristic of d' is the convolution of pdf (f_1) and pdf (f_2), if the random variables are independent (Reference 4.)

$$\text{pdf}(d') = \int_{-\infty}^{\infty} \text{pdf}(d' - f_1) \text{pdf}(f_1) df_1 \quad \text{Eq. 24.}$$

where

$$d' = d \frac{V_s}{F\lambda}.$$

Each frequency bin in the linear photodiode array exactly corresponds to Δd bin coverage in displacement space.

The output frequency of the detector array is

$$f_o = K_2 d \quad \text{Eq. 25.}$$

Substituting Equation 25 into Equation 23, the result is:

$$f_o = \frac{K_2 F \lambda (f_1 + f_2)}{V_s}. \quad \text{Eq. 26.}$$

The Bragg-cell receiver's measured output frequency can be stated in terms of the input IF signal's frequency by using Equations 26 and a modified version of Equation 7. The output frequency is:

$$f_D = K_3 (f_{IF} + f_2^1) \quad \text{Eq. 27.}$$

where

$$K_3 = \frac{K_2 F \lambda}{K V_s}$$

f_2^1 = The equivalent IF frequency of unwanted acoustic signal components approximated as acoustic frequency f_2 .

f_D is a linear combination of two random variables f_{IF} and f_2^1 , which are assumed to be independent. The pdf (f_D) is the convolution of pdf (f_{IF}) and pdf (f_2^1), which is expressed mathematically as:

$$\text{pdf}(f_D) = \int_{-\infty}^{\infty} \text{pdf}(f_D - f_{IF}) \text{pdf}(f_{IF}) df_{IF} \quad \text{Eq. 28.}$$

The pdf (f_D) characteristic is functionally divided into sampled Δf_D bins by the photodiode cells in the linear detector array. This frequency domain binning process is equivalent to discrete sampling of the pdf (f_D)

characteristics in Δf_D bin widths. Δf_D is the basic frequency resolution of the Bragg-cell receiver at the linear detector array. The actual pdf characteristic of the Bragg-cell receiver's frequency parameter is a discrete characteristic, which is a function of the pdf of the IF signal frequency and pdf characteristic of the equivalent unwanted signal components.

SIGNAL PROCESSING ANALYSIS

INTRODUCTION

Signal processing analysis results are presented in this section. The Bragg-cell receiver model is implemented on a Hewlett Packard Integral computer. Computer software program listings are contained in Appendix A of this report.

PDF analysis of the Bragg-cell receiver's frequency parameter is performed, assuming constant and Gaussian pdf characteristics for the input signal's IF frequency. PDF analysis is performed for selected frequency resolutions of the Bragg-cell receiver. Also, statistical analysis are performed on output pdf signals and summary results are presented.

BRAGG-CELL RECEIVER MODEL RESULTS

The Bragg-cell receiver is math modeled in the previous section. First-order model implementation is shown to be a convolution of pdf (f_{IF}) and pdf (f_2^1) for the Bragg-cell receiver's output frequency pdf characteristic. Equation 28 is the final descriptive equation for the output frequency pdf characteristic.

Bragg-cell receiver signal processing results are summarized in Table 1. Signal processing analysis programs are presented in Appendix A. Figures 5 through 70 contain detailed pdf plots for the Bragg-cell receiver's output frequency parameters. These plots are made for selected pdf characteristic of f_{IF} and f_2^1 and selected Bragg-cell receiver frequency resolutions.

Table 1 defines the input signal or f_{IF} in terms of DF1 or DF1 and σ_1 . The pdf (f_{IF}) is assumed to be a constant if only a value for DF1 is given. DF1 (MHz) indicates the frequency excursion of the input frequency (f_{IF})

For a Gaussian pdf (f_{IF}), DF1(MHz) and σ_1 (MHz) is selected as 1.166 MHz or 4.166 MHz for Gaussian pdf's.

TABLE 1

BRAGG-CELL RECEIVER
SIGNAL PROCESSING RESULTS

FIGURE	INPUT SIGNAL		DISTORTION SIGNAL		FREQUENCY RESOLUTION (MHz)	OUTPUT FREQUENCY: STATISTICAL RESULTS		
	DFI(MHz)	σ_1 (MHz)	DF2(MHz)	σ_2 (MHz)		σ (MHz)	SKEW	KURTOSIS
5	10		2		0.5	2.964	0.216	1.907
6	10		2		1.0	3.404	1.257	2.253
7	10		2		2.0	3.103	1.010	2.165
8	10		5		0.5	3.250	-0.119	2.192
9	10		5		1.0	3.422	-0.864	2.319
10	10		5		2.0	4.168	1.395	2.369
11	10		9		0.5	3.910	0.038	2.394
12	10		9		1.0	3.922	-0.228	2.402
13	10		9		2.0	4.017	0.730	2.442
14	25		5		1.0	7.395	0.000	1.895
15	25		5		2.0	7.571	-0.581	1.967
16	25		5		5.0	7.356	0.495	1.946
17	25		15		1.0	8.471	0.000	2.272
18	25		15		2.0	8.498	-0.155	2.281
19	25		15		5.0	8.420	-0.077	2.268
20	25		24		1.0	10.071	0.000	2.399
21	25		24		2.0	10.062	0.096	2.396
22	25		24		5.0	9.996	0.026	2.389

TABLE 1 CONT'D
BRAGG-CELL RECEIVER
SIGNAL PROCESSING RESULTS

FIGURE	INPUT SIGNAL		DISTORTION SIGNAL		FREQUENCY RESOLUTION (MHz)	OUTPUT FREQUENCY: STATISTICAL RESULTS		
	DFI(MHz)	α_1 (MHz)	DF2(MHz)	σ_2 (MHz)		σ (MHz)	SKEW	KURTOSIS
23	10	1.166	2		0.5	1.755	0.007	2.850
24	10	1.166	2		1.0	1.755	0.086	2.844
25	10	1.166	2		2.0	1.753	0.111	2.824
26	10	1.166	5		0.5	2.208	-0.006	2.713
27	10	1.166	5		1.0	2.209	-0.042	2.714
28	10	1.166	5		2.0	2.207	0.023	2.704
29	25	4.166	15		1.0	6.026	-0.001	2.624
30	25	4.166	15		2.0	6.026	-0.008	2.625
31	25	4.166	15		5.0	6.022	0.009	2.617
32	25	4.166	24		1.0	8.124	0.000	2.327
33	25	4.166	24		2.0	8.124	0.003	2.327
34	25	4.166	24		5.0	8.122	0.000	2.324
35	10		2	0.333	0.5	2.915	0.003	1.831
36	10		2	0.333	1.0	3.257	1.174	2.192
37	10		2	0.333	2.0	2.748	0.080	1.799
38	10		5	0.833	0.5	3.012	-0.004	1.973
39	10		5	0.833	1.0	3.102	-0.019	1.973
40	10		5	0.833	2.0	3.055	0.564	2.059

TABLE 1 CONT'D
BRAGG-CELL RECEIVER
SIGNAL PROCESSING RESULTS

FIGURE	INPUT SIGNAL		DISTORTION SIGNAL		FREQUENCY RESOLUTION (MHz)	OUTPUT FREQUENCY: STATISTICAL RESULTS		
	DFI(MHz)	σ_1 (MHz)	DF2(MHz)	σ_2 (MHz)		σ (MHz)	SKEW	KURTOSIS
41	10		9	1.5	0.5	3.255	0.001	2.241
42	10		9	1.5	1.0	3.255	-0.008	2.241
43	10		9	1.5	2.0	3.255	0.027	2.239
44	25		5.0	0.833	1.0	7.288	0.000	1.831
45	25		5.0	0.833	2.0	7.306	-0.165	1.834
46	25		5.0	0.833	5.0	6.87	1.001	1.799
47	25		15	2.5	1.0	7.653	0.000	2.037
48	25		15	2.5	2.0	7.653	-0.002	2.037
49	25		15	2.5	5.0	7.645	0.063	2.041
50	25		24	4.0	1.0	8.254	0.000	2.281
51	25		24	4.0	2.0	8.254	0.002	2.280
52	25		24	4.0	5.0	8.252	0.006	2.278
53	10	1.666	2.0	0.333	0.5	1.683	-0.003	2.842
54	10	1.666	2.0	0.333	1.0	1.683	0.076	2.842
55	10	1.666	2.0	0.333	2.0	1.680	0.039	2.804
56	10	1.666	5.0	0.833	0.5	1.845	-0.003	2.884
57	10	1.666	5.0	0.833	1.0	1.845	-0.003	2.884
58	10	1.666	5.0	0.833	2.0	1.845	0.002	2.882

TABLE 1 CONT'D
BRAGG-CELL RECEIVER
SIGNAL PROCESSING RESULTS

FIGURE	INPUT SIGNAL		DISTORTION SIGNAL		FREQUENCY RESOLUTION (MHz)	OUTPUT FREQUENCY: STATISTICAL RESULTS		
	DF1(MHz)	σ_1 (MHz)	DF2(MHz)	σ_2 (MHz)		σ (MHz)	SKEW	KURTOSIS
59	10	1.666	9	1.5	0.5	2.220	-0.001	2.915
60	10	1.666	9	1.5	1.0	2.220	-0.002	2.915
61	10	1.666	9	1.5	2.0	2.220	-0.001	2.915
62	25	4.166	5	0.833	1.0	4.207	-0.003	2.842
63	25	4.166	5	0.833	1.0	4.207	-0.003	2.842
64	25	4.166	5	0.833	5.0	4.200	0.001	2.805
65	25	4.166	15	2.5	1.0	4.811	-0.002	2.896
66	25	4.166	15	2.5	2.0	4.811	-0.002	2.896
67	25	4.166	15	2.5	5.0	4.811	-0.001	2.895
68	25	4.166	24	4.0	1.0	5.719	-0.001	2.916
69	25	4.166	24	4.0	2.0	5.719	-0.001	2.916
70	25	4.166	24	4.0	5.0	5.719	-0.001	2.915

The distortion signal or f_2^1 is quantified in terms of DF2 or DF2 and σ_2 . The pdf(f_2^1) is assumed to be a constant if only a value for DF2 is given. DF2(MHz) indicates the frequency excursion of the distortion signal f_2^1 .

For a Gaussian pdf(f_2^1), DF2(MHz) and σ_2 (MHz) indicates six times sigma and standard deviation, respectively. DF2 is selected as 2, 5, 9, 15, and 24 MHz. σ_2 (MHz) is selected as 0.333, 0.833, 1.5, 2.5 and 4.0 MHz for Gaussian pdfs.

Bragg-cell receiver frequency resolution (MHz) is chosen to be 0.5, 1.0, 2.0 or 5.0 MHz. These frequency resolution selections are readily expected with current Bragg-cell receiver technology.

The last three columns of Table 1 contain statistical results of the Bragg-cell receiver's output frequency. Sigma (MHz), skew and kurtosis are computed for each output frequency pdf characteristic shown in Figure 5 through 70.

The pdf(f_d) characteristic is a staircased trapezoidal function for pdf(f_{IF}) = constant and pdf(f_2^1) = constant. Figures 5 through 22 show numerous examples of pdf(f_d) characteristics for selected input signal and distortion signal constant pdf characteristics. Pdf(f_d) is observed to significantly depart from a constant characteristic and approach a staircased triangular characteristic as DF2 approaches DF1.

Figures 23 through 34 reveal output frequency pdf(f_d) characteristics with input frequency characteristics assumed to be Gaussian pdf and distortion signal frequency characteristics assumed to be constant pdf. These pdf characteristics are staircased Gaussian characteristics. The pdf characteristic departs from the Gaussian characteristics as the Bragg-cell receiver's frequency resolution is decreased.

Figures 23 through 34 reveal output frequency $\text{pdf}(f_d)$ characteristics with input frequency characteristics assumed to be Gaussian pdf and distortion signal frequency characteristics assumed to be constant pdf. These pdf characteristics are staircased Gaussian characteristics. The pdf characteristic departs from the Gaussian characteristics as the Bragg-cell receiver's frequency resolution is decreased.

Figures 35 through 52 reveal output frequency $\text{pdf}(f_d)$ characteristics with input frequency characteristics assumed to be constant pdf and distortion signal frequency characteristics assumed to be Gaussian pdf. For most example plots the long constant pdf characteristic of the input frequency tends to dominate the overall pdf characteristic. The pdf characteristics are approximately a staircased trapezoidal characteristic.

The $\text{pdf}(f_d)$ characteristic is a staircased Gaussian function for $\text{pdf}(f_{IF}) = \text{Gaussian}$ and $\text{pdf}(f_2^1) = \text{Gaussian}$. Figures 53 through 70 show numerous examples of $\text{pdf}(f_d)$ for selected input signal and distortion signal frequency characteristics. $\text{pdf}(f_d)$ is observed to be close to a Gaussian characteristic for all DF2 and DF1 selections. For low frequency resolution in the Bragg-cell receiver, the pdf characteristic departs from a Gaussian characteristic.

Figure 5

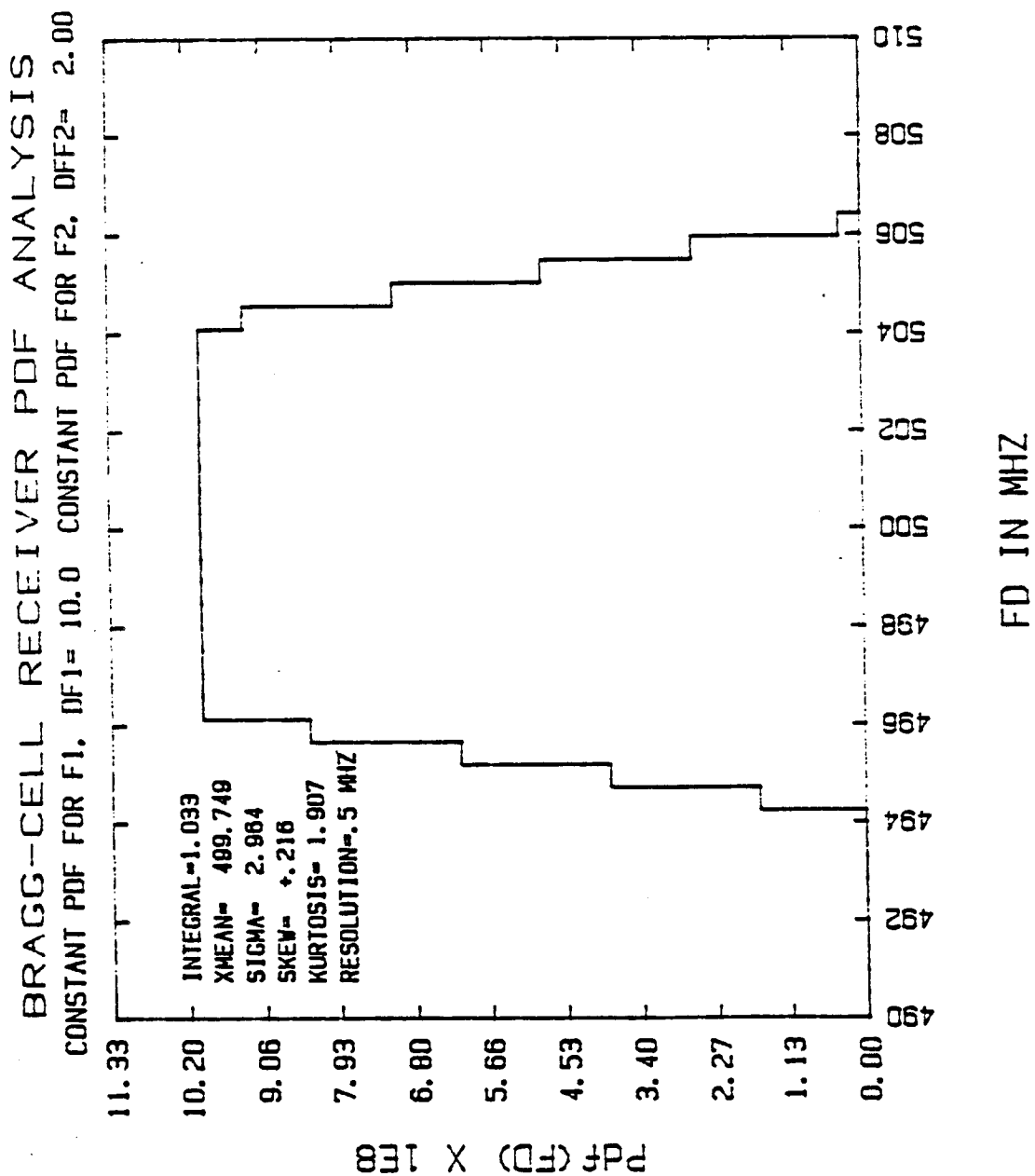


Figure 6

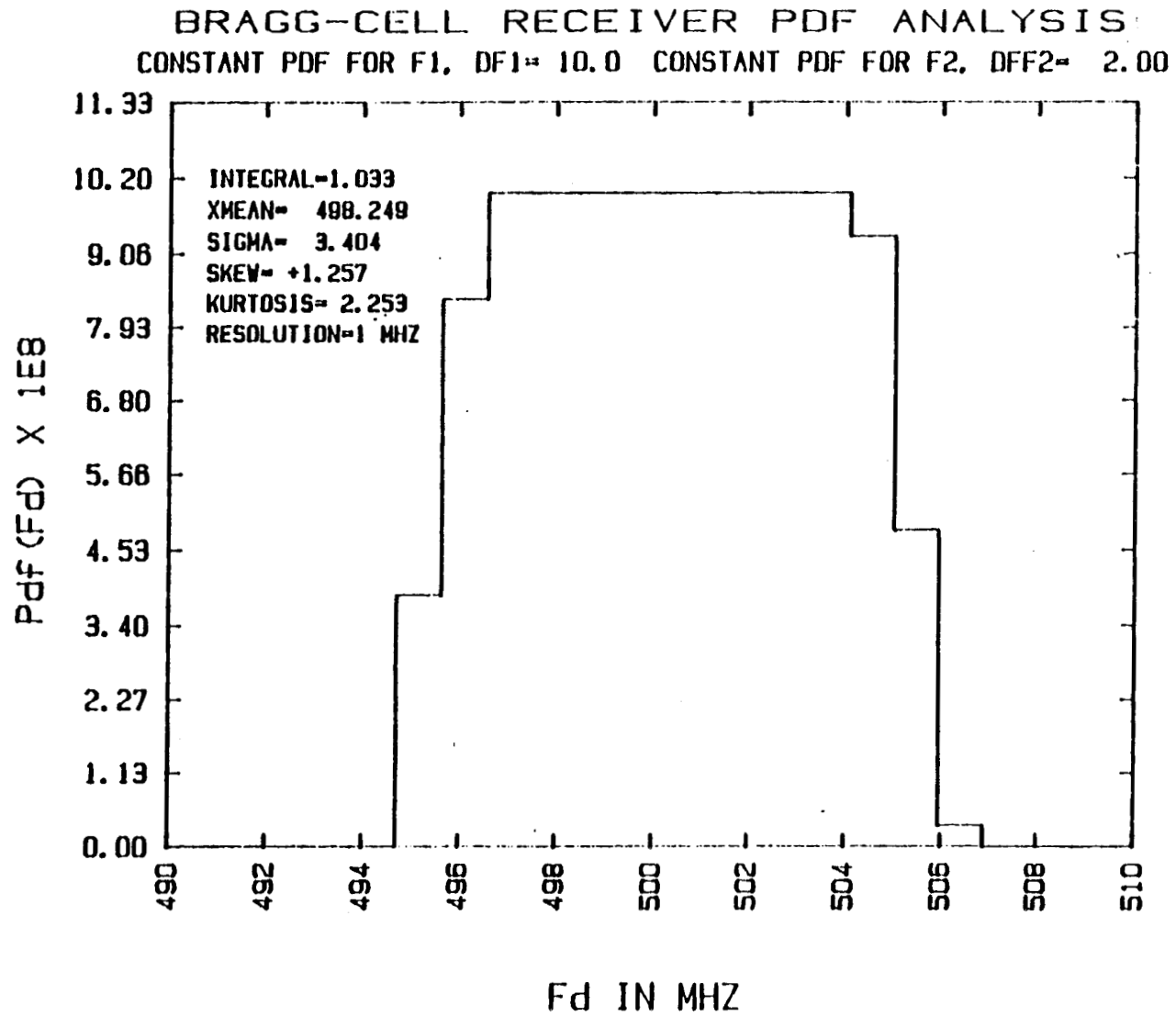


Figure 7

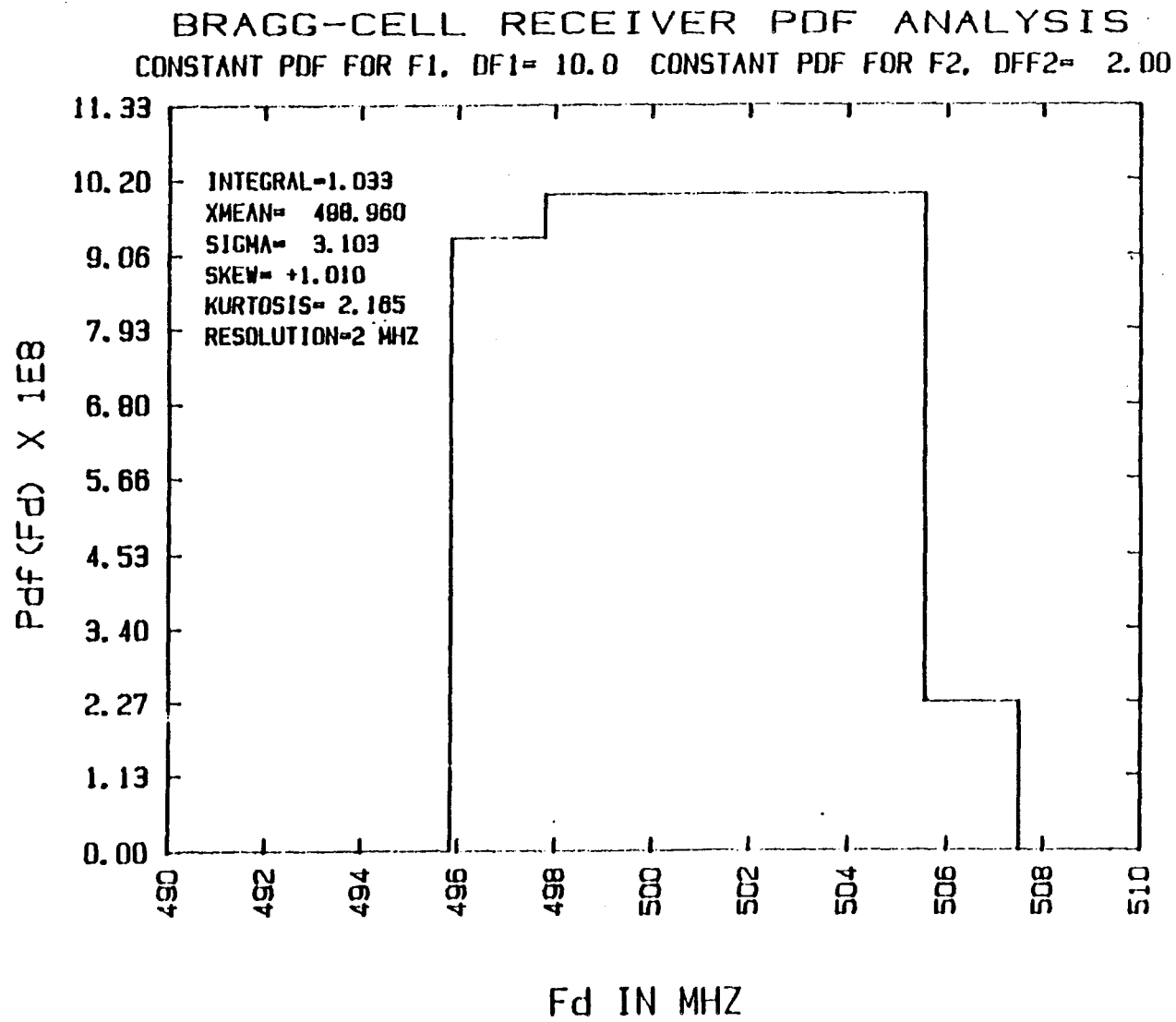


Figure 8

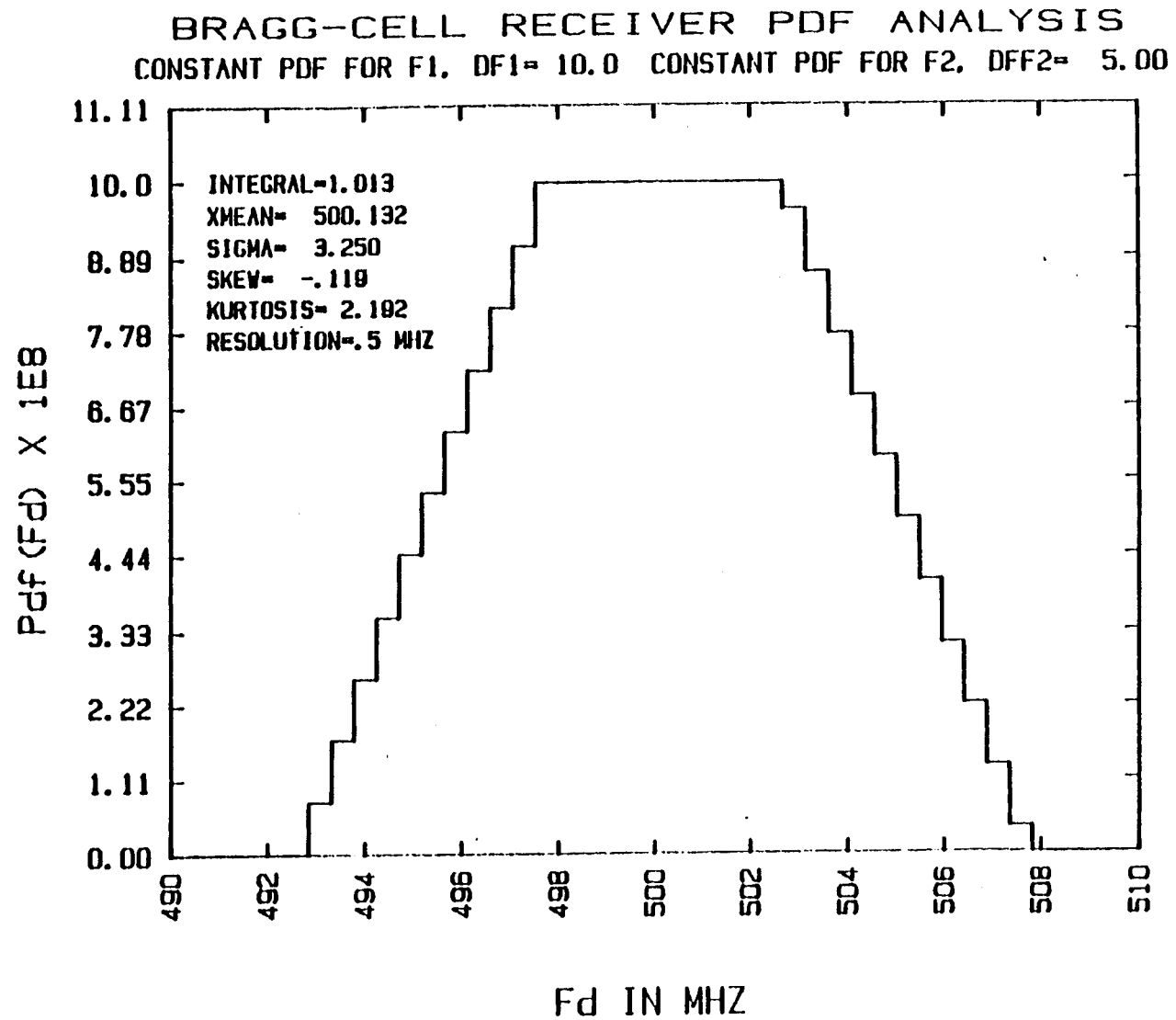


Figure 9

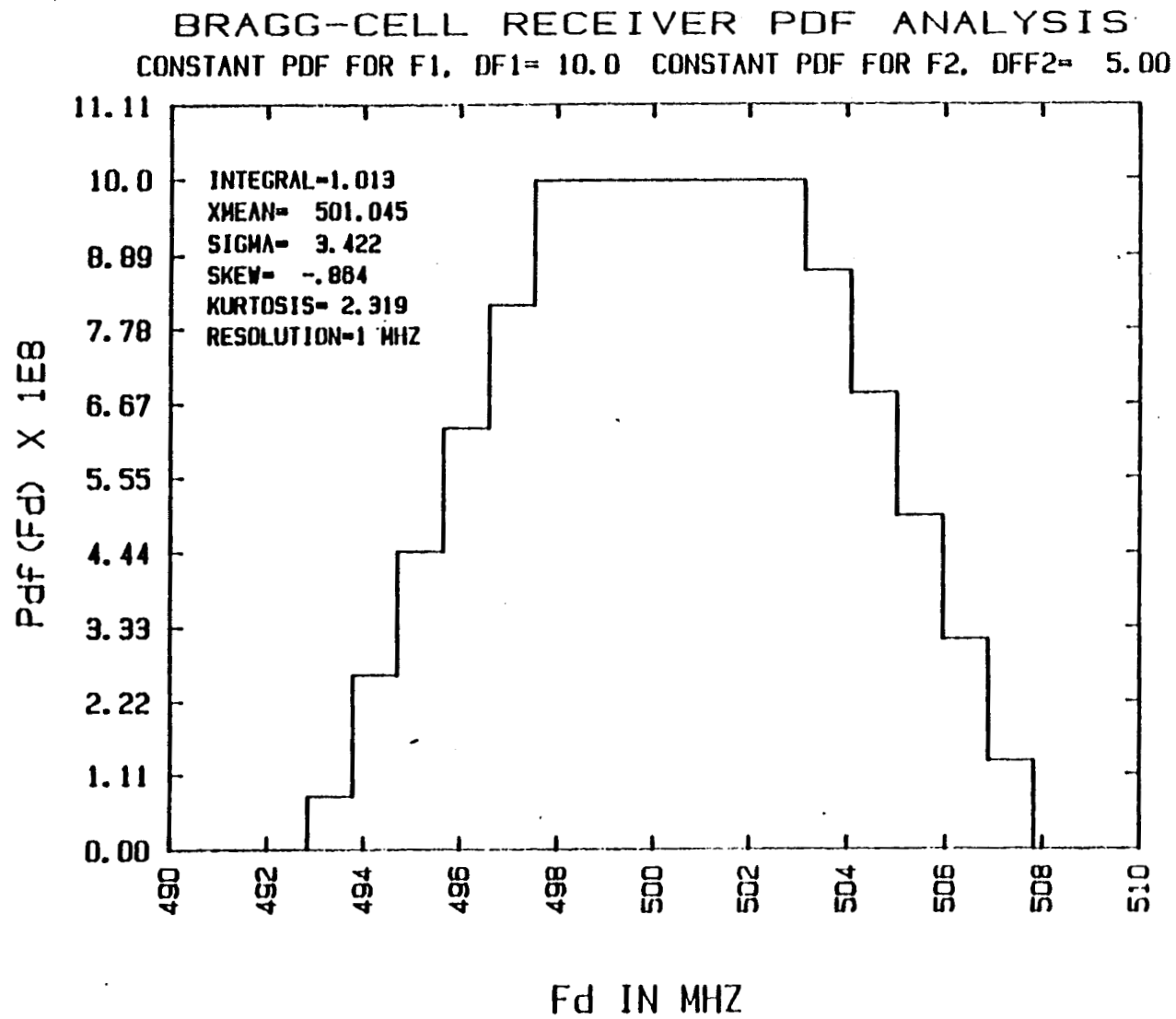


Figure 10

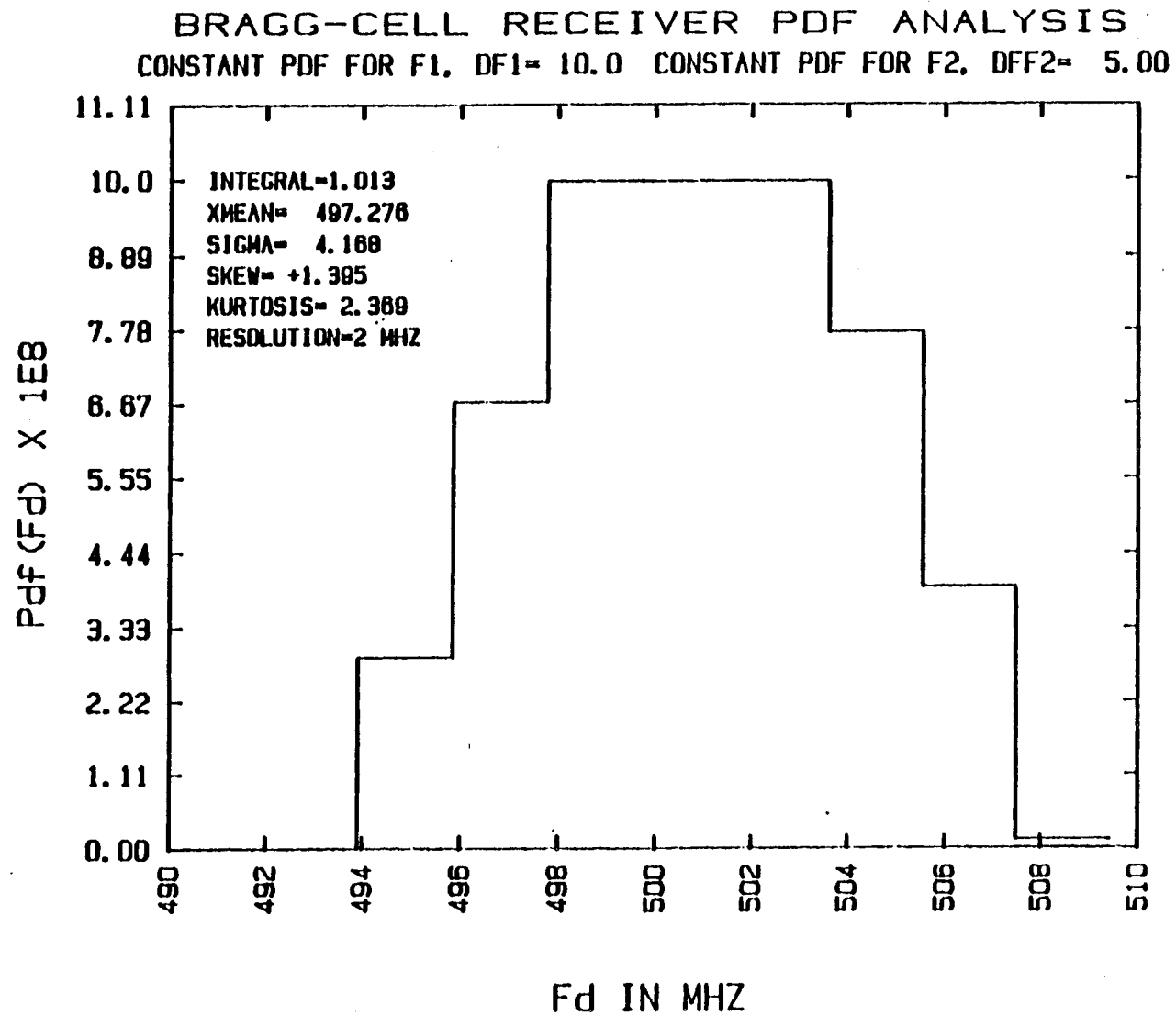


Figure 11

BRAGG-CELL RECEIVER PDF ANALYSIS
CONSTANT PDF FOR F1, DF1= 10.0 CONSTANT PDF FOR F2, DFF2= 9.00

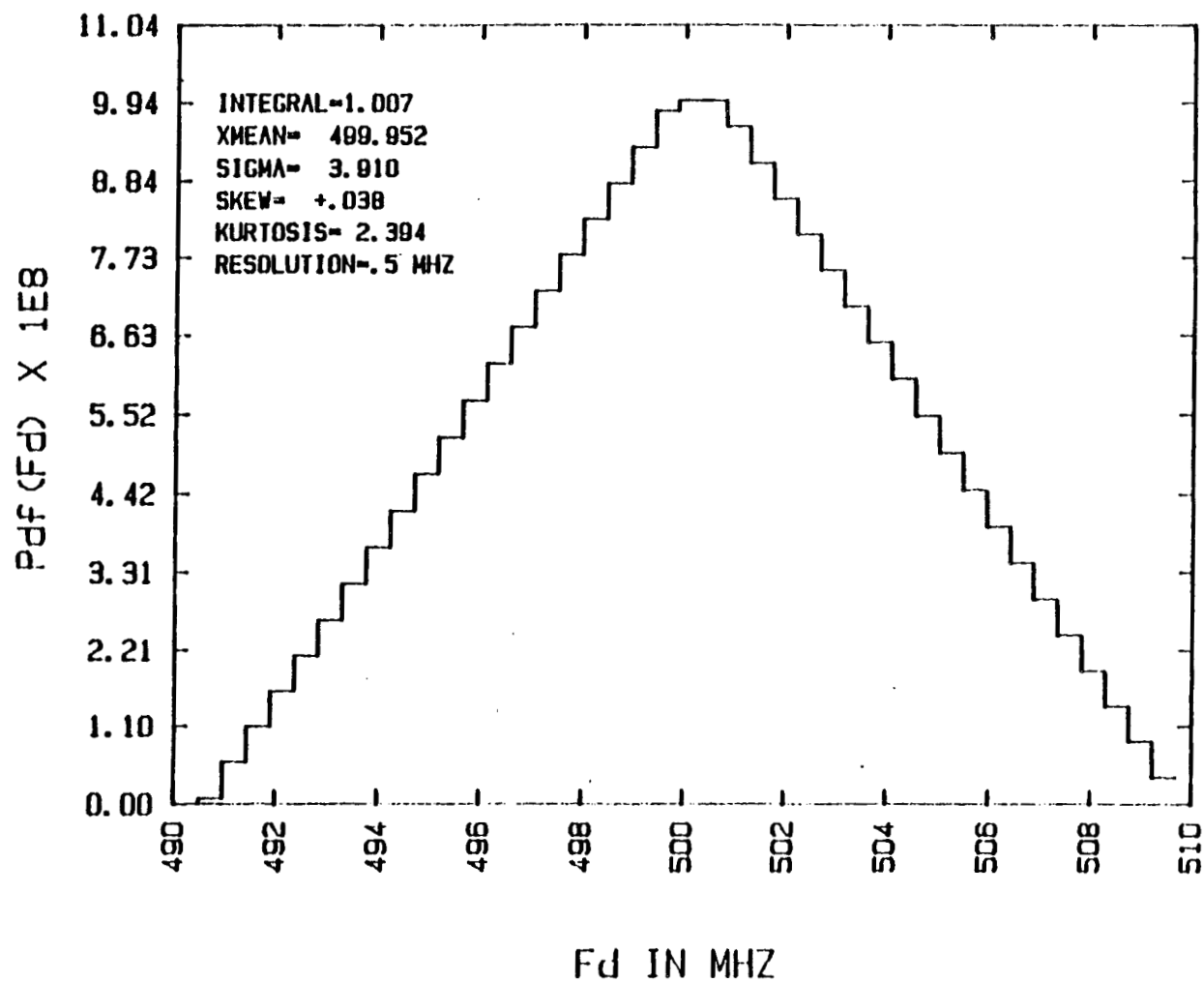


Figure 12

BRAGG-CELL RECEIVER PDF ANALYSIS
CONSTANT PDF FOR F1, DF1= 10.0 CONSTANT PDF FOR F2, DFF2= 9.00

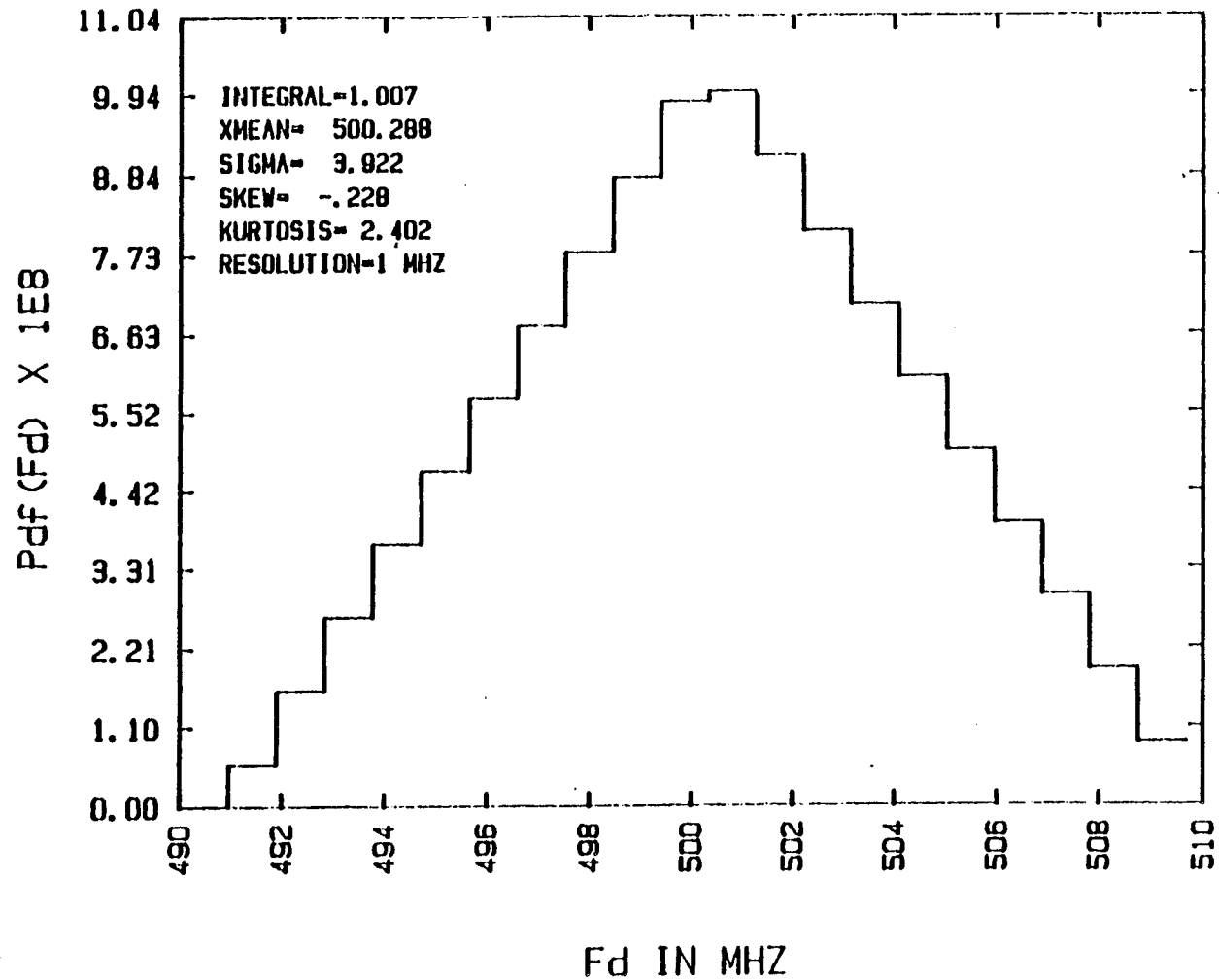


Figure 13

BRAGG-CELL RECEIVER PDF ANALYSIS

CONSTANT PDF FOR F1, DF1= 10.0 CONSTANT PDF FOR F2, DFF2= 9.00

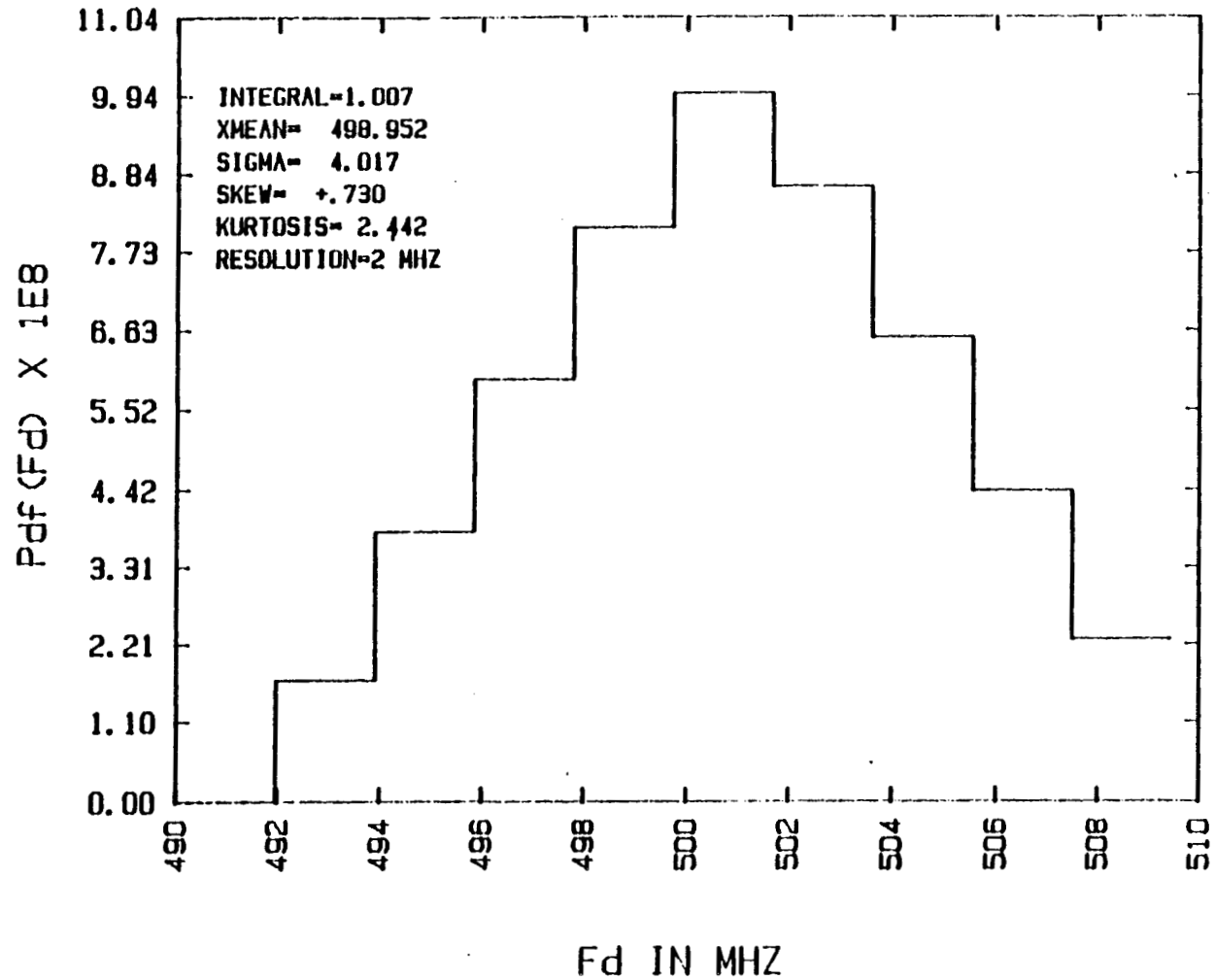


Figure 14
BRAGG-CELL RECEIVER PDF ANALYSIS
CONSTANT PDF FOR F1, DF1= 25.0 CONSTANT PDF FOR F2, DFF2= 5.00

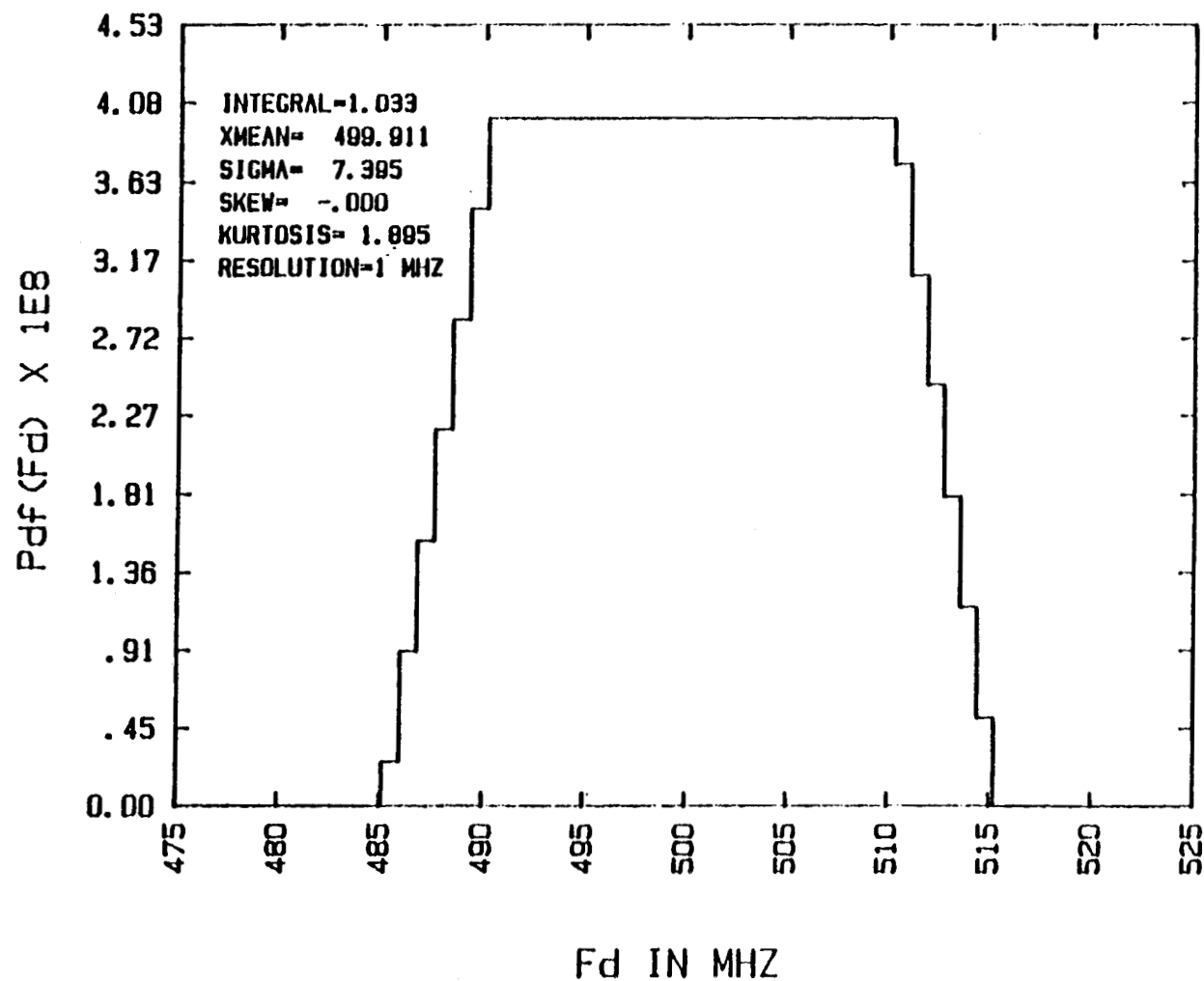


Figure 15

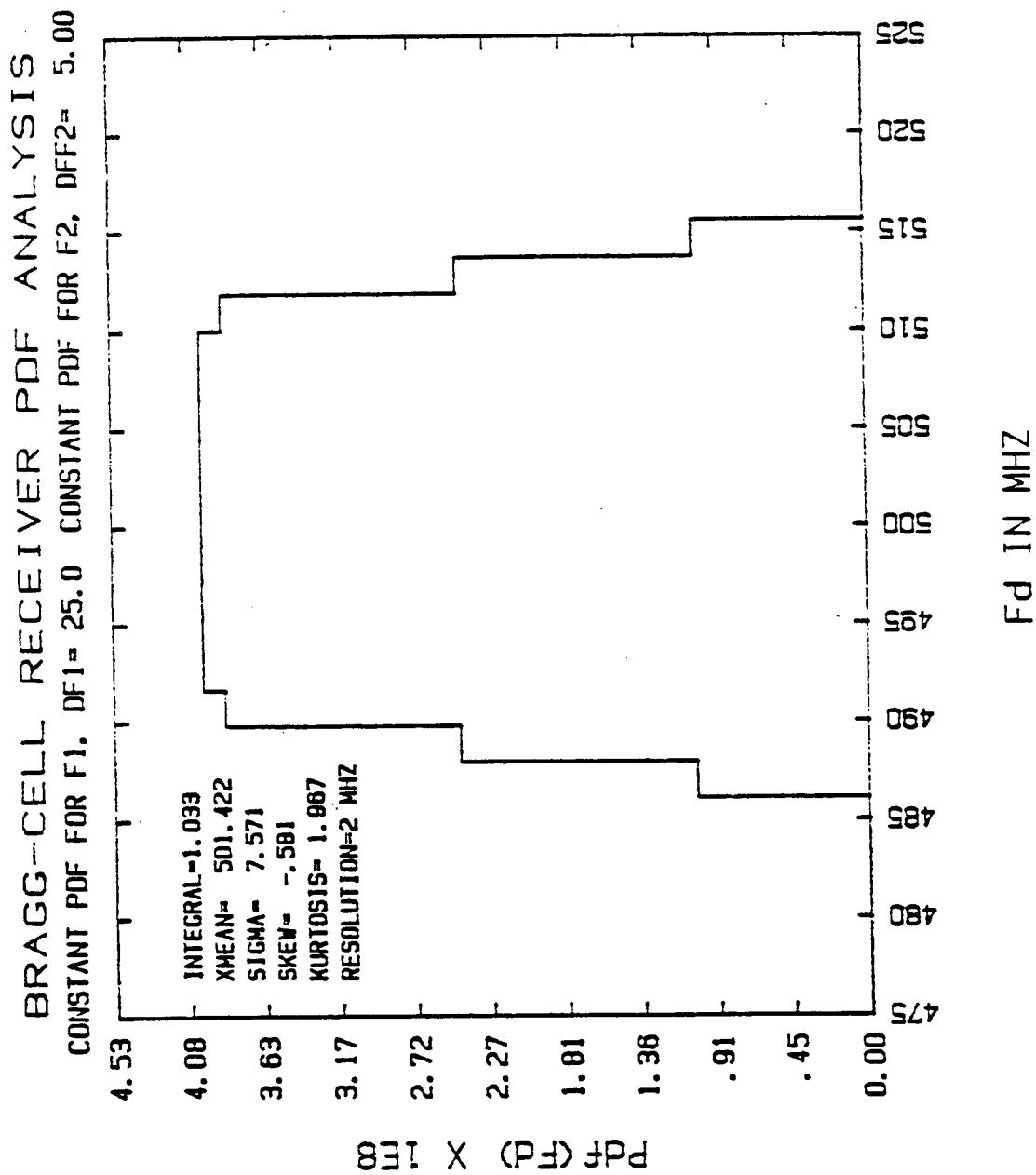


Figure 16

BRAGG-CELL RECEIVER PDF ANALYSIS
CONSTANT PDF FOR F1, DF1= 25.0 CONSTANT PDF FOR F2, DFF2= 5.00

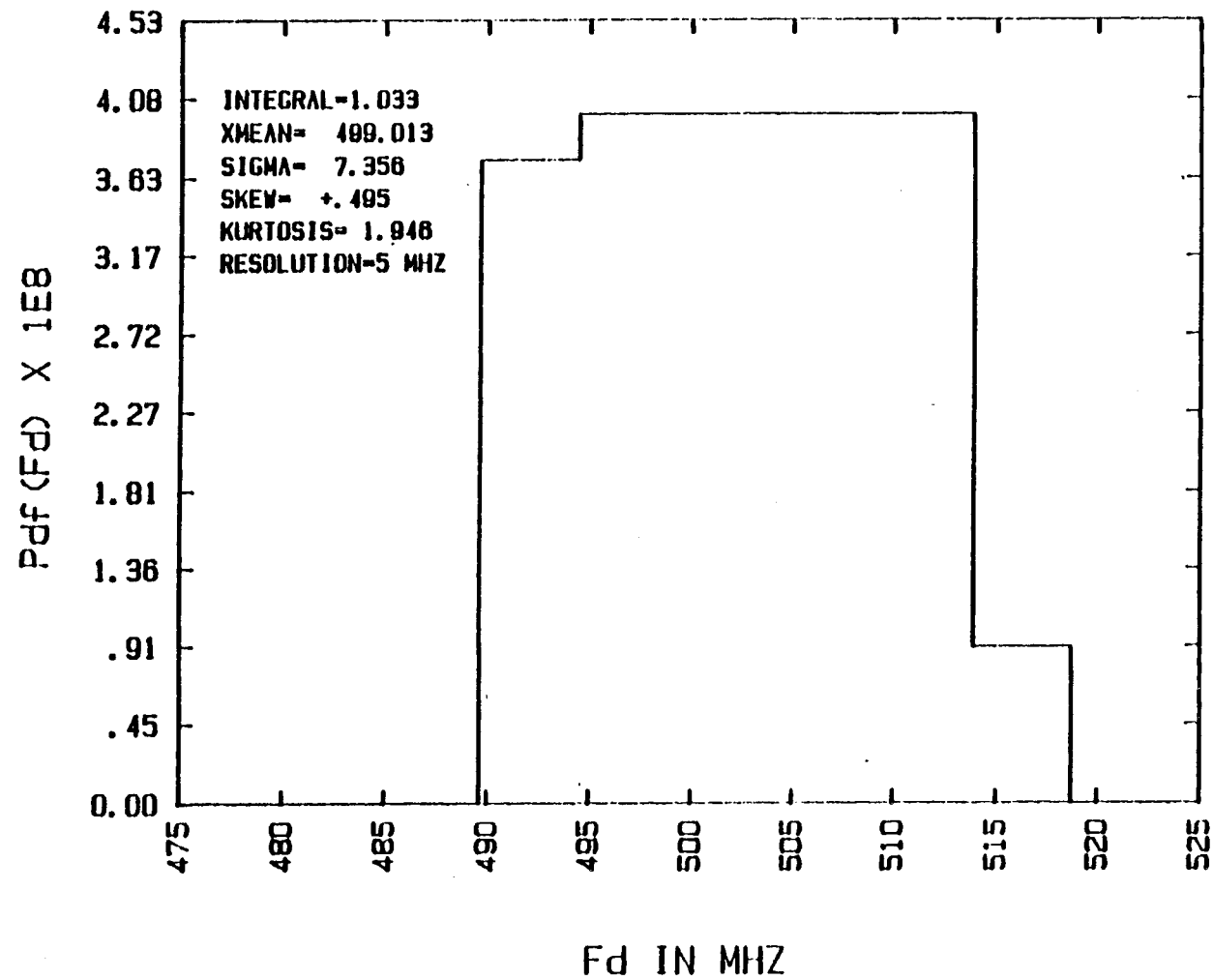


Figure 17

BRAGG-CELL RECEIVER PDF ANALYSIS
CONSTANT PDF FOR F1, DF1= 25.0 CONSTANT PDF FOR F2, DFF2= 15.00

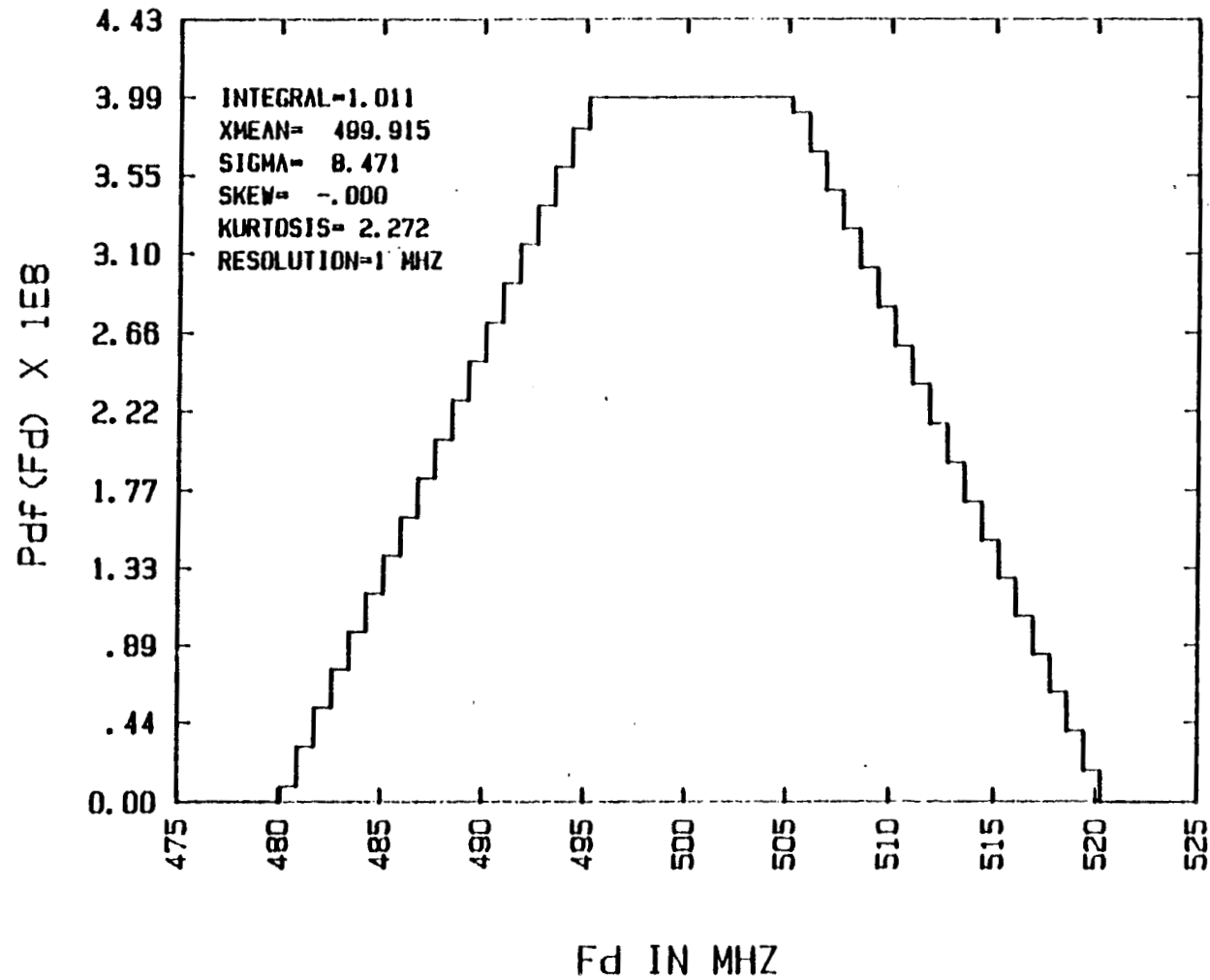


Figure 18

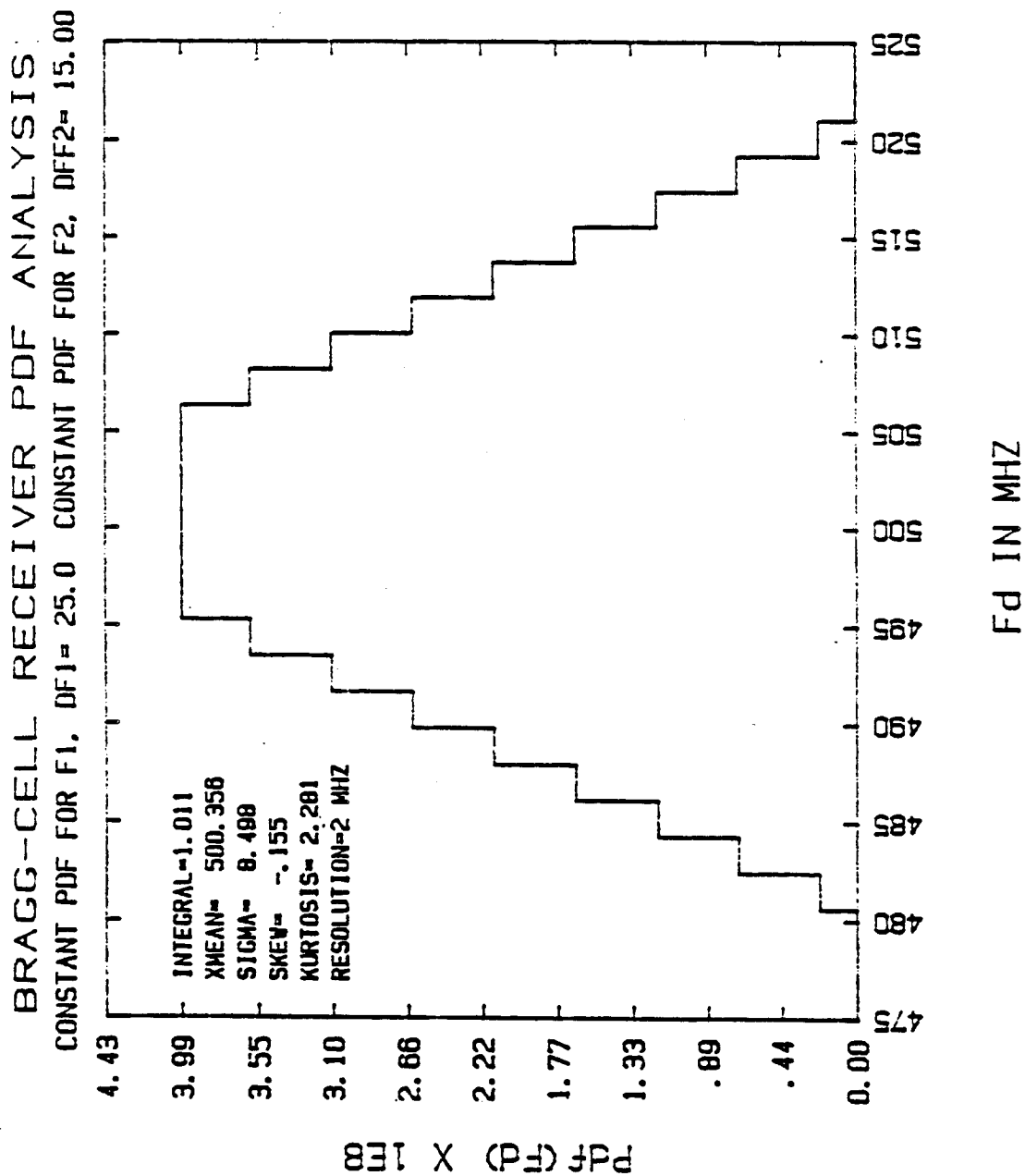


Figure 19

BRAGG-CELL RECEIVER PDF ANALYSIS
CONSTANT PDF FOR F1, DF1= 25.0 CONSTANT PDF FOR F2, DFF2= 15.00

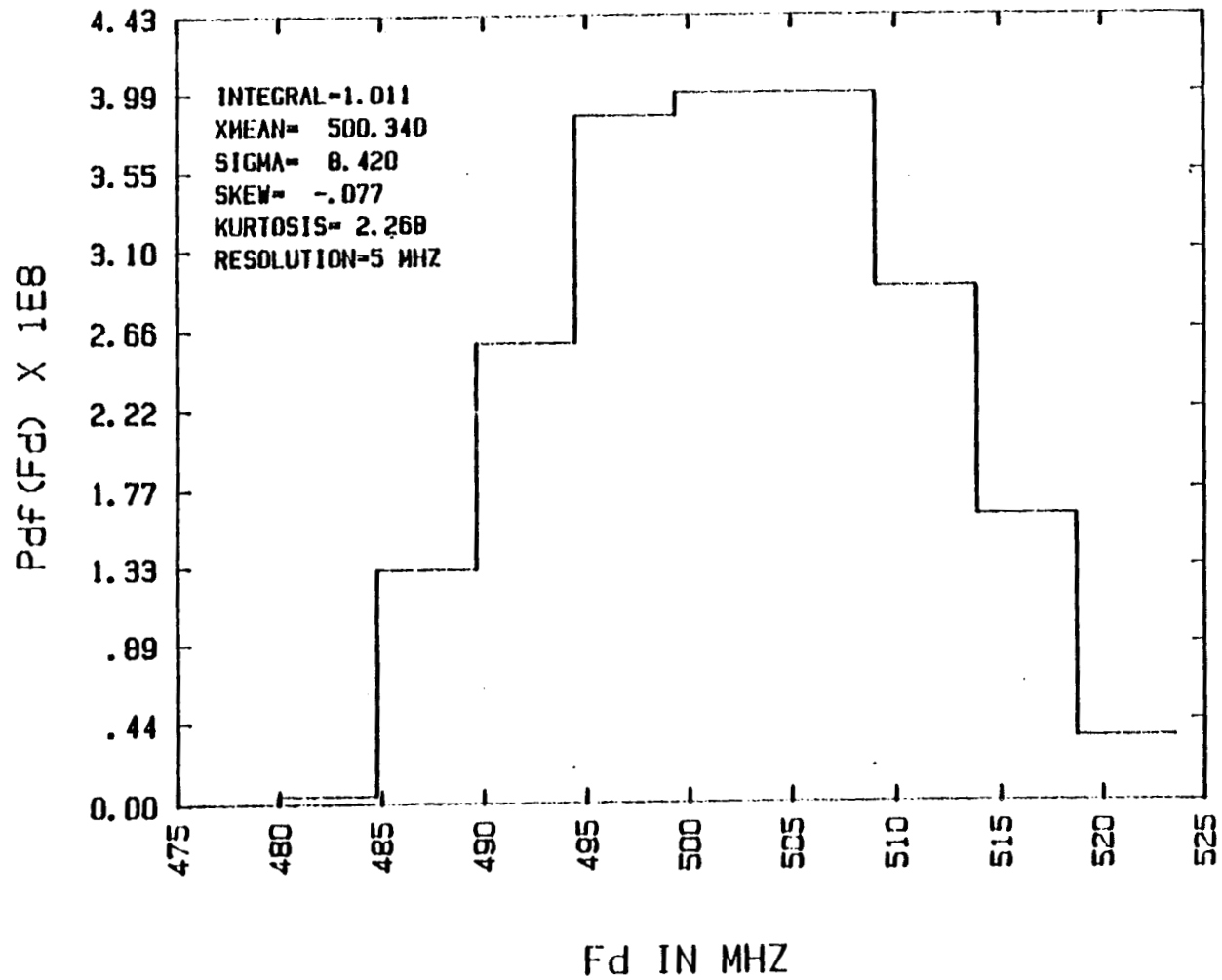


Figure 20

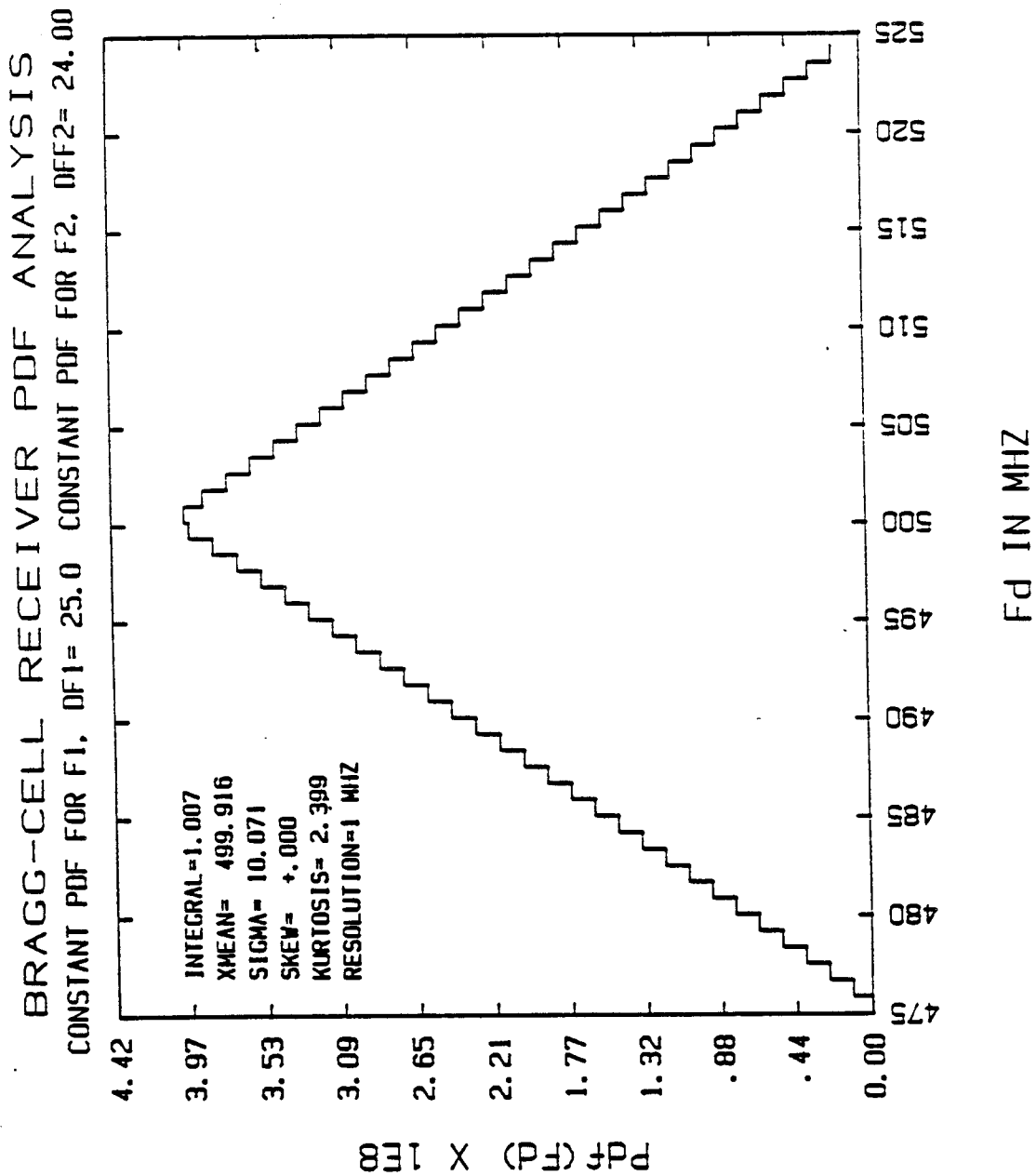


Figure 21

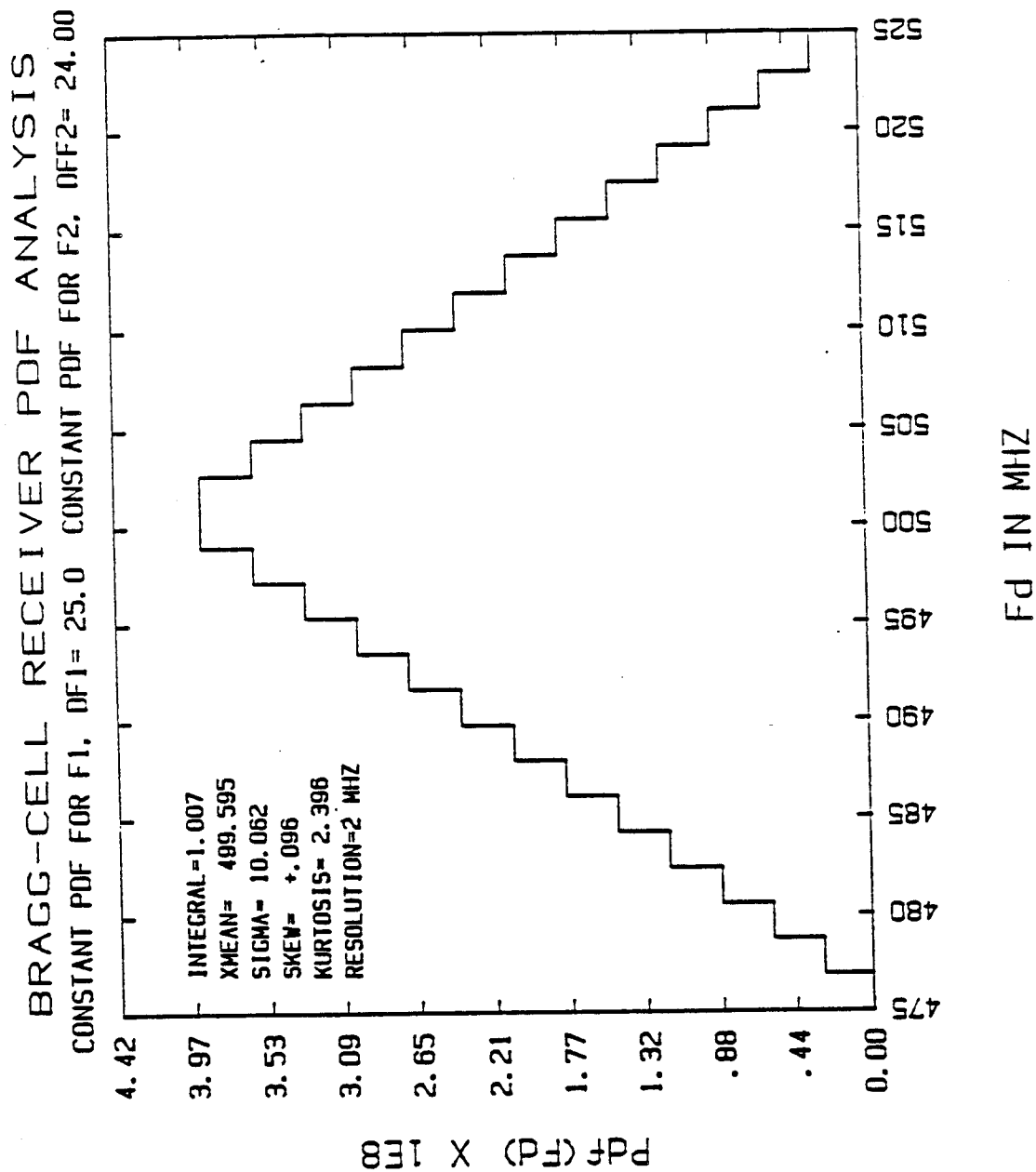
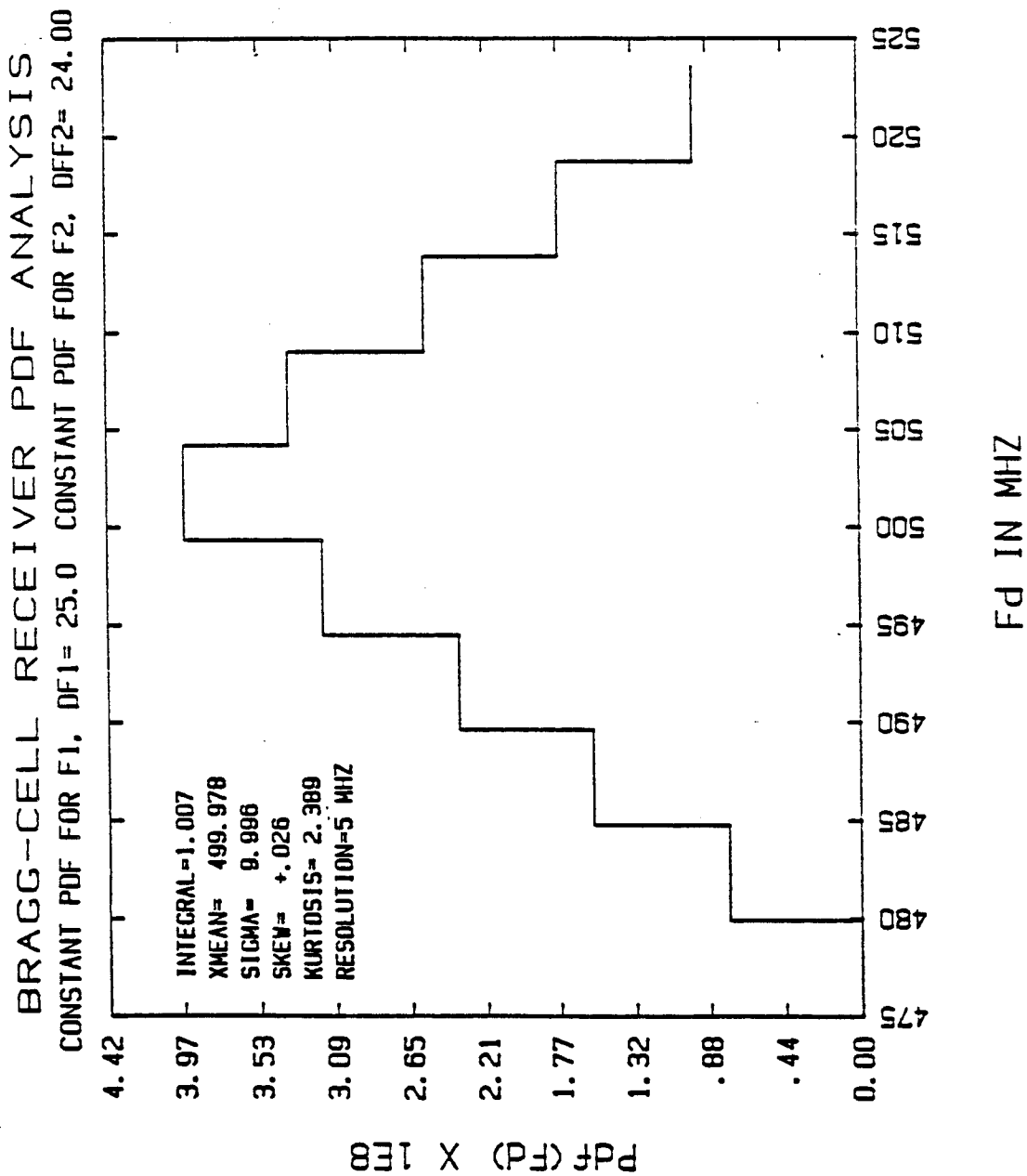


Figure 22



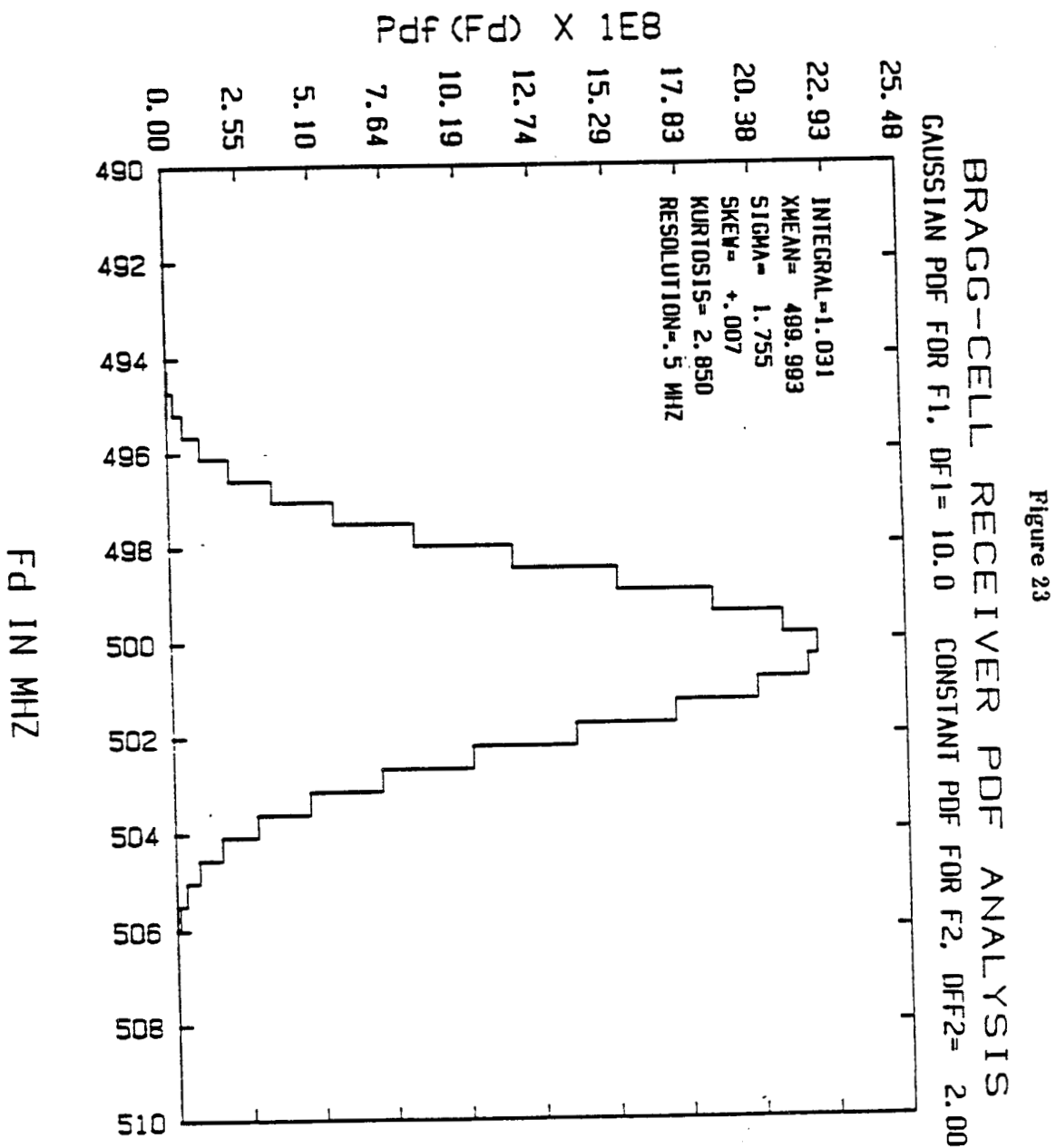


Figure 24

BRAGG-CELL RECEIVER PDF ANALYSIS
GAUSSIAN PDF FOR F1, DF1= 10.0 CONSTANT PDF FOR F2, DFF2= 2.00

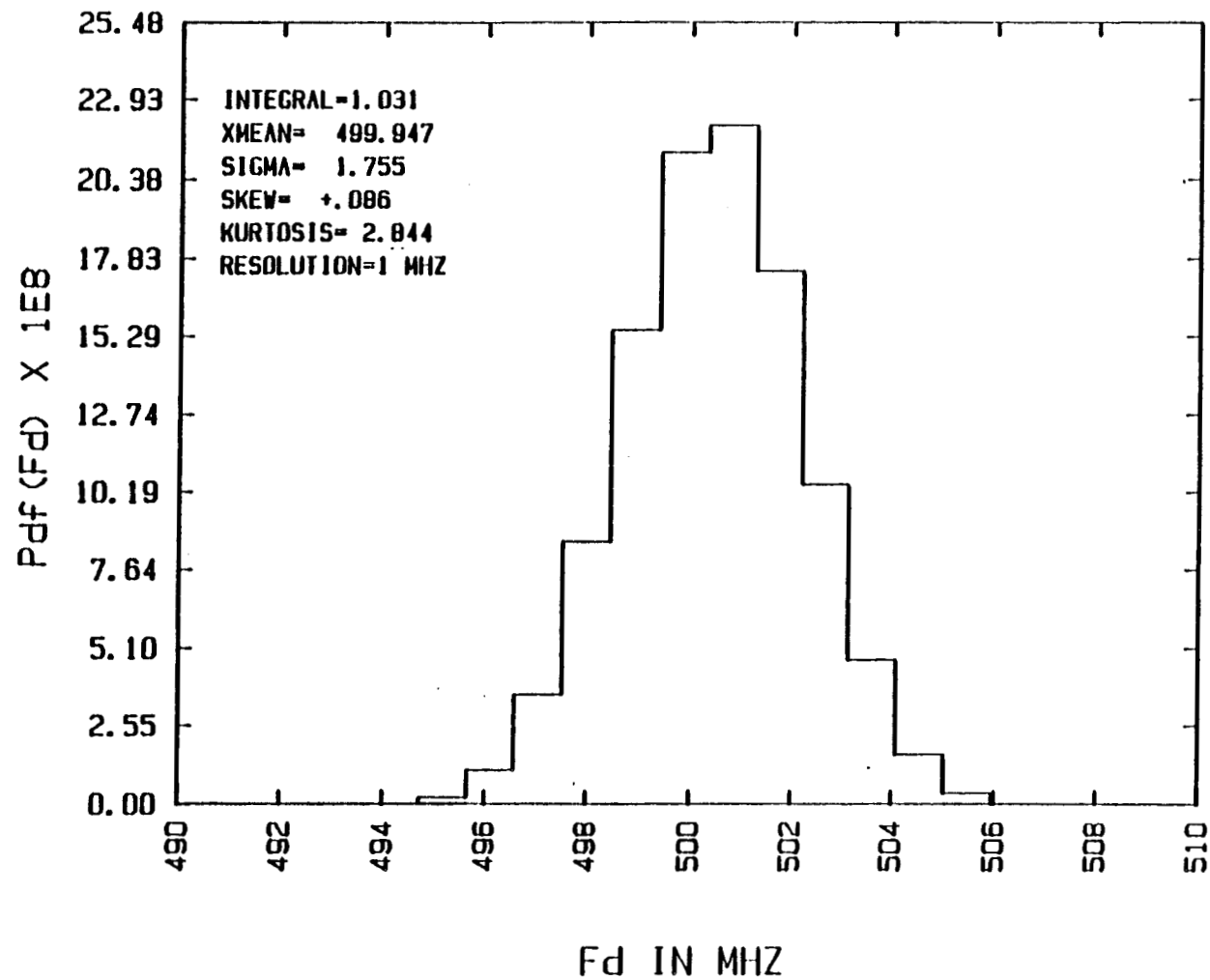


Figure 25

BRAGG-CELL RECEIVER PDF ANALYSIS

GAUSSIAN PDF FOR F1, DF1= 10.0 CONSTANT PDF FOR F2, DFF2= 2.00

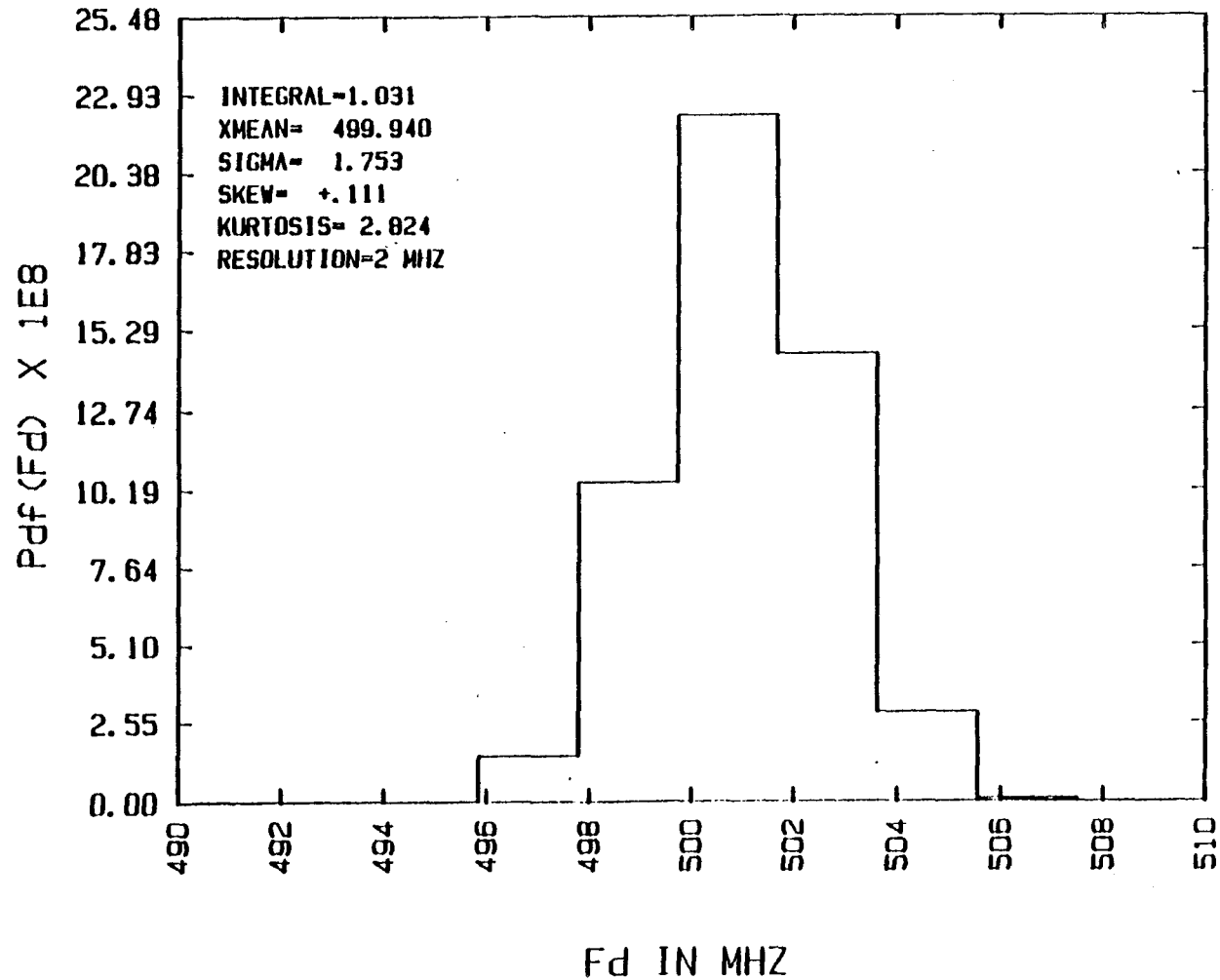


Figure 26

BRAGG-CELL RECEIVER PDF ANALYSIS
GAUSSIAN PDF FOR F1, DF1= 10.0 CONSTANT PDF FOR F2, DFF2= 5.00

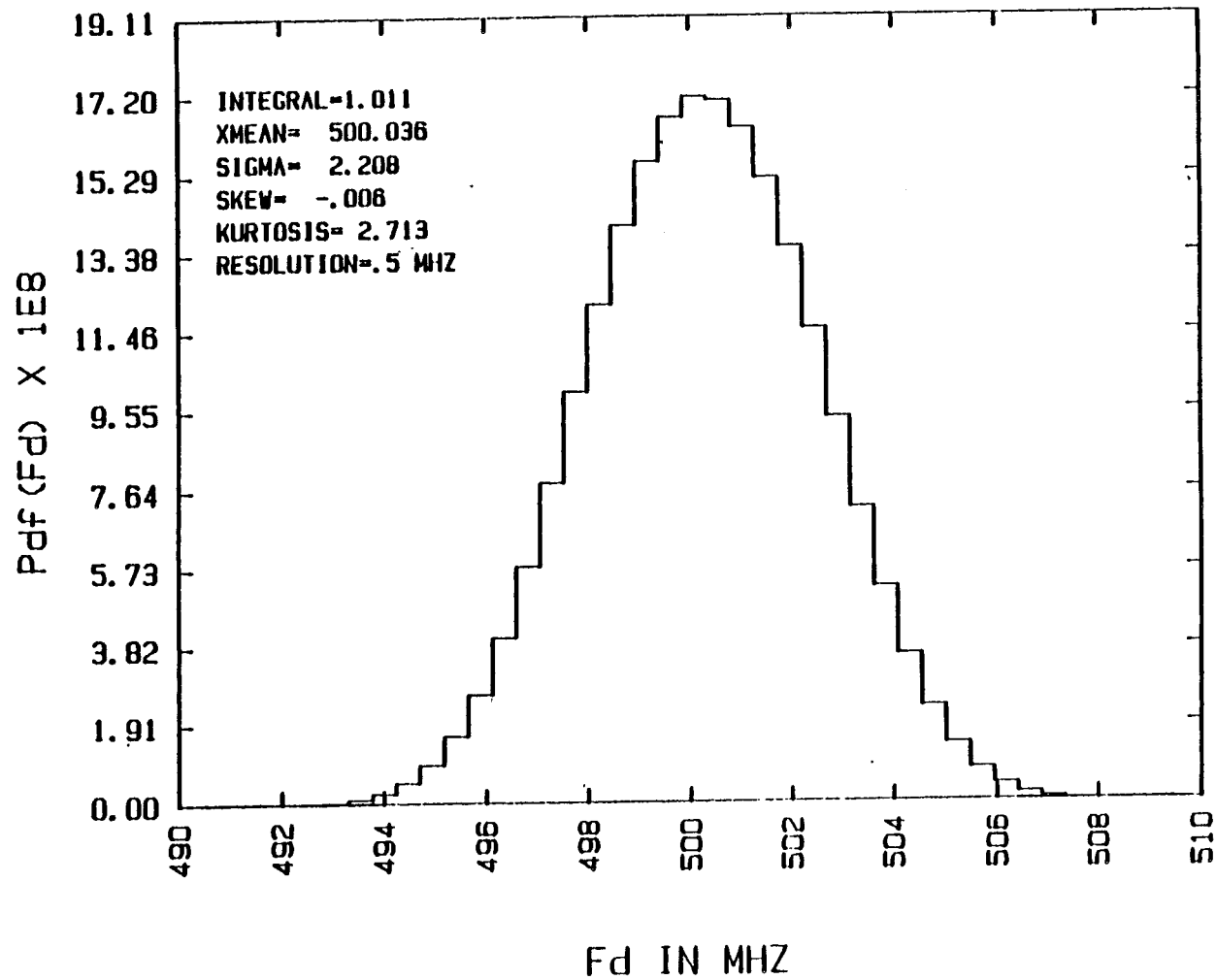


Figure 27

BRAGG-CELL RECEIVER PDF ANALYSIS

GAUSSIAN PDF FOR F1, DF1= 10.0 CONSTANT PDF FOR F2, DFF2= 5.00

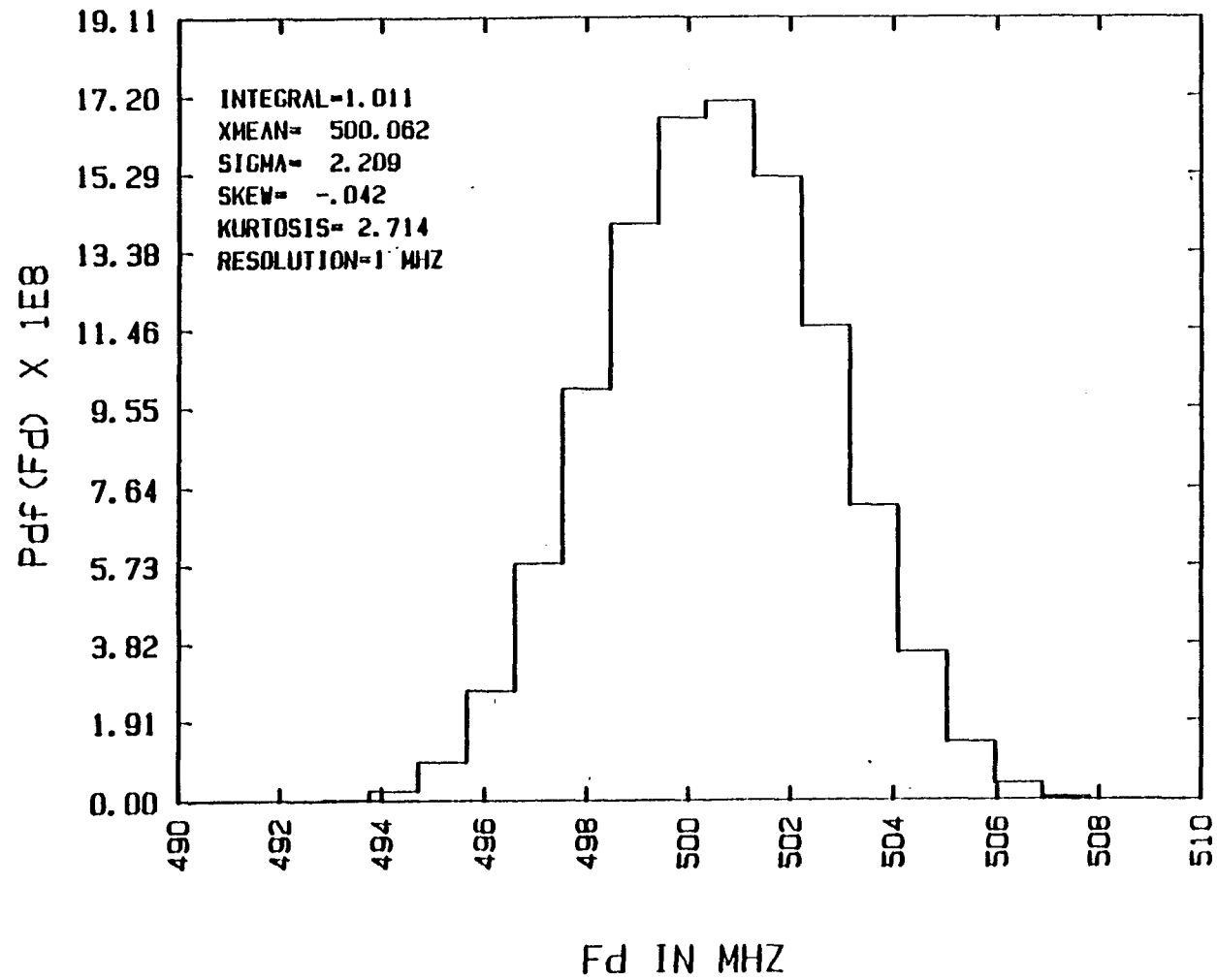


Figure 28

BRAGG-CELL RECEIVER PDF ANALYSIS
GAUSSIAN PDF FOR F1, DF1= 10.0 CONSTANT PDF FOR F2, DFF2= 5.00

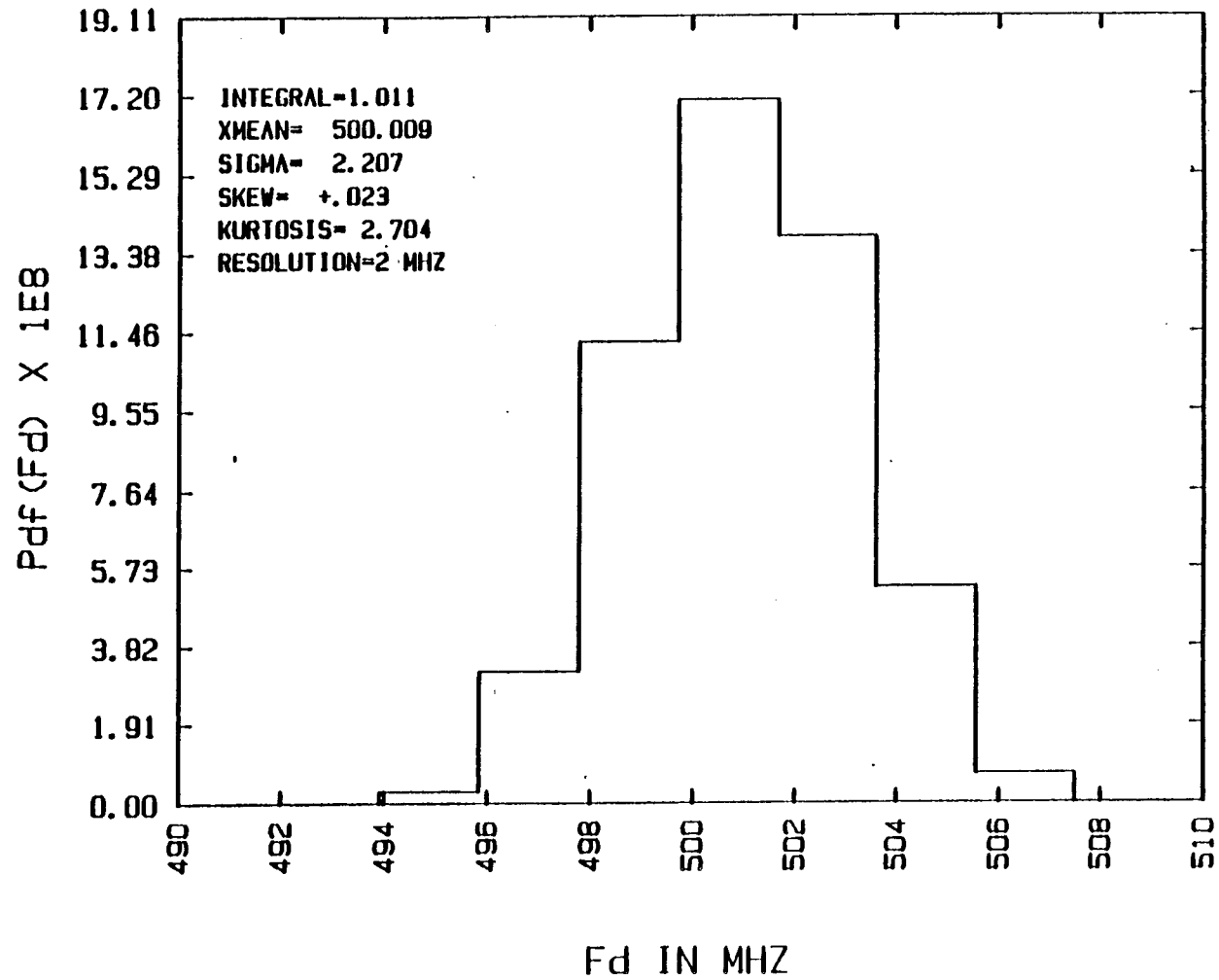


Figure 29

BRAGG-CELL RECEIVER PDF ANALYSIS
GAUSSIAN PDF FOR F1, DF1= 25.0 CONSTANT PDF FOR F2, DFF2= 15.00

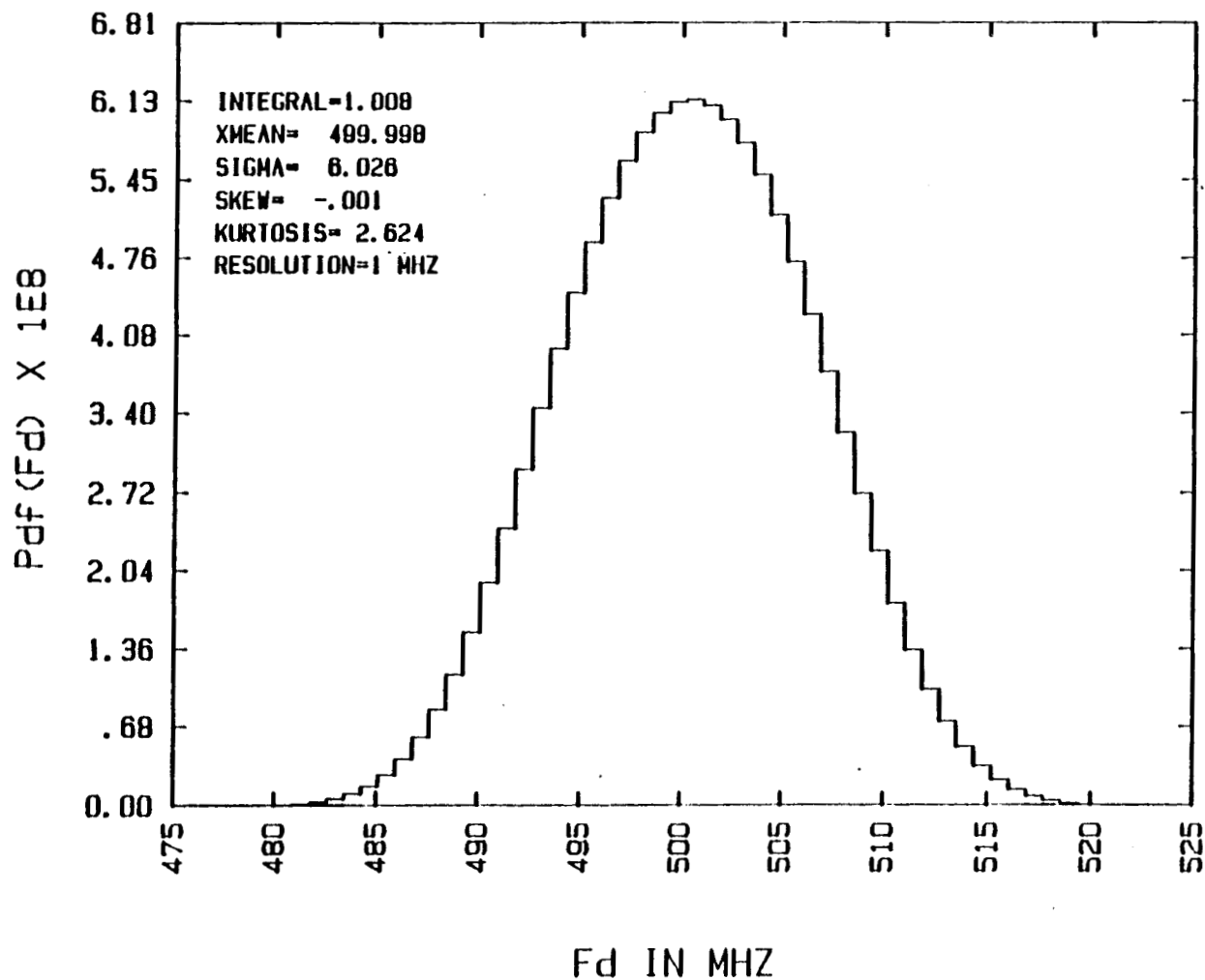


Figure 30
BRAGG-CELL RECEIVER PDF ANALYSIS
GAUSSIAN PDF FOR F1, DF1= 25.0 CONSTANT PDF FOR F2, DFF2= 15.00

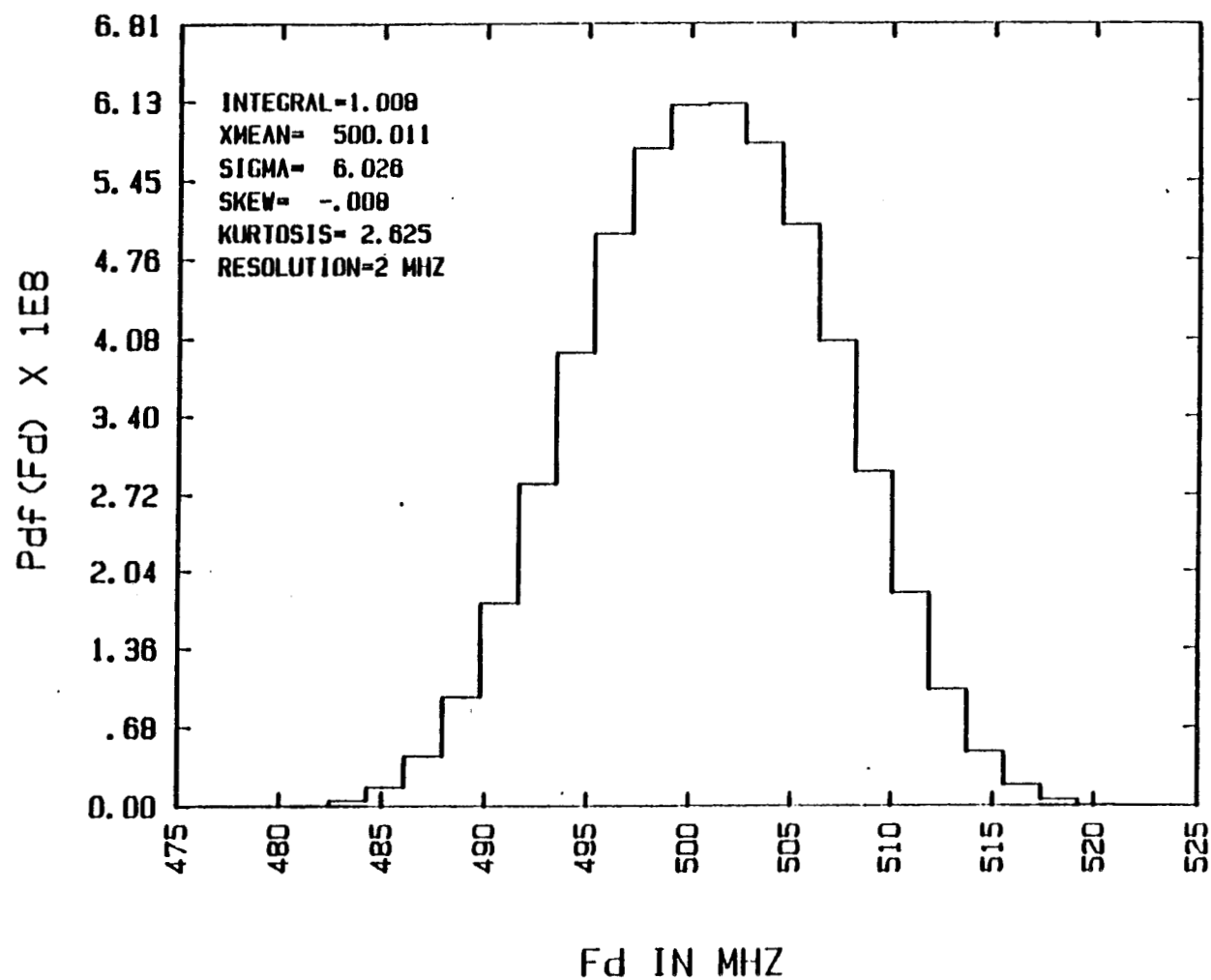


Figure 31

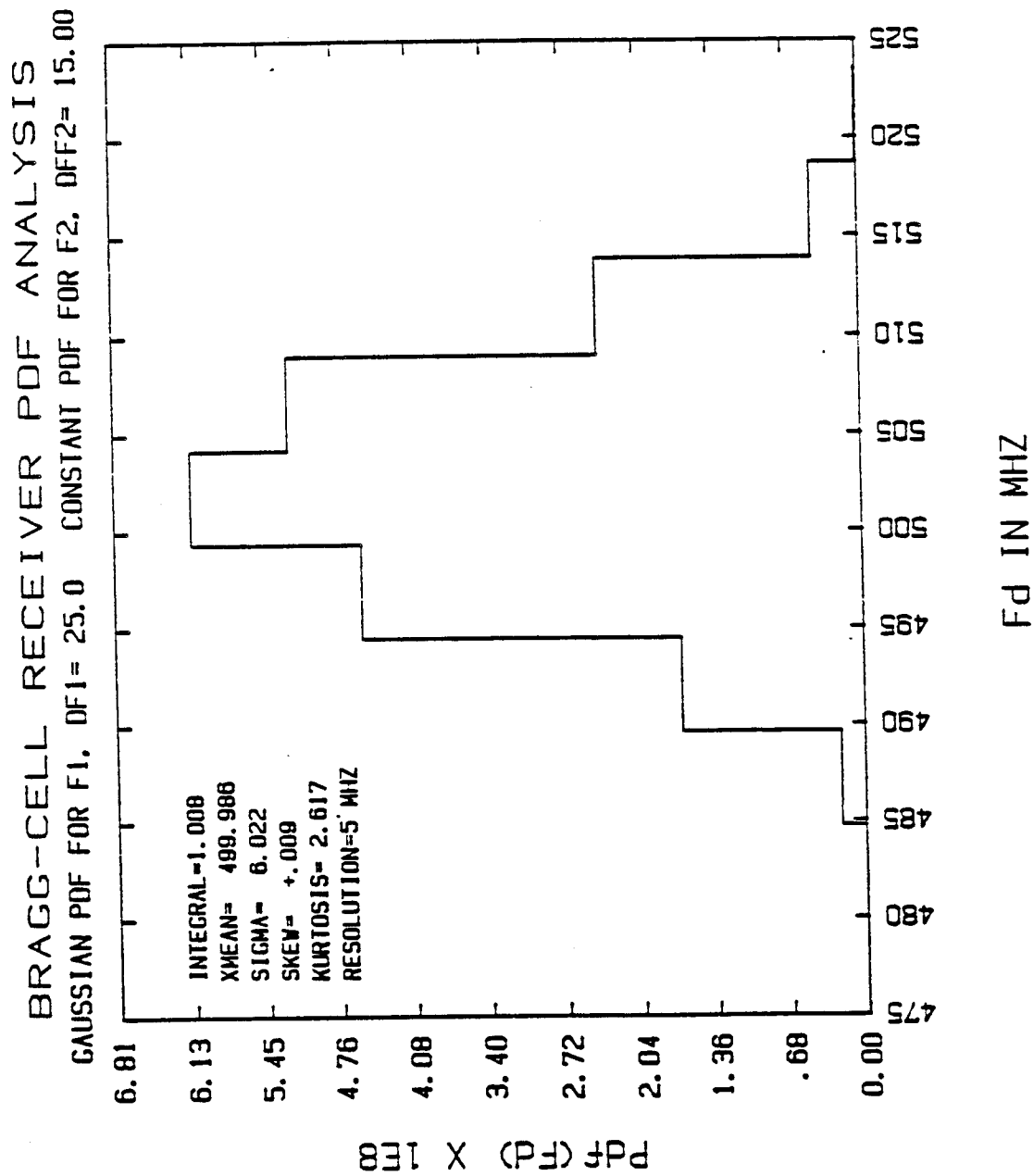


Figure 32

BRAGG-CELL RECEIVER PDF ANALYSIS
GAUSSIAN PDF FOR F1, DF1= 25.0 CONSTANT PDF FOR F2, DFF2= 24.00

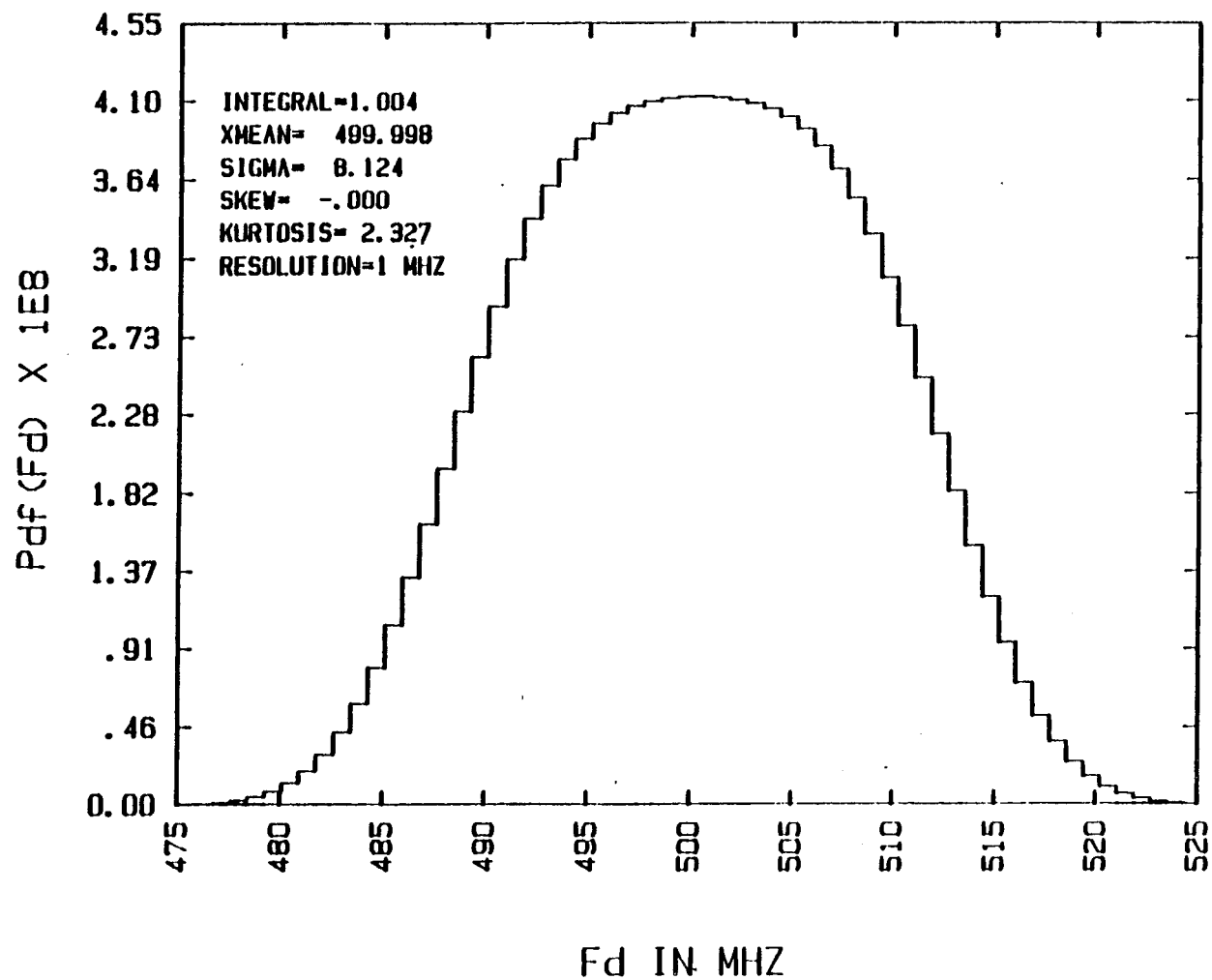


Figure 33

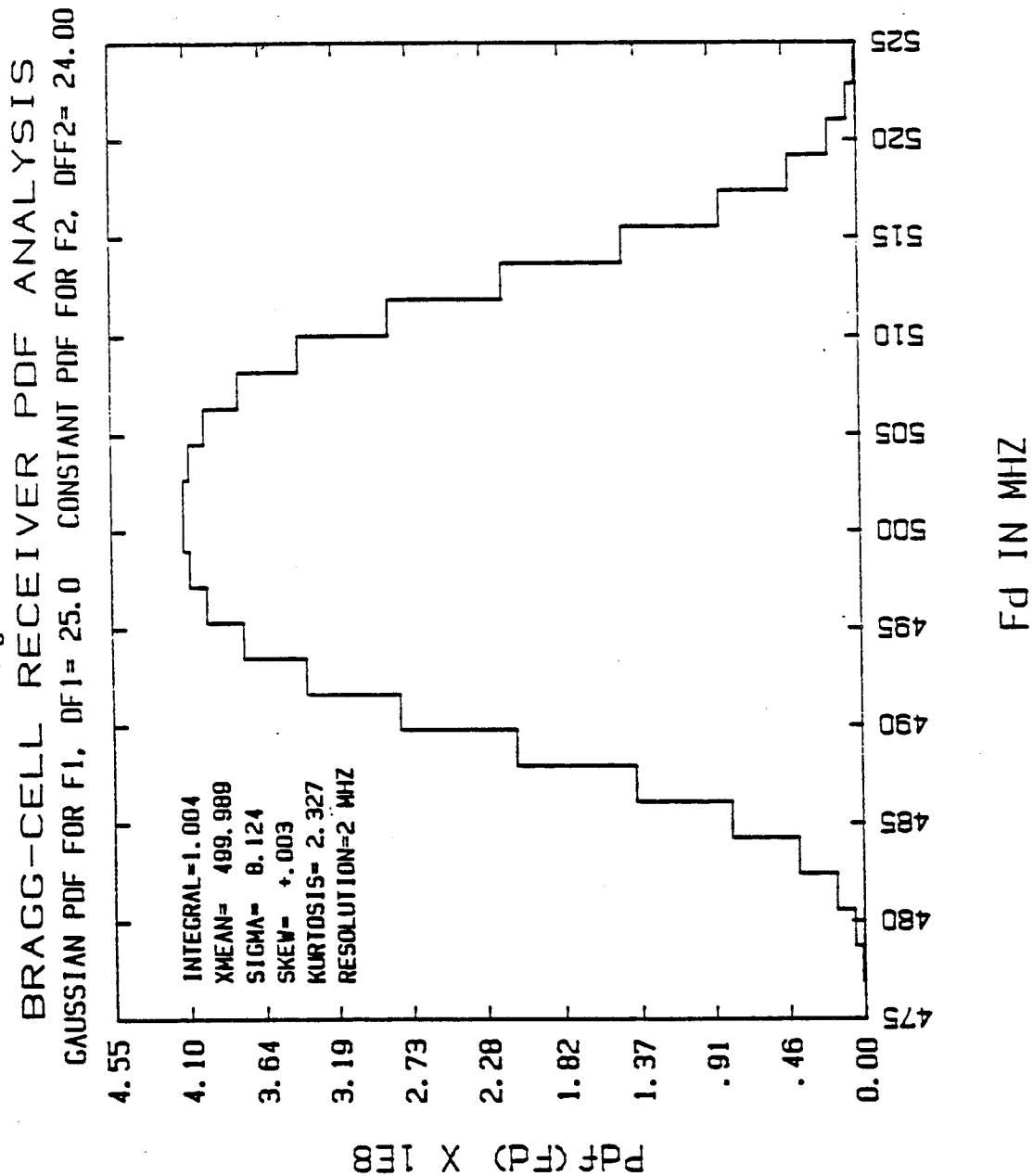


Figure 34

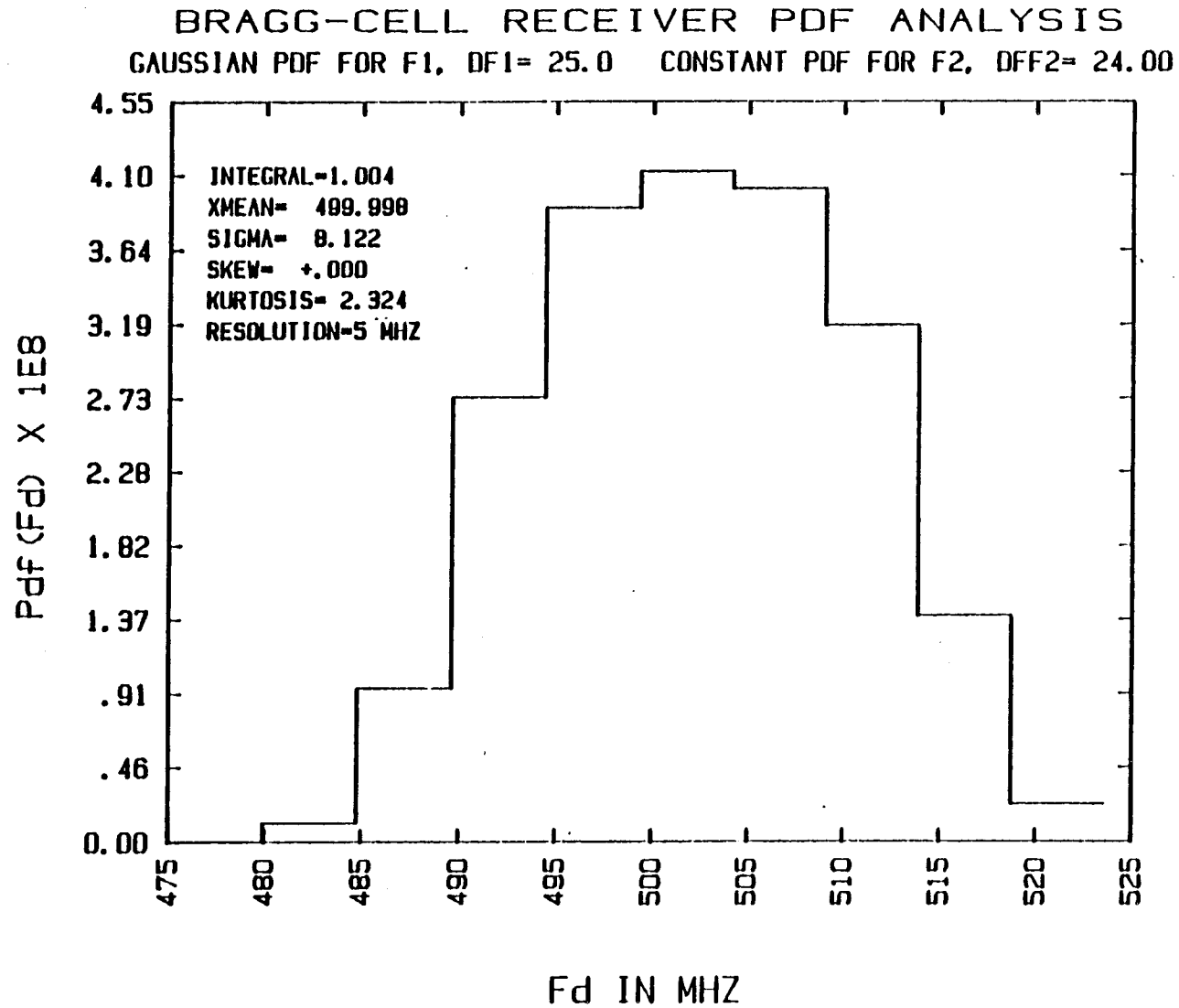


Figure 35

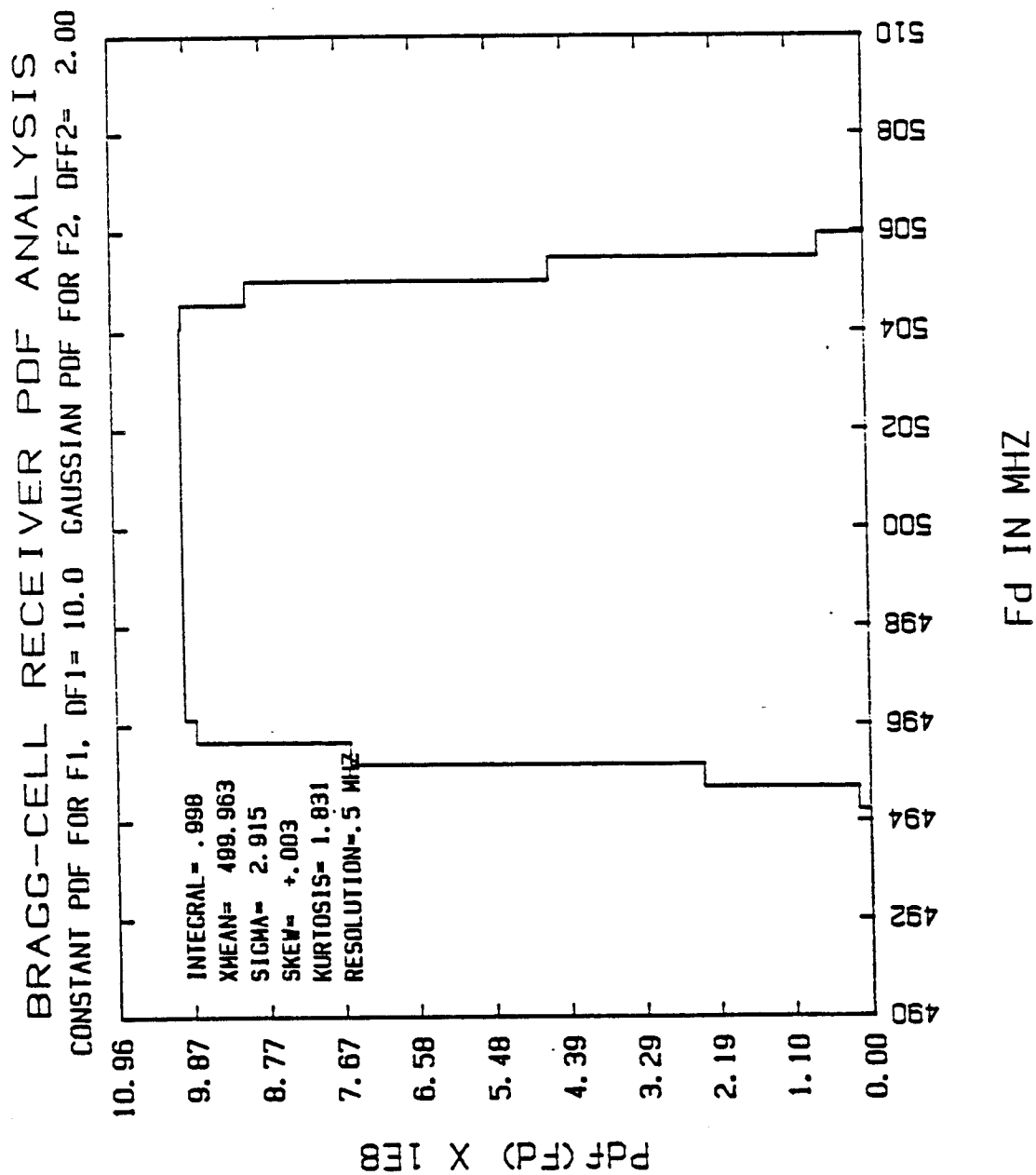


Figure 36

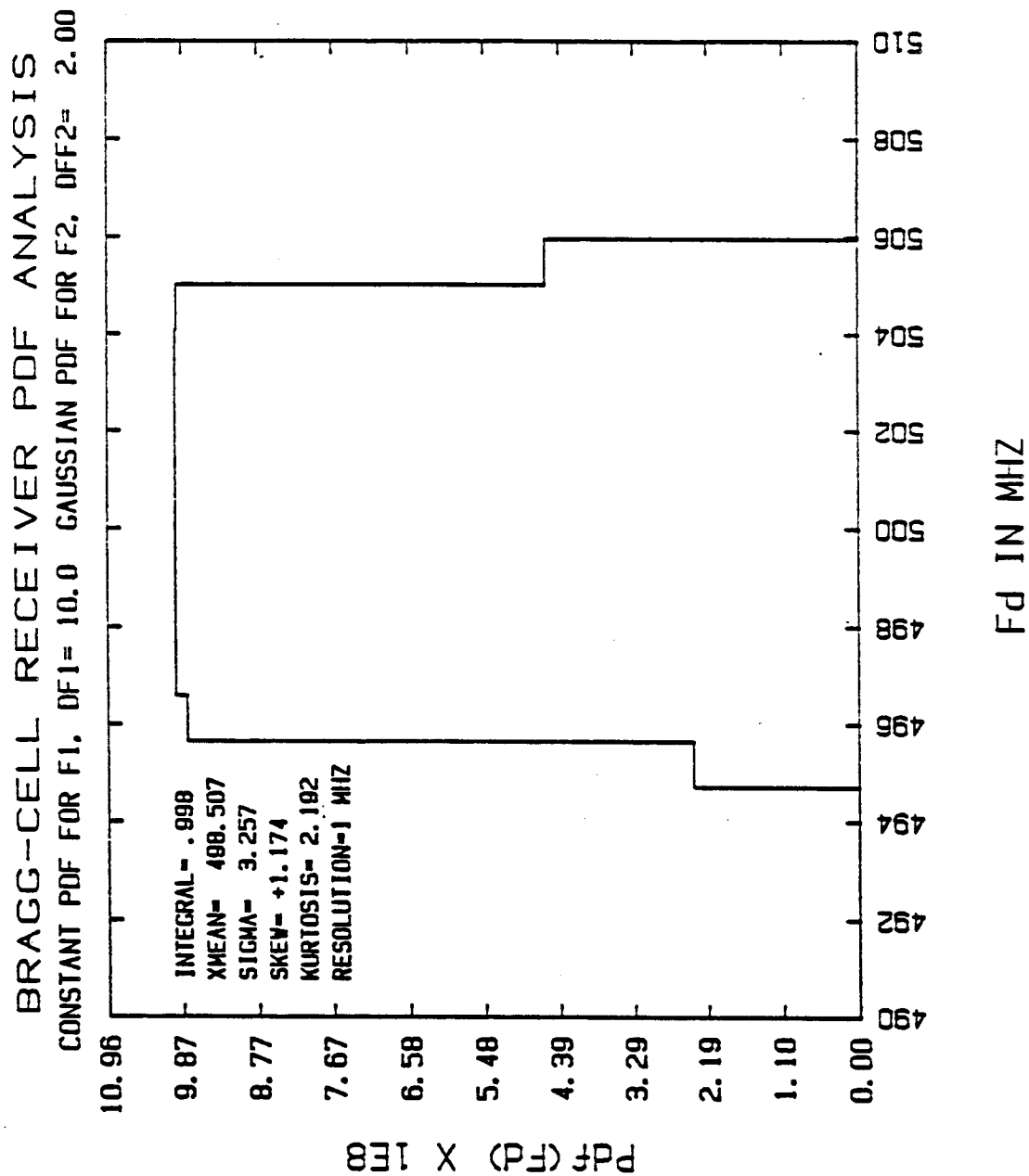


Figure 37

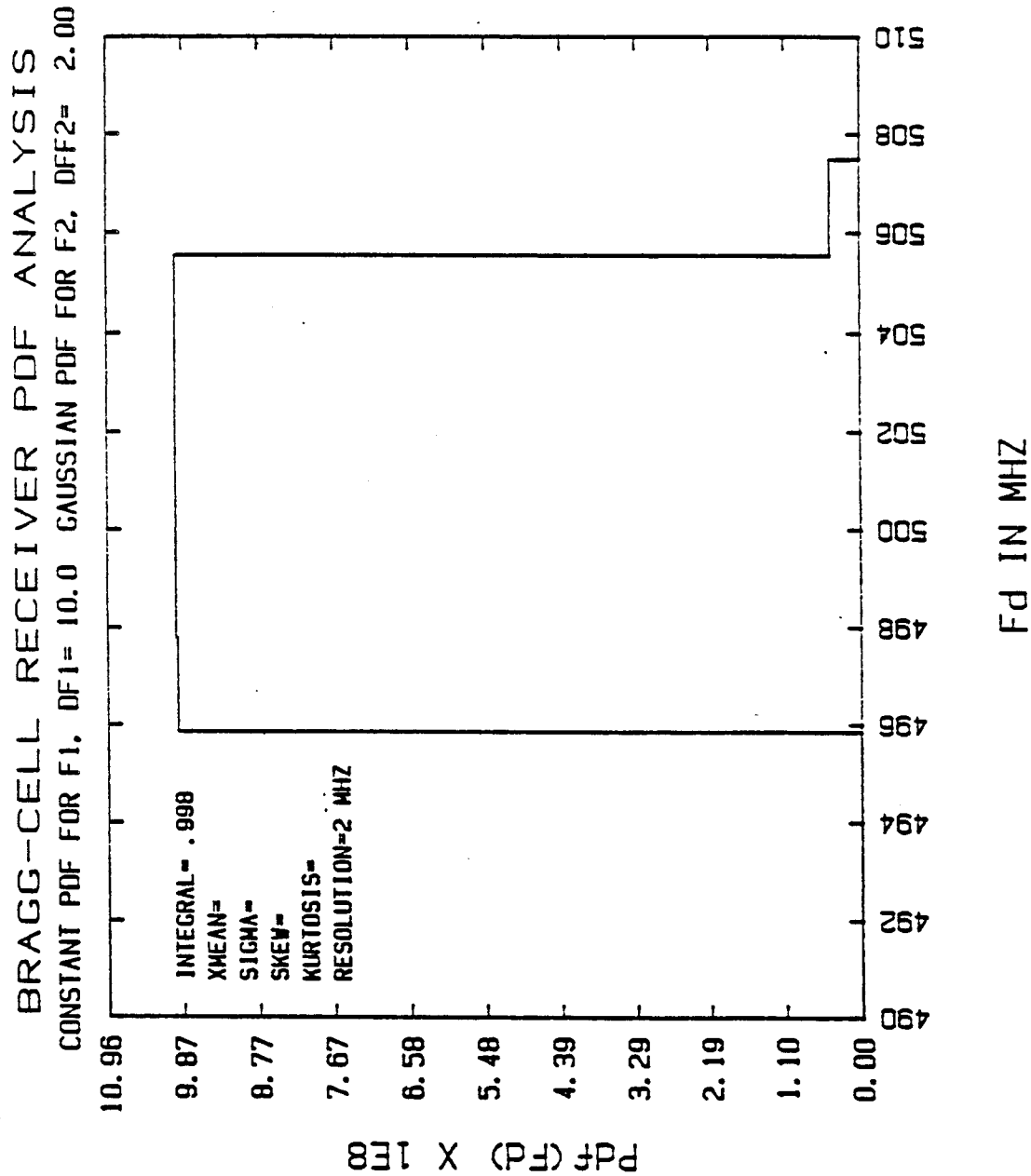


Figure 38

BRAGG-CELL RECEIVER PDF ANALYSIS
CONSTANT PDF FOR F1, DF1= 10.0 GAUSSIAN PDF FOR F2, DFF2= 5.00

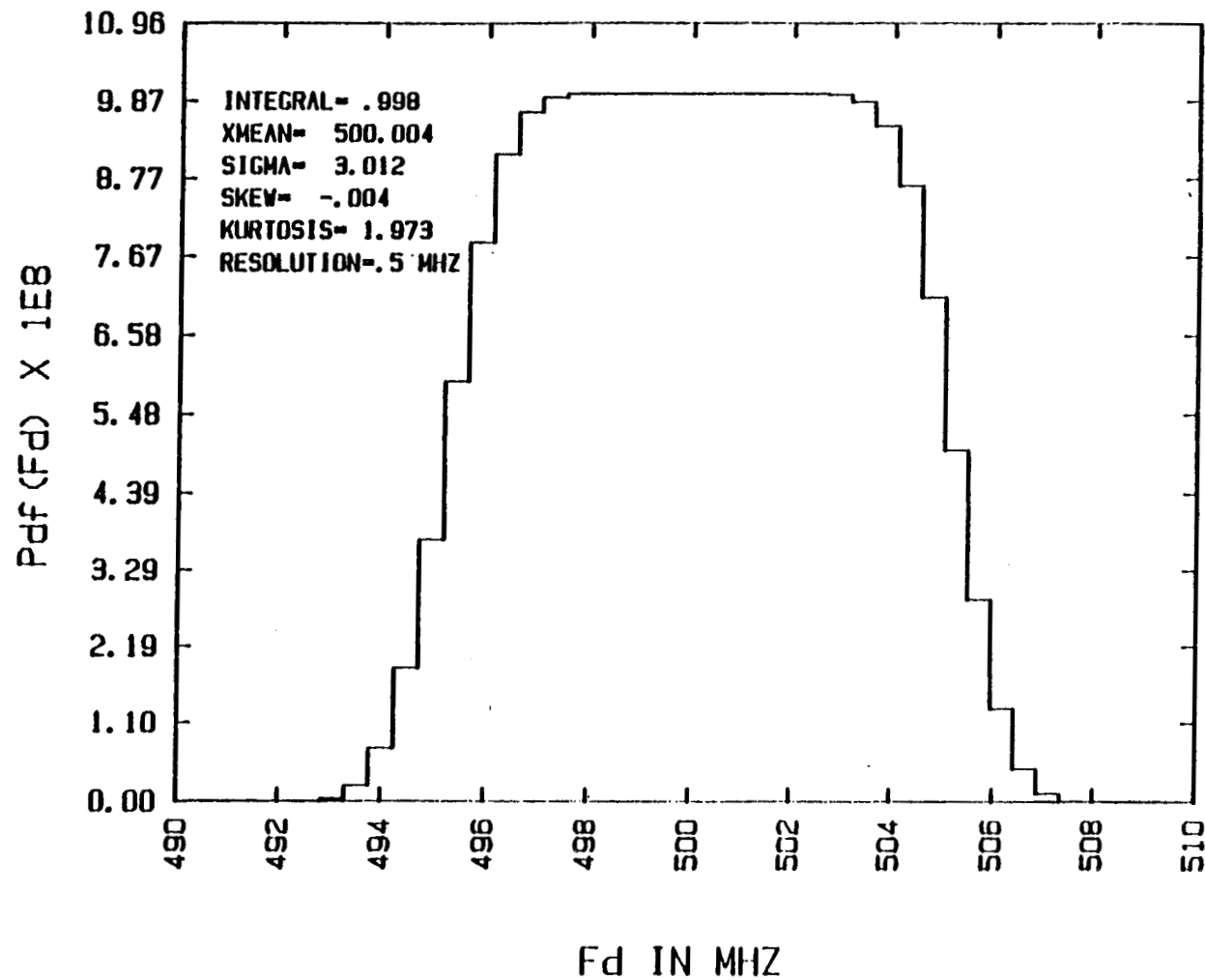


Figure 39

BRAGG-CELL RECEIVER PDF ANALYSIS
CONSTANT PDF FOR F1, DF1= 10.0 GAUSSIAN PDF FOR F2, DFF2= 5.00

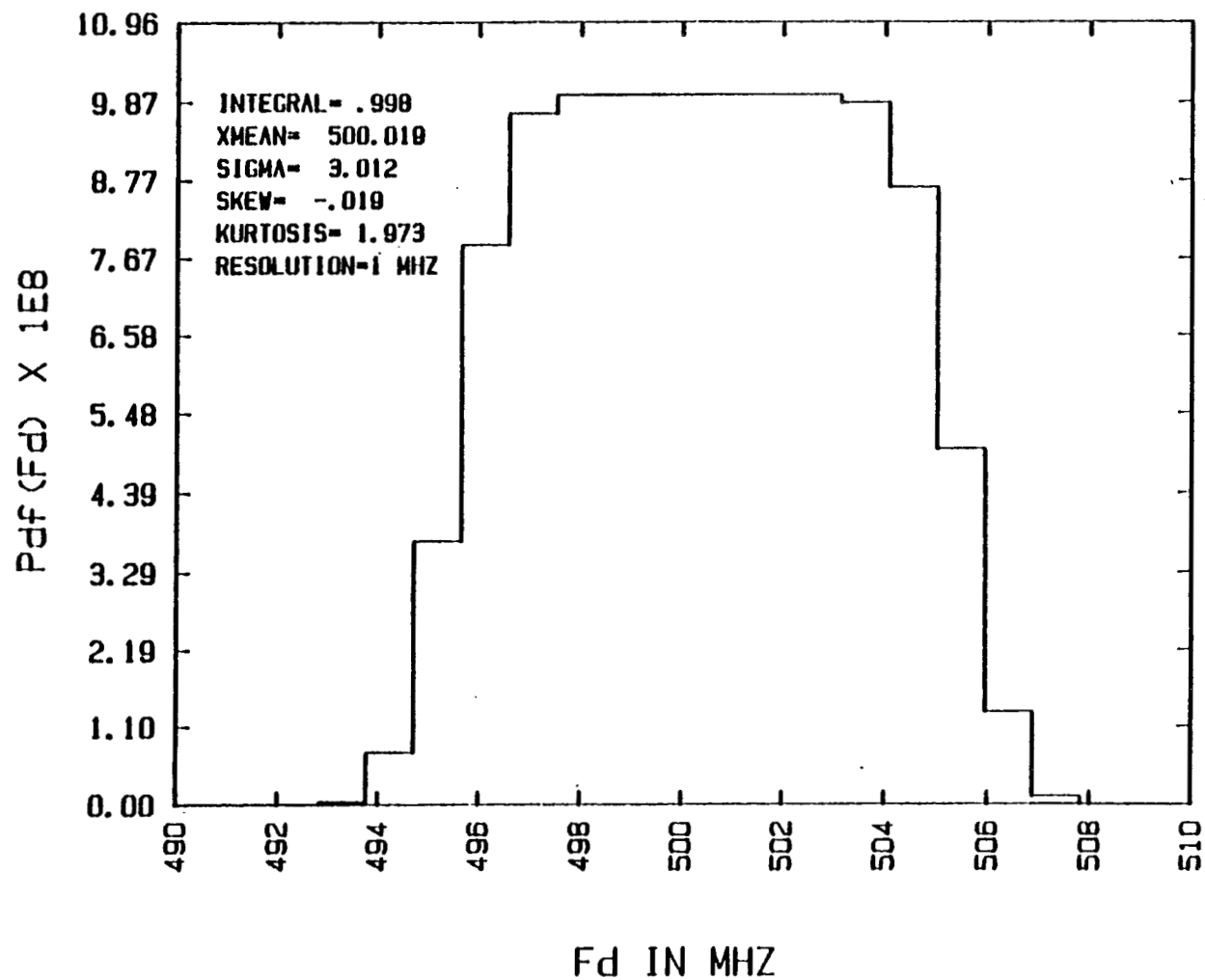


Figure 40
BRAGG-CELL RECEIVER PDF ANALYSIS
CONSTANT PDF FOR F1, DF1= 10.0 GAUSSIAN PDF FOR F2, DFF2= 5.00

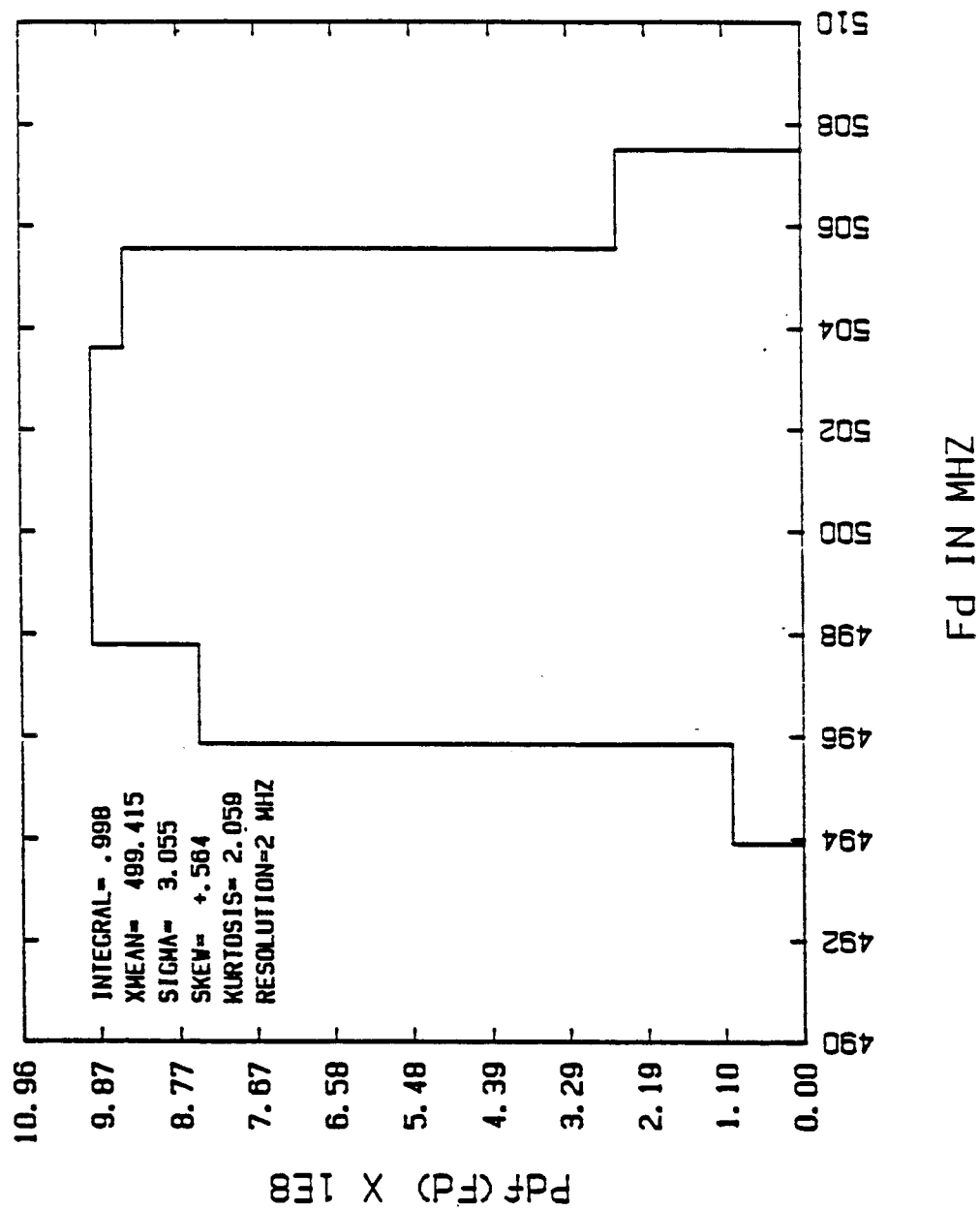


Figure 41

BRAGG-CELL RECEIVER PDF ANALYSIS
CONSTANT PDF FOR F1, DF1= 10.0 GAUSSIAN PDF FOR F2, DFF2= 9.00

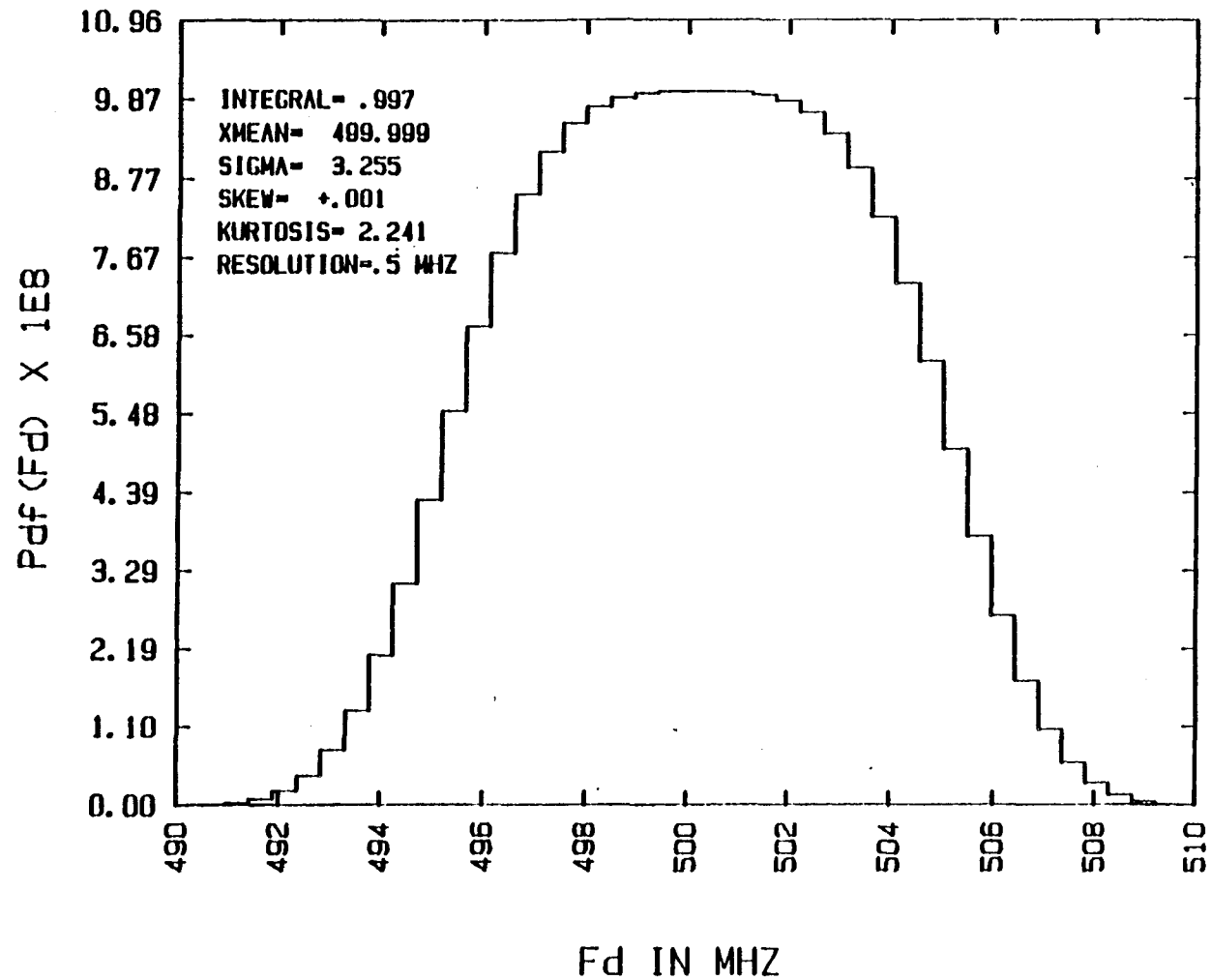


Figure 42

BRAGG-CELL RECEIVER PDF ANALYSIS
CONSTANT PDF FOR F1, DF1= 10.0 GAUSSIAN PDF FOR F2, DFF2= 9.00

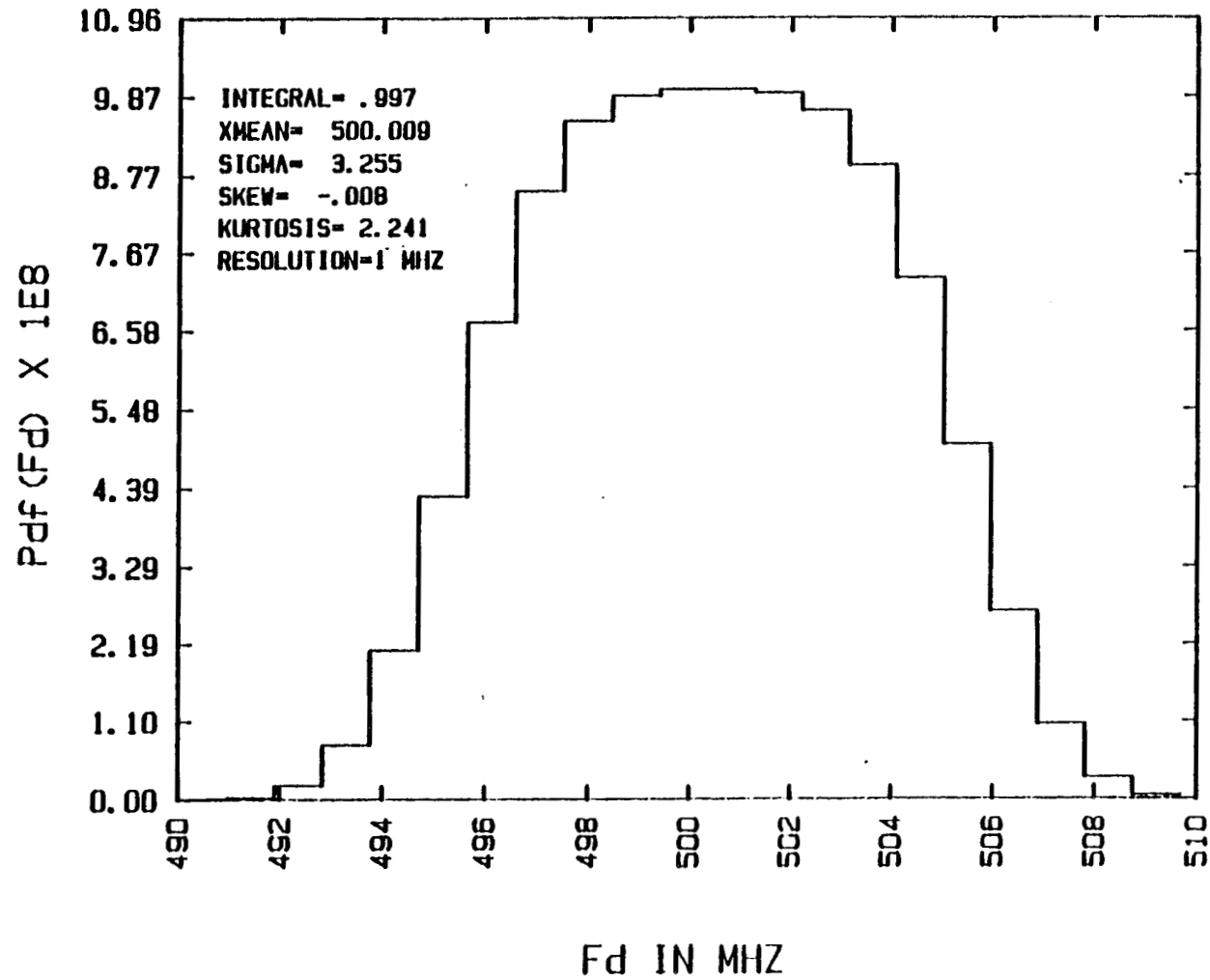


Figure 43

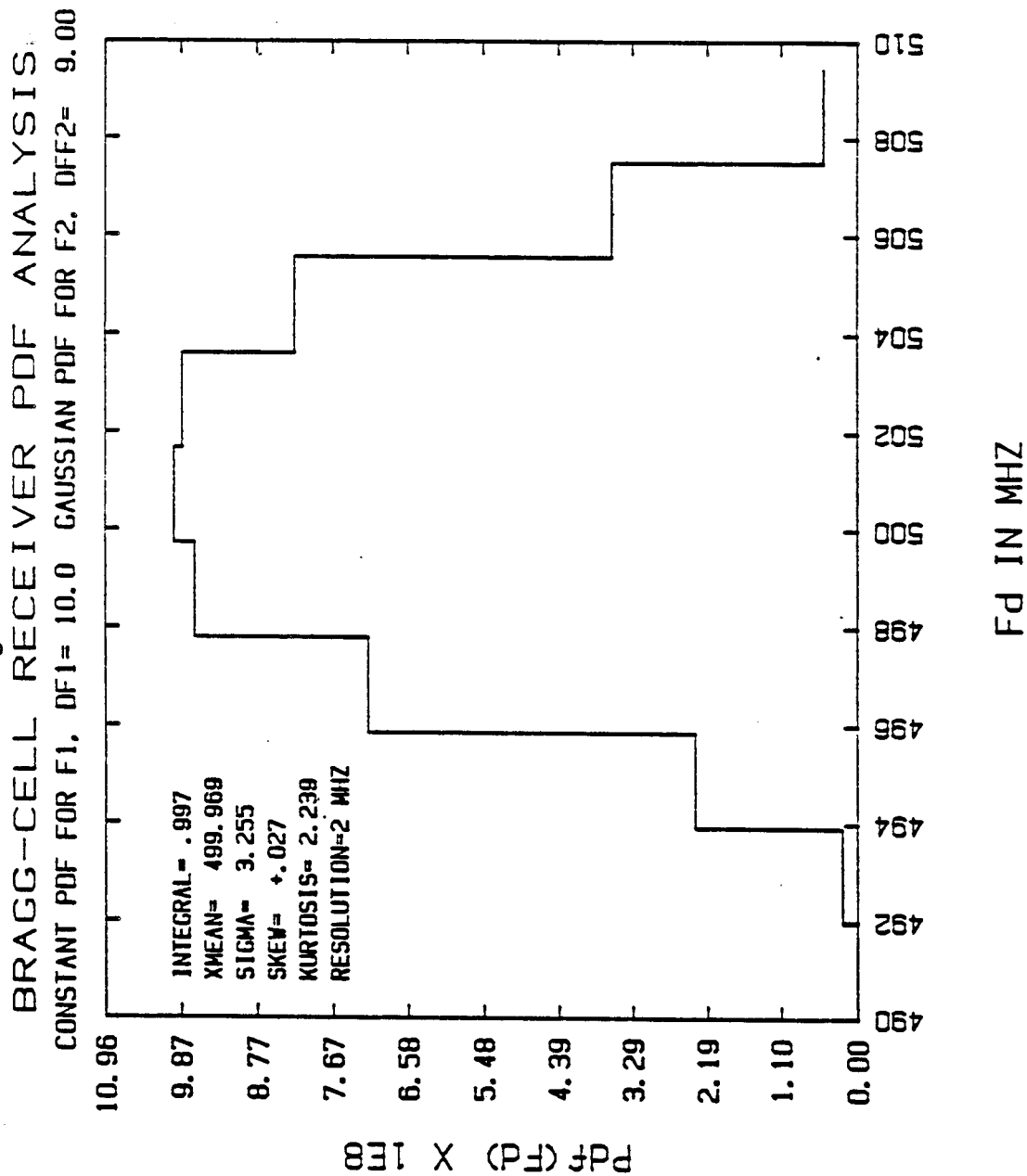


Figure 44

BRAGG-CELL RECEIVER PDF ANALYSIS
CONSTANT PDF FOR F1, DF1= 25.0 GAUSSIAN PDF FOR F2, DFF2= 5.00

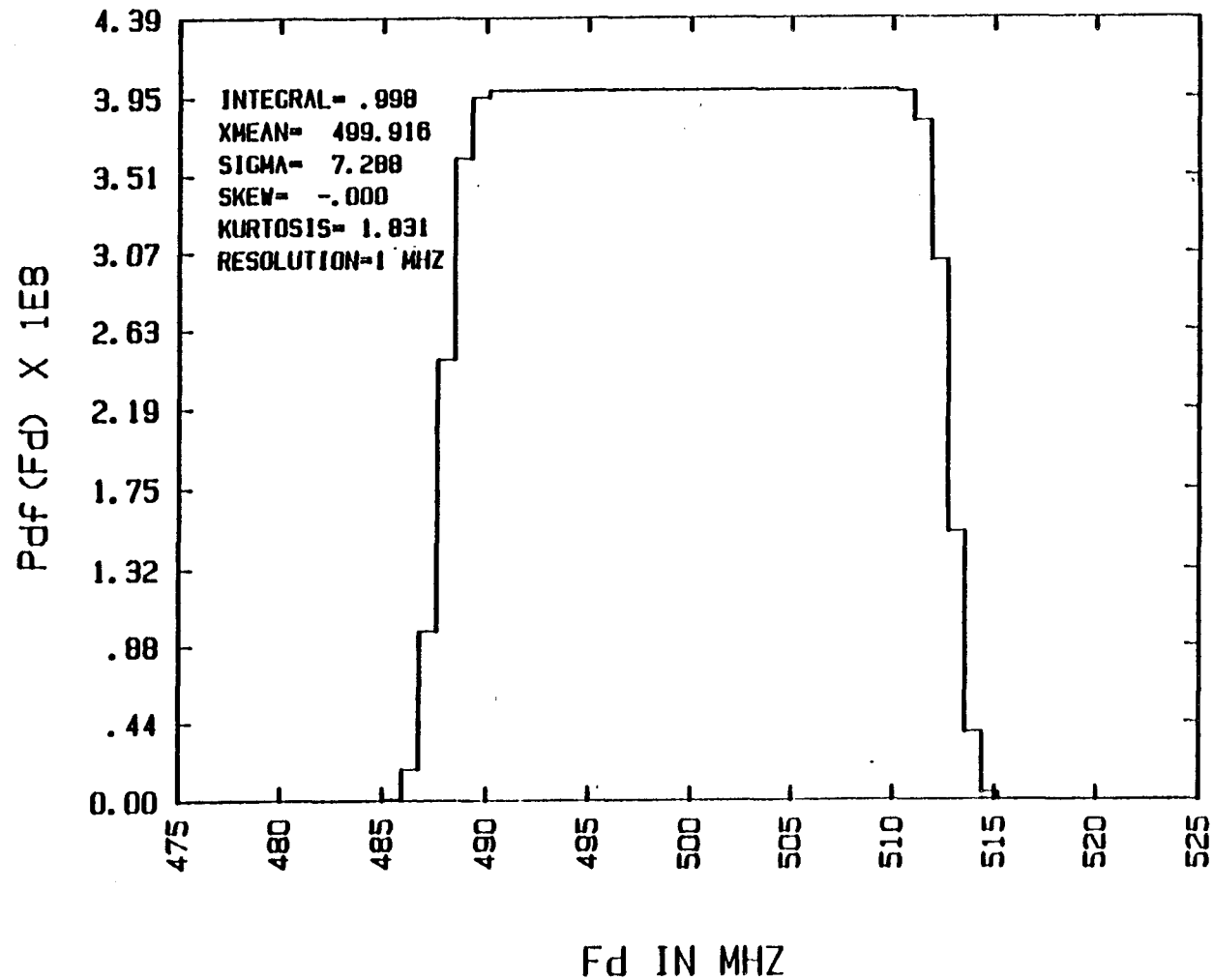


Figure 45
 BRAGG-CELL RECEIVER PDF ANALYSIS
 CONSTANT PDF FOR F1, DF1= 25.0 GAUSSIAN PDF FOR F2, DFF2= 5.00

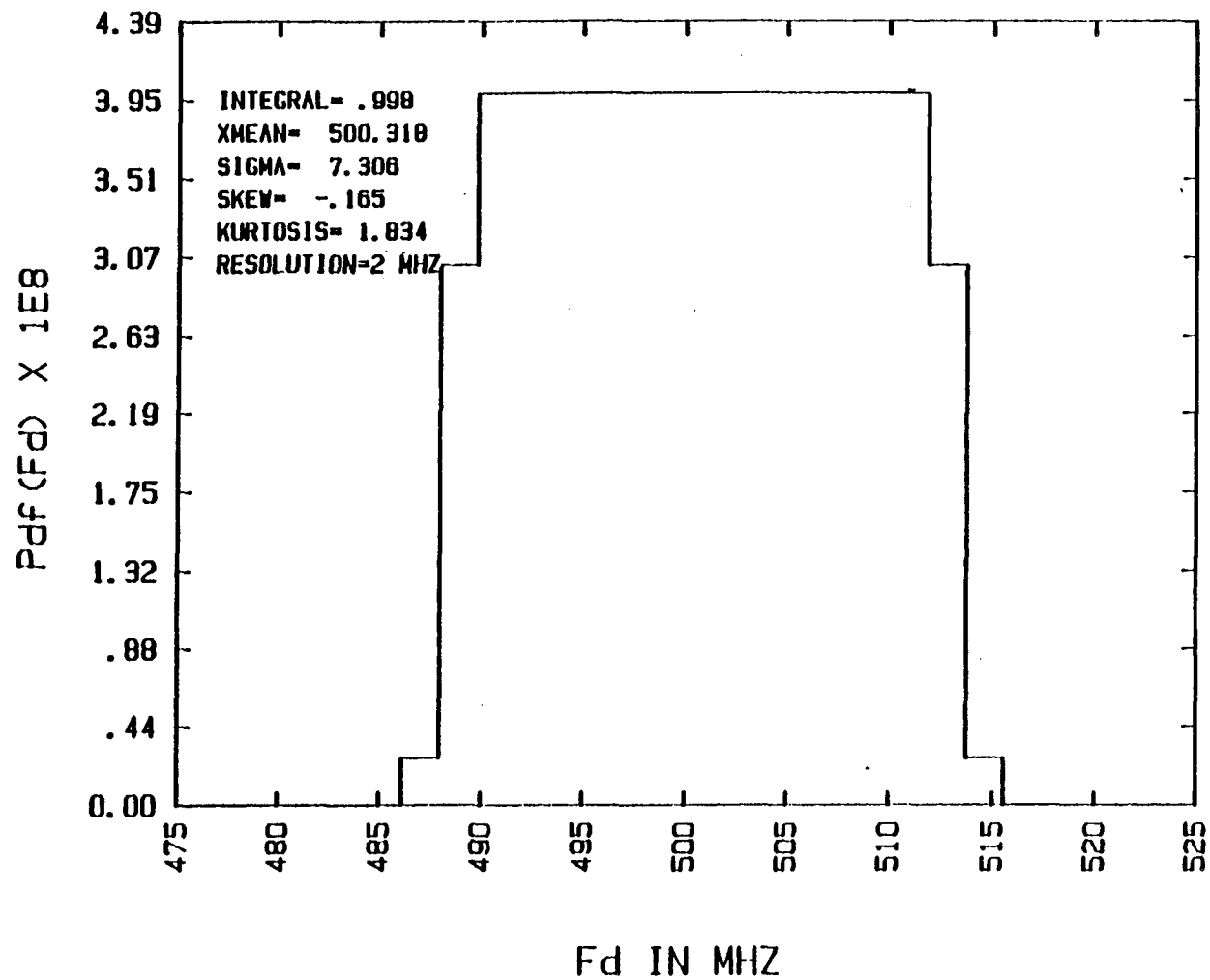


Figure 46

BRAGG-CELL RECEIVER PDF ANALYSIS
CONSTANT PDF FOR F1, DF1= 25.0 GAUSSIAN PDF FOR F2, DFF2= 5.00

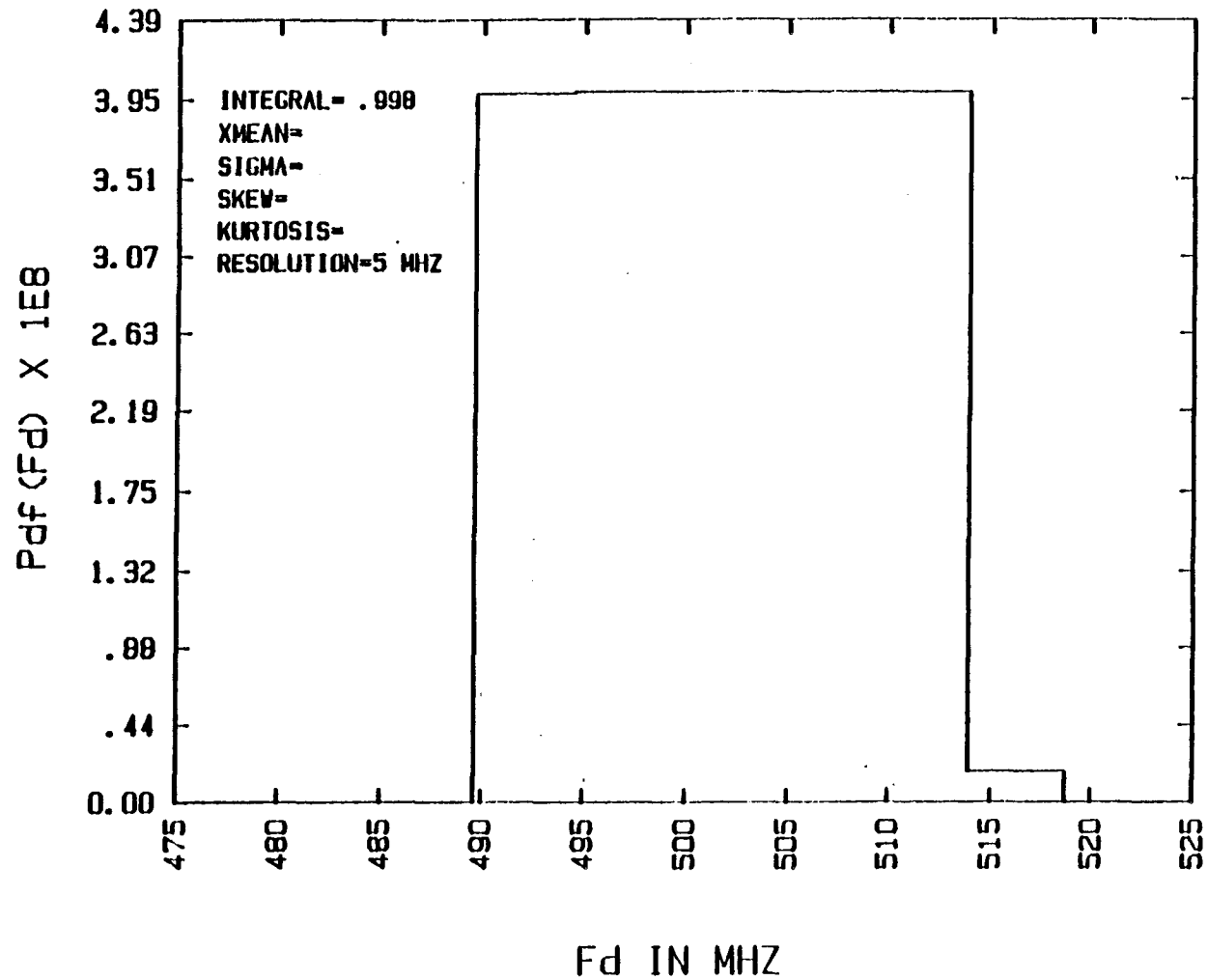


Figure 47

BRAGG-CELL RECEIVER PDF ANALYSIS
CONSTANT PDF FOR F1, DF1= 25.0 GAUSSIAN PDF FOR F2, DFF2= 15.00

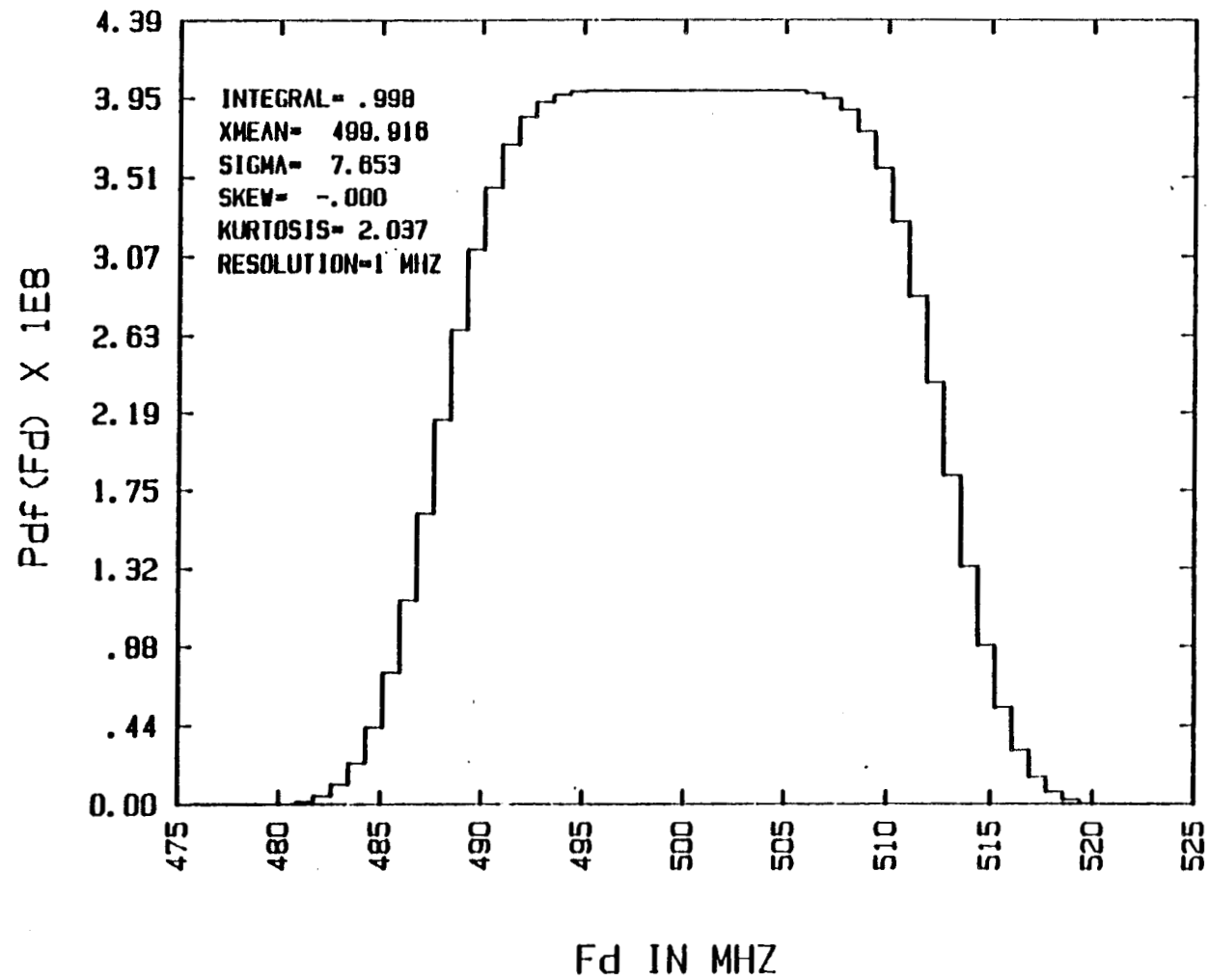


Figure 48

BRAGG-CELL RECEIVER PDF ANALYSIS
CONSTANT PDF FOR F1, DF1= 25.0 GAUSSIAN PDF FOR F2, DFF2= 15.00

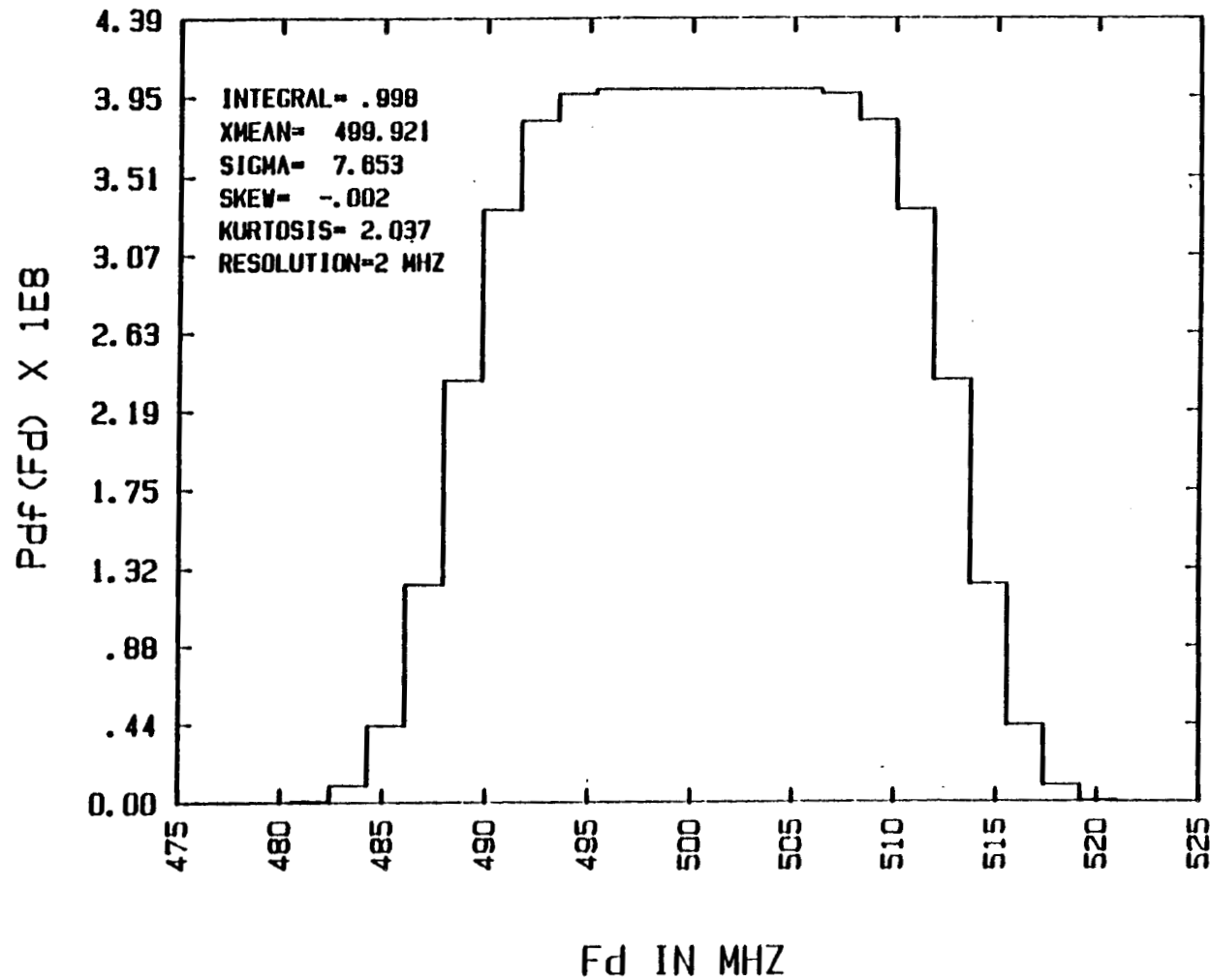


Figure 49

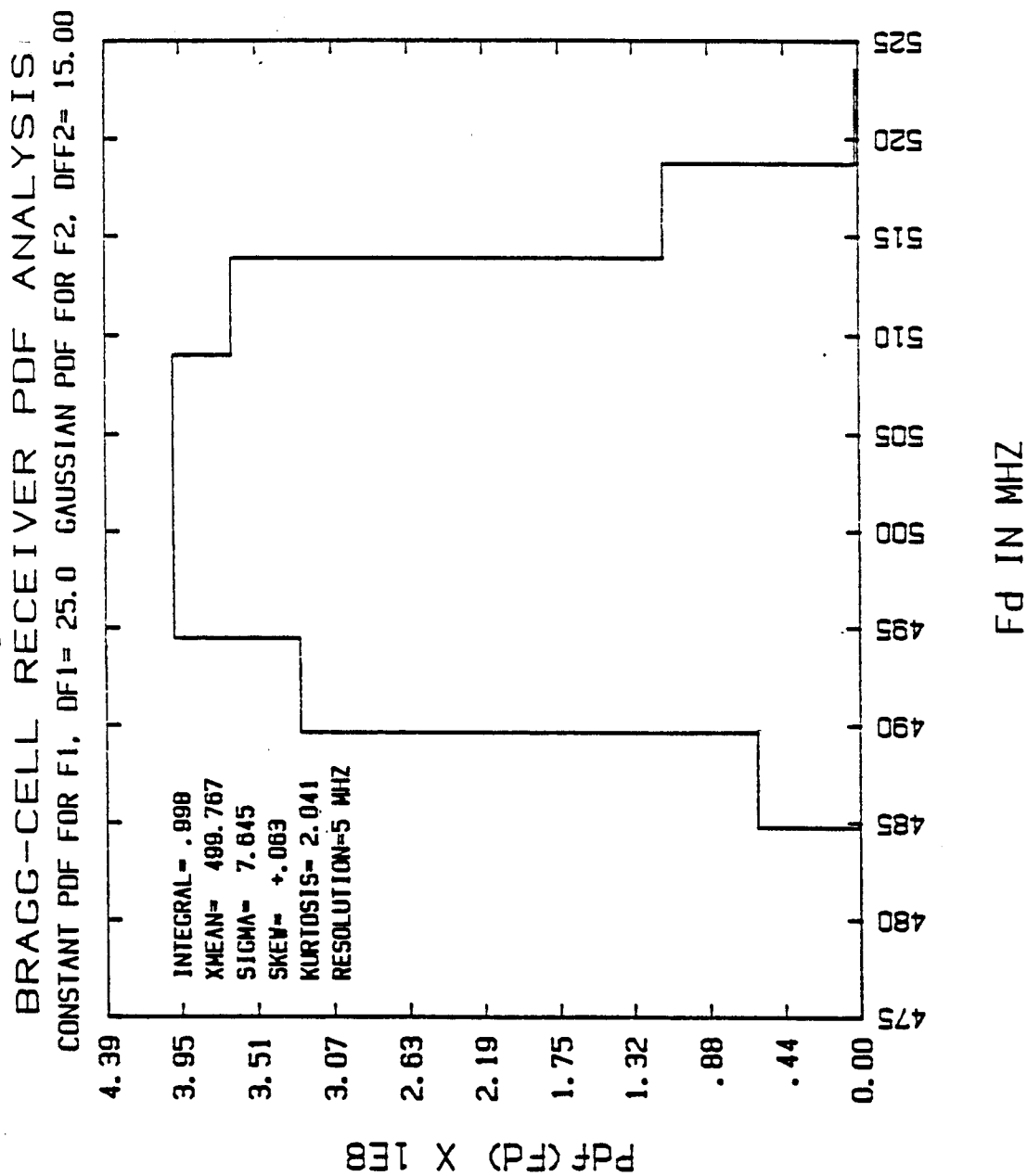


Figure 50

BRAGG-CELL RECEIVER PDF ANALYSIS
CONSTANT PDF FOR F1, DF1= 25.0 GAUSSIAN PDF FOR F2, OFF2= 24.00

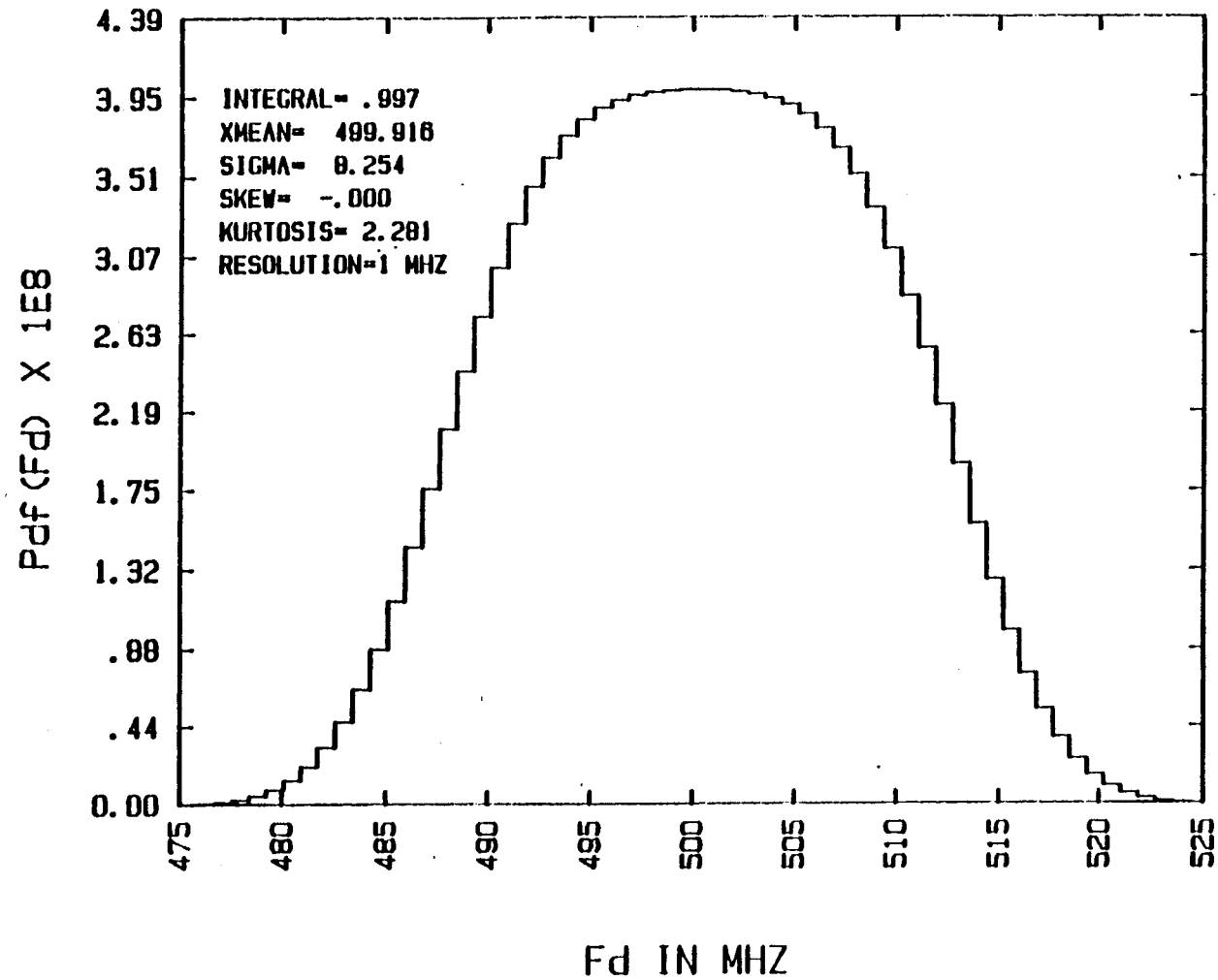


Figure 51

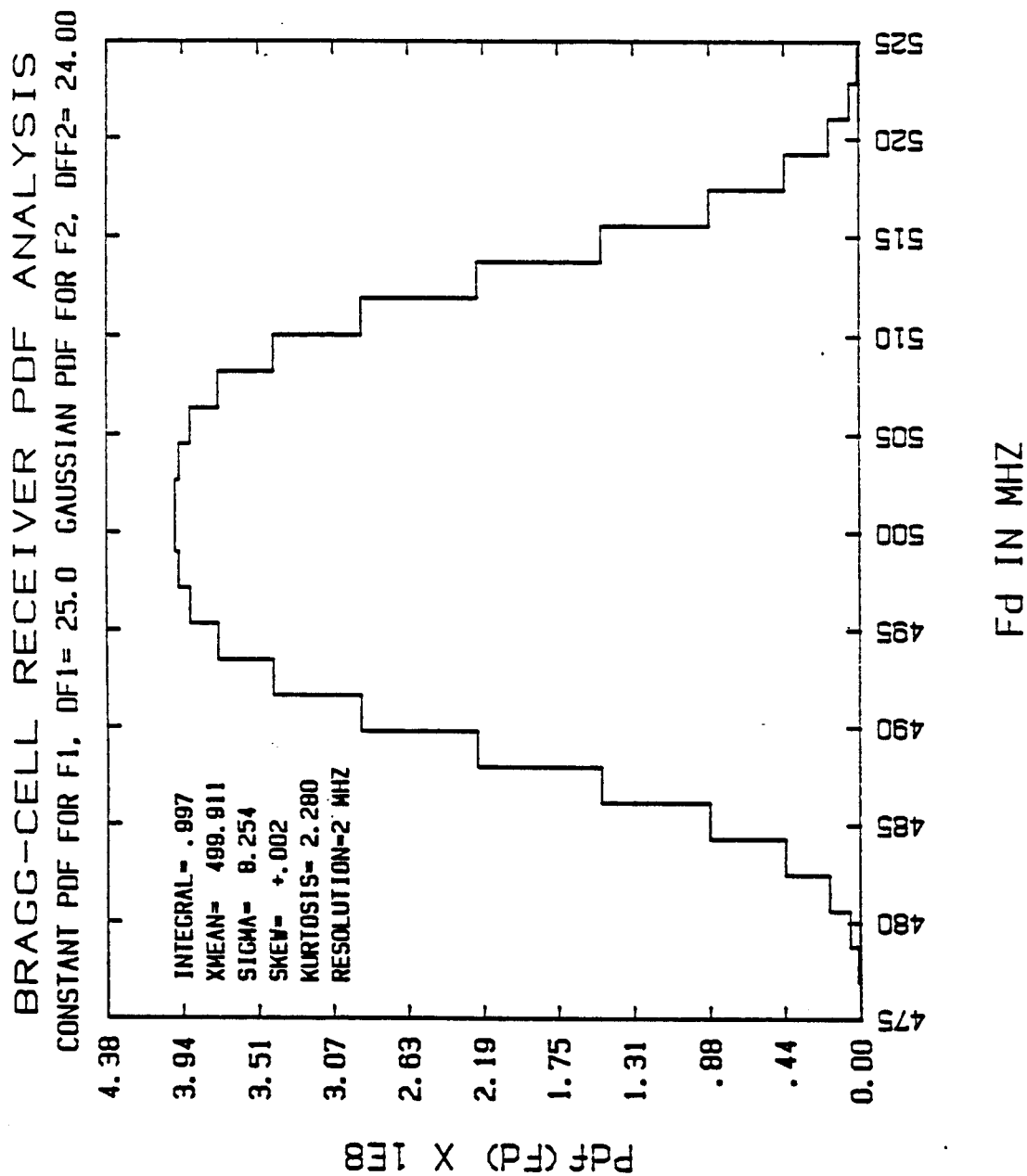


Figure 52

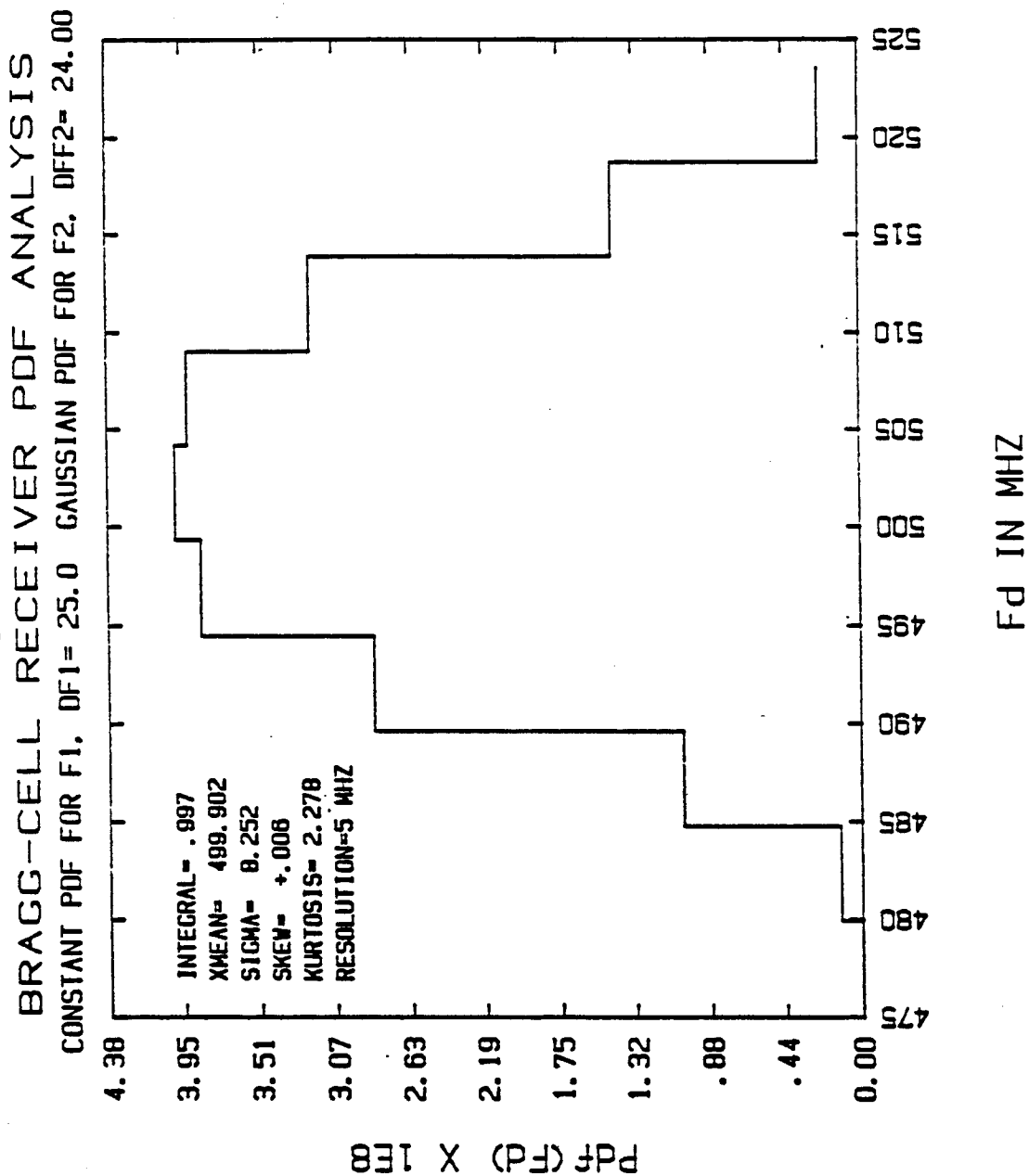


Figure 53

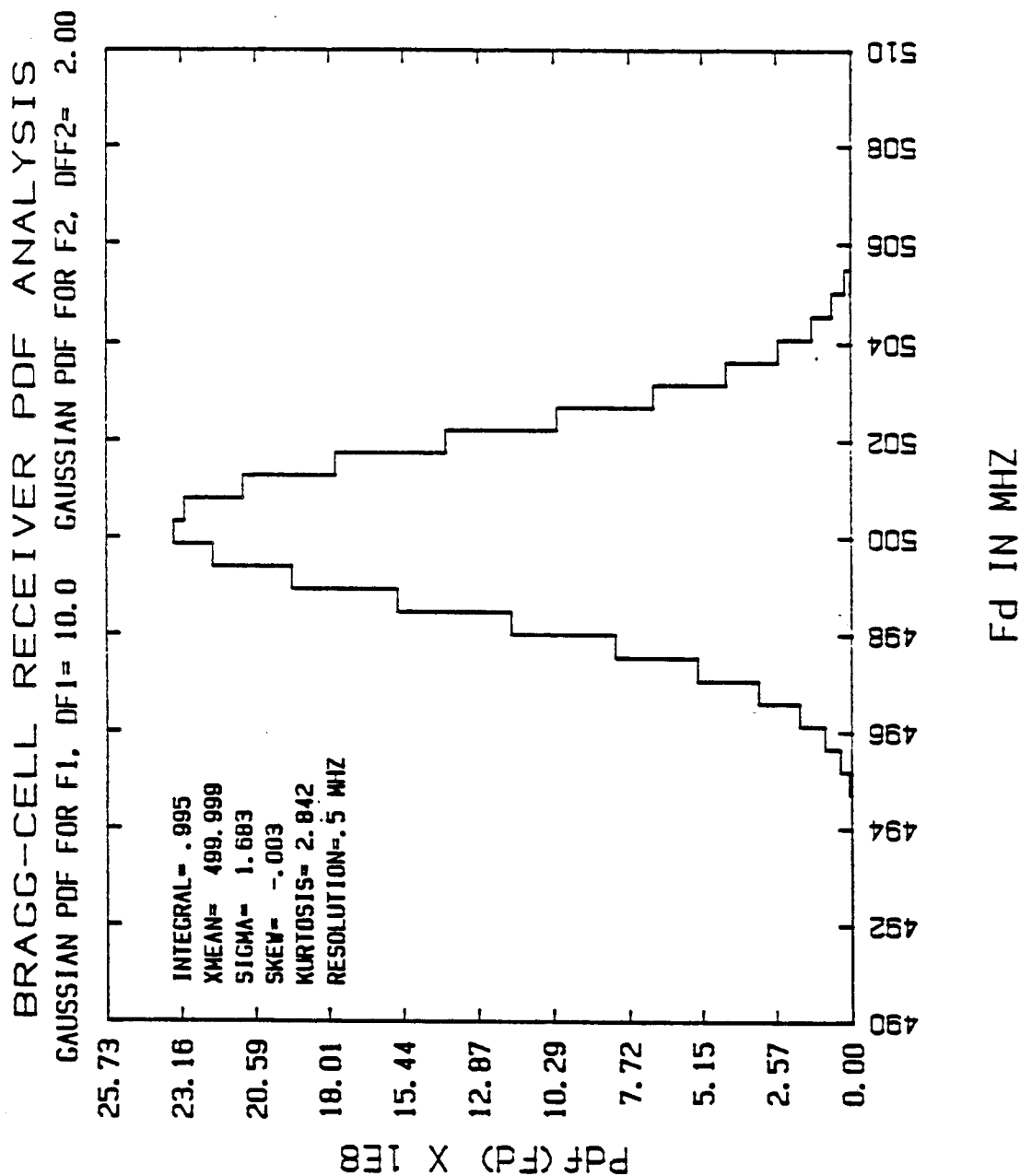


Figure 54

BRAGG-CELL RECEIVER PDF ANALYSIS
GAUSSIAN PDF FOR F1, DF1= 10.0 GAUSSIAN PDF FOR F2, DFF2= 2.00

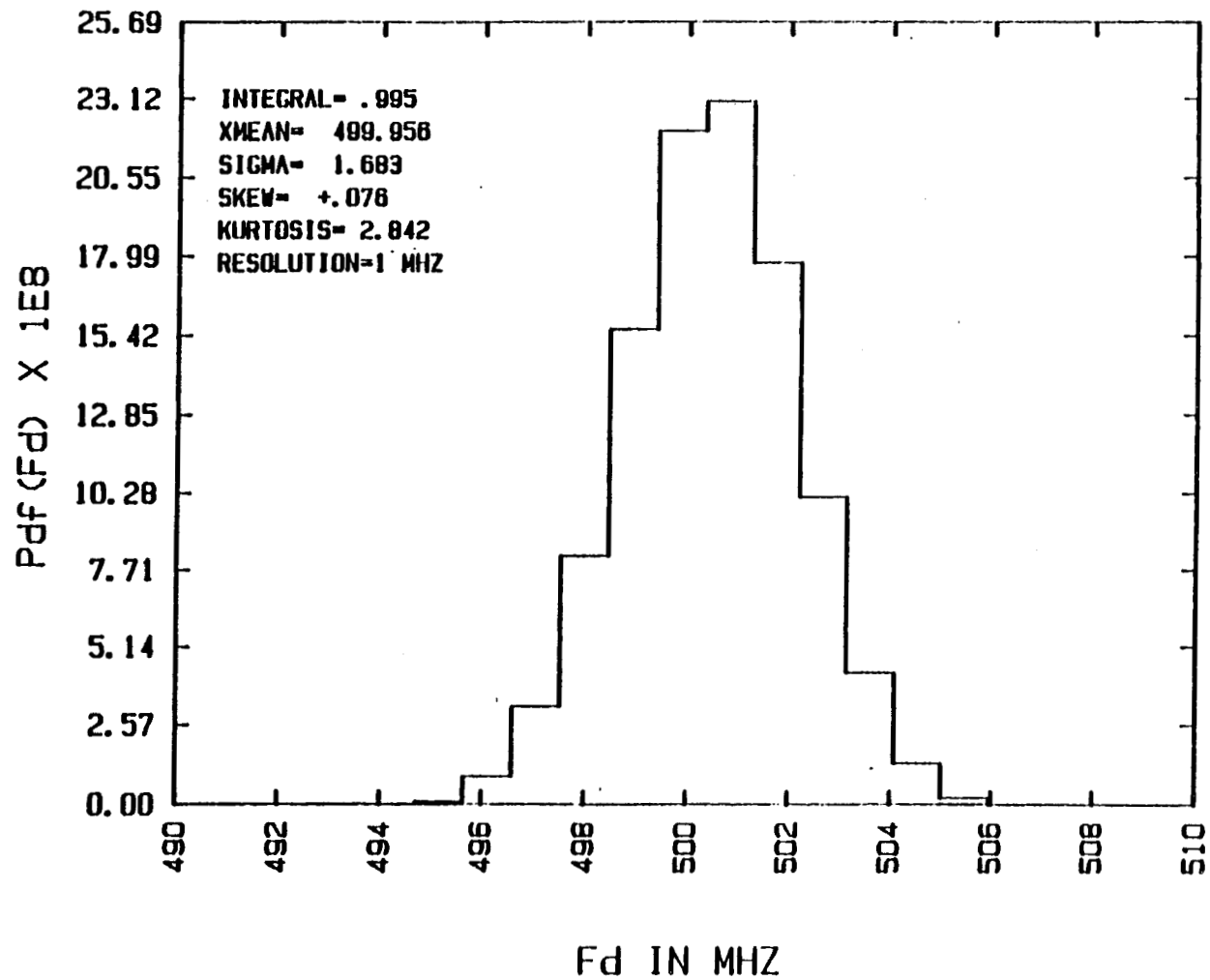


Figure 55

BRAGG-CELL RECEIVER PDF ANALYSIS
GAUSSIAN PDF FOR F1, DF1= 10.0 GAUSSIAN PDF FOR F2, DFF2= 2.00

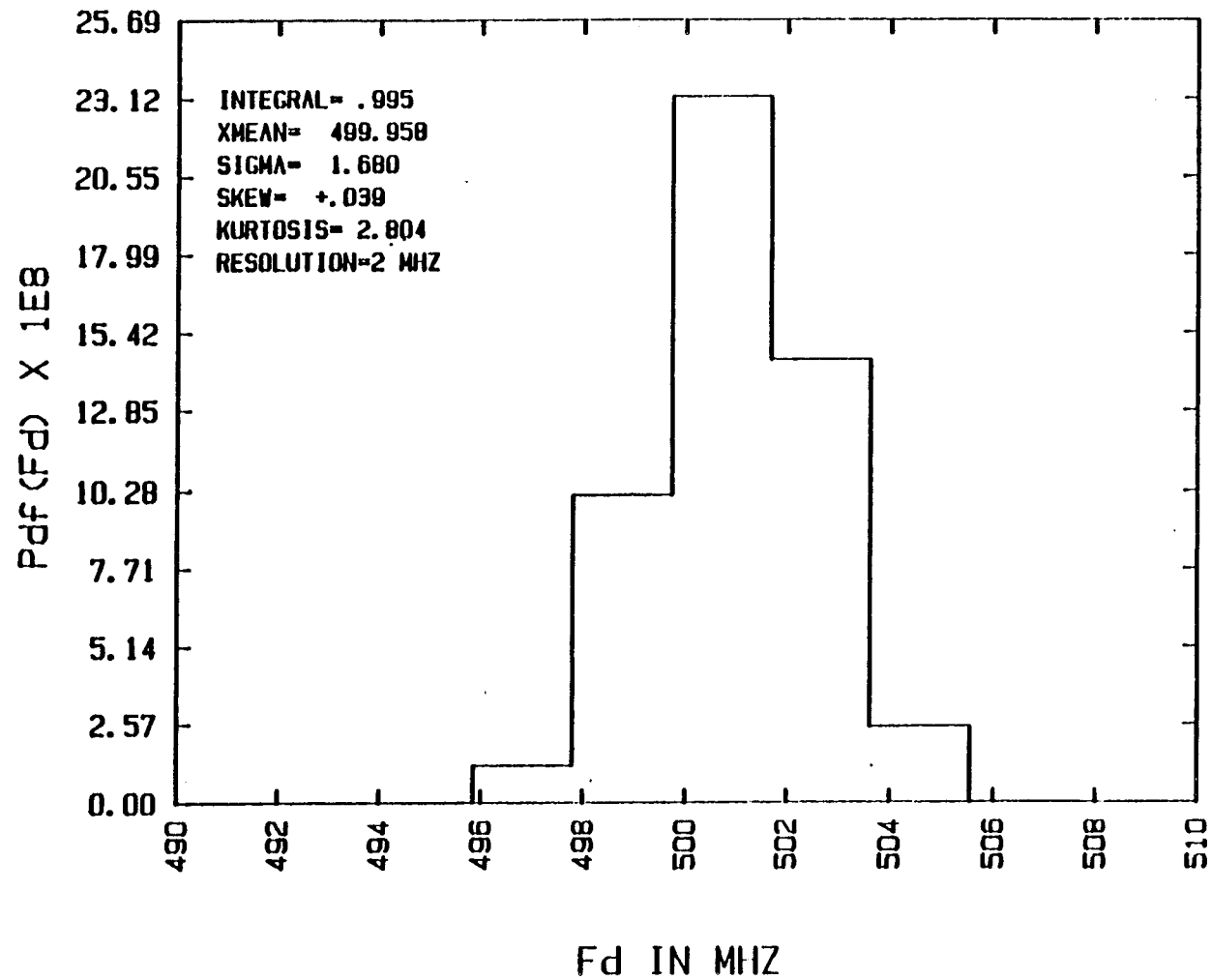


Figure 56

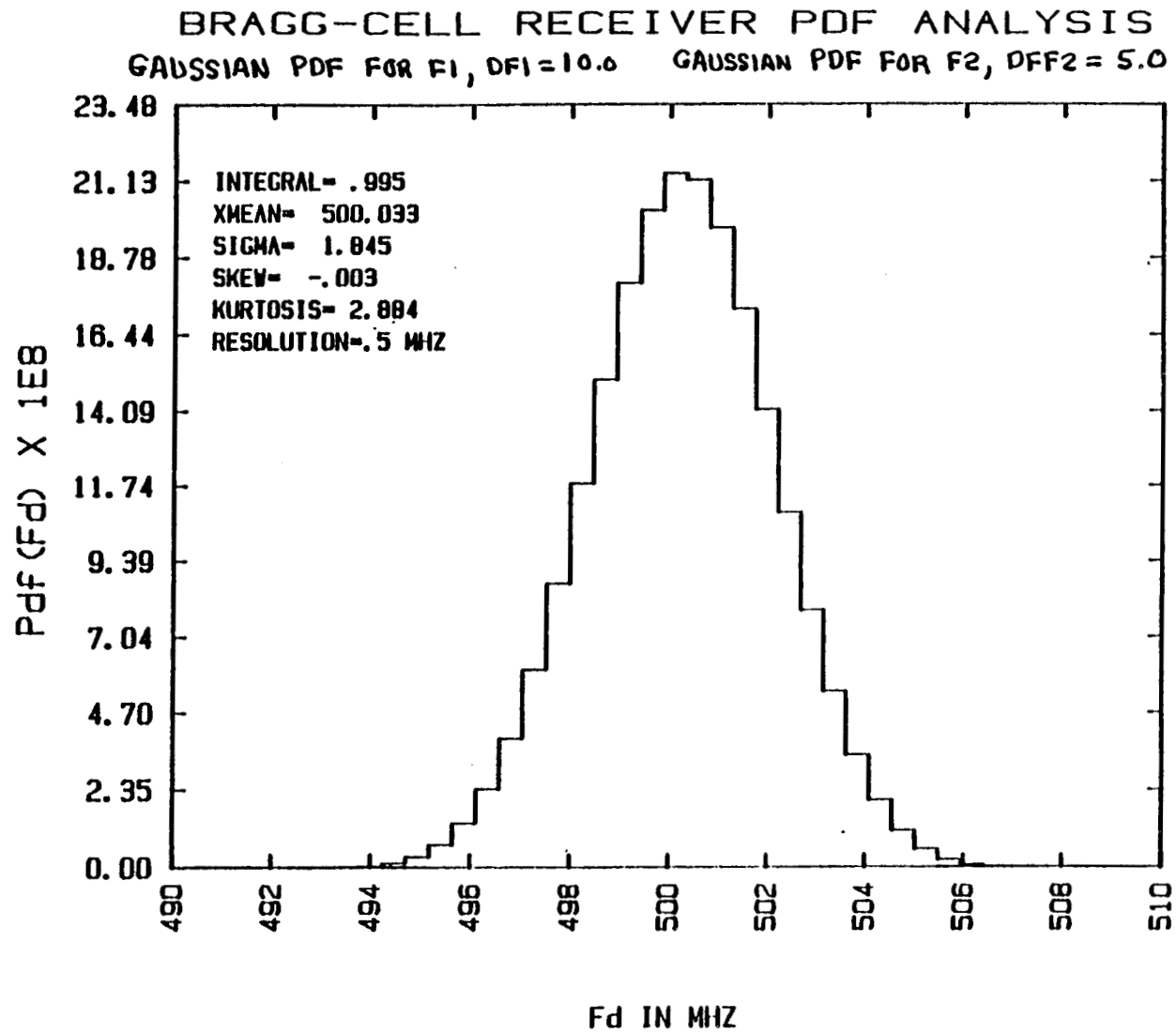


Figure 57

BRAGG-CELL RECEIVER PDF ANALYSIS

GAUSSIAN PDF FOR F1, DFF1=10.0

GAUSSIAN PDF FOR F2, DFF2=5.0

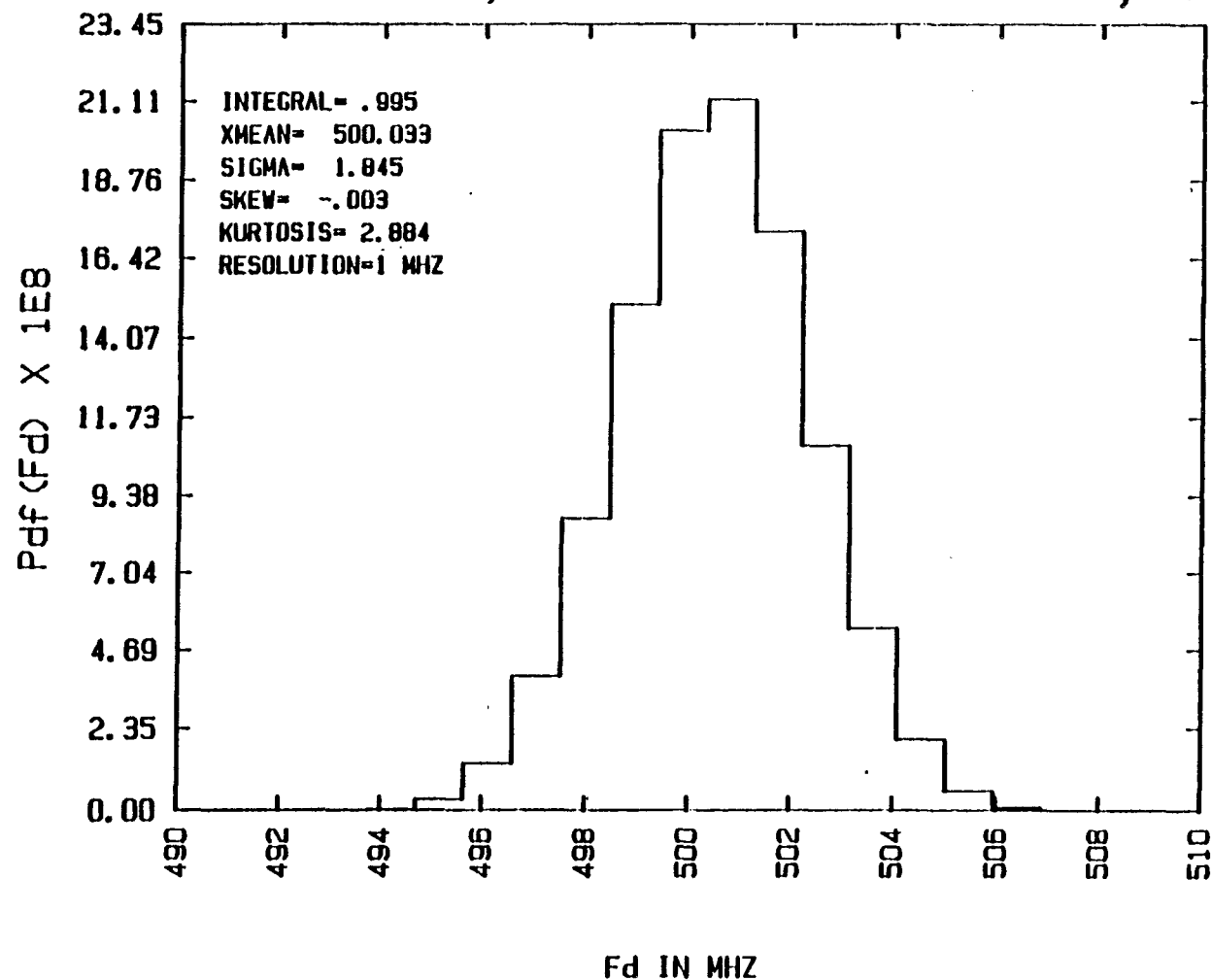


Figure 58

BRAGG-CELL RECEIVER PDF ANALYSIS

GAUSSIAN PDF FOR F1, DFI=10.0

GAUSSIAN PDF FOR F2, DFF2=5.0

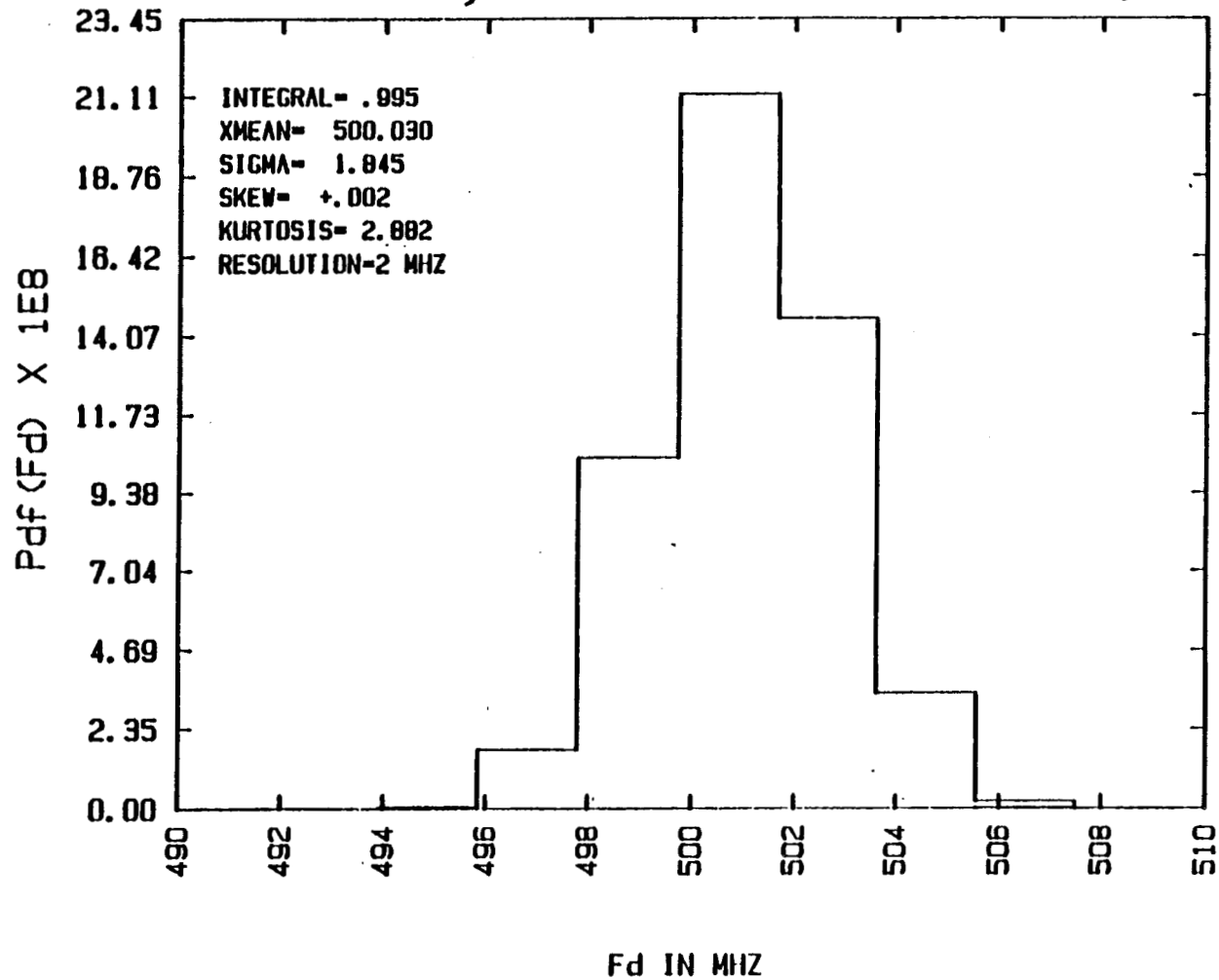


Figure 59

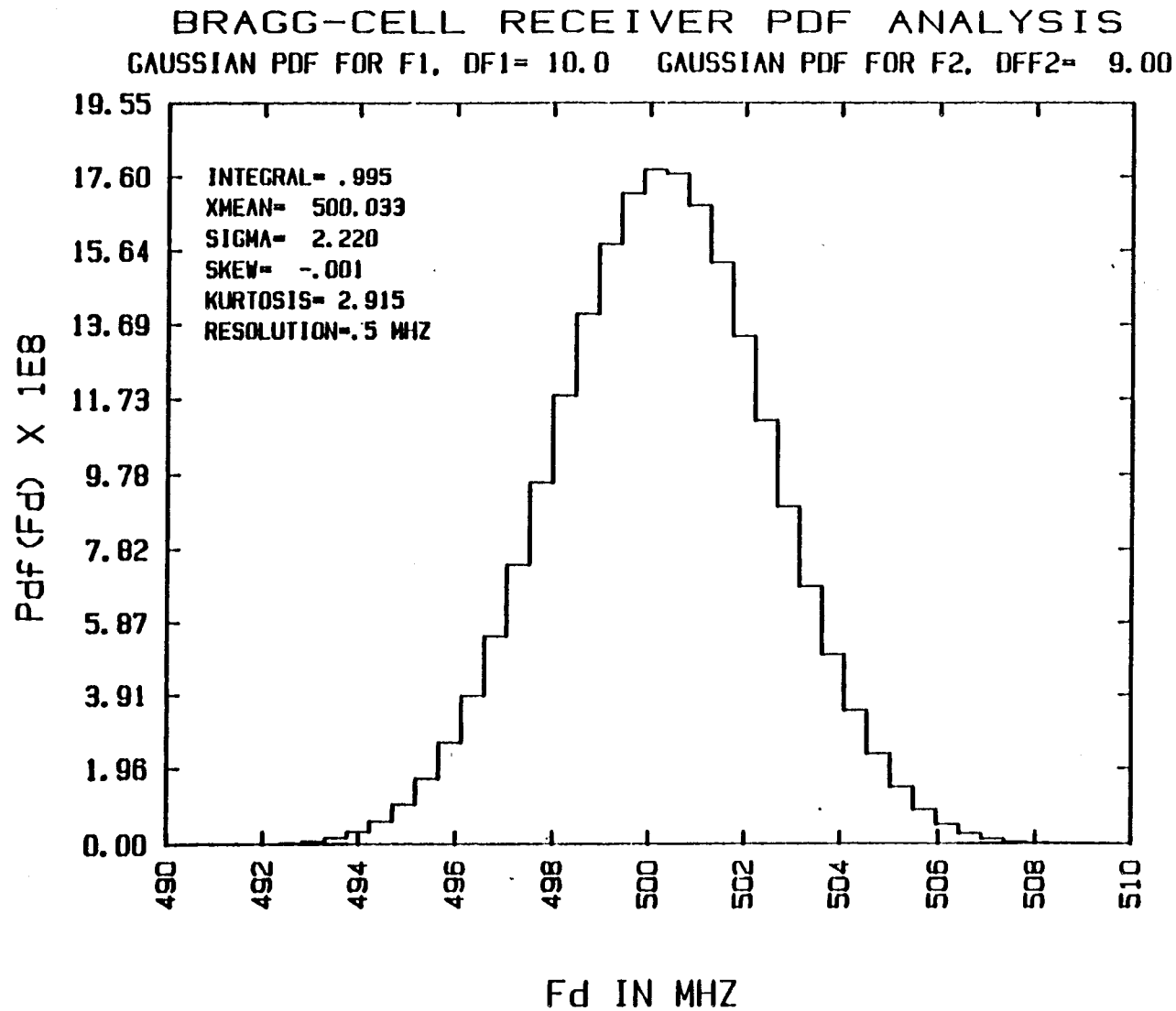
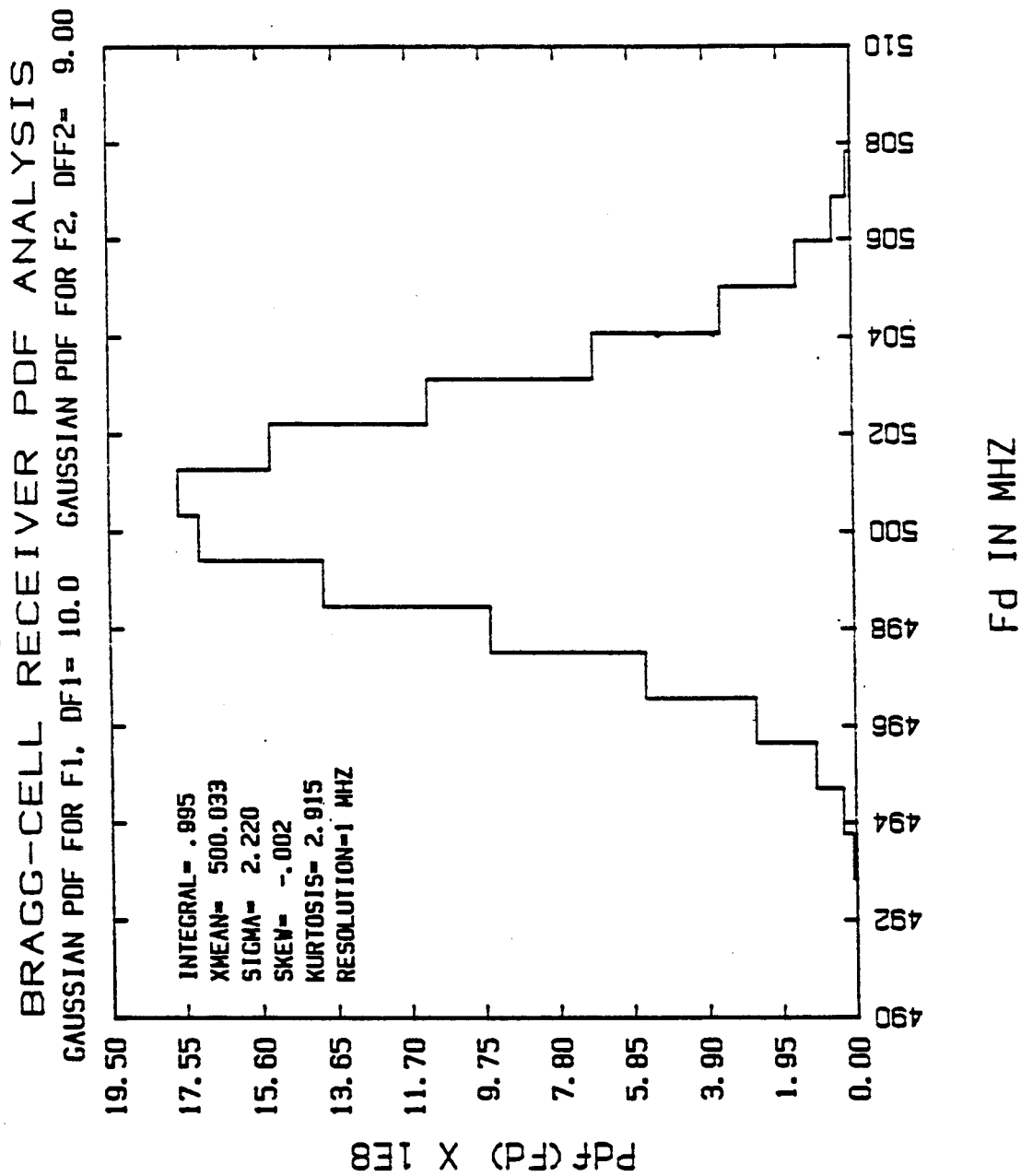


Figure 60



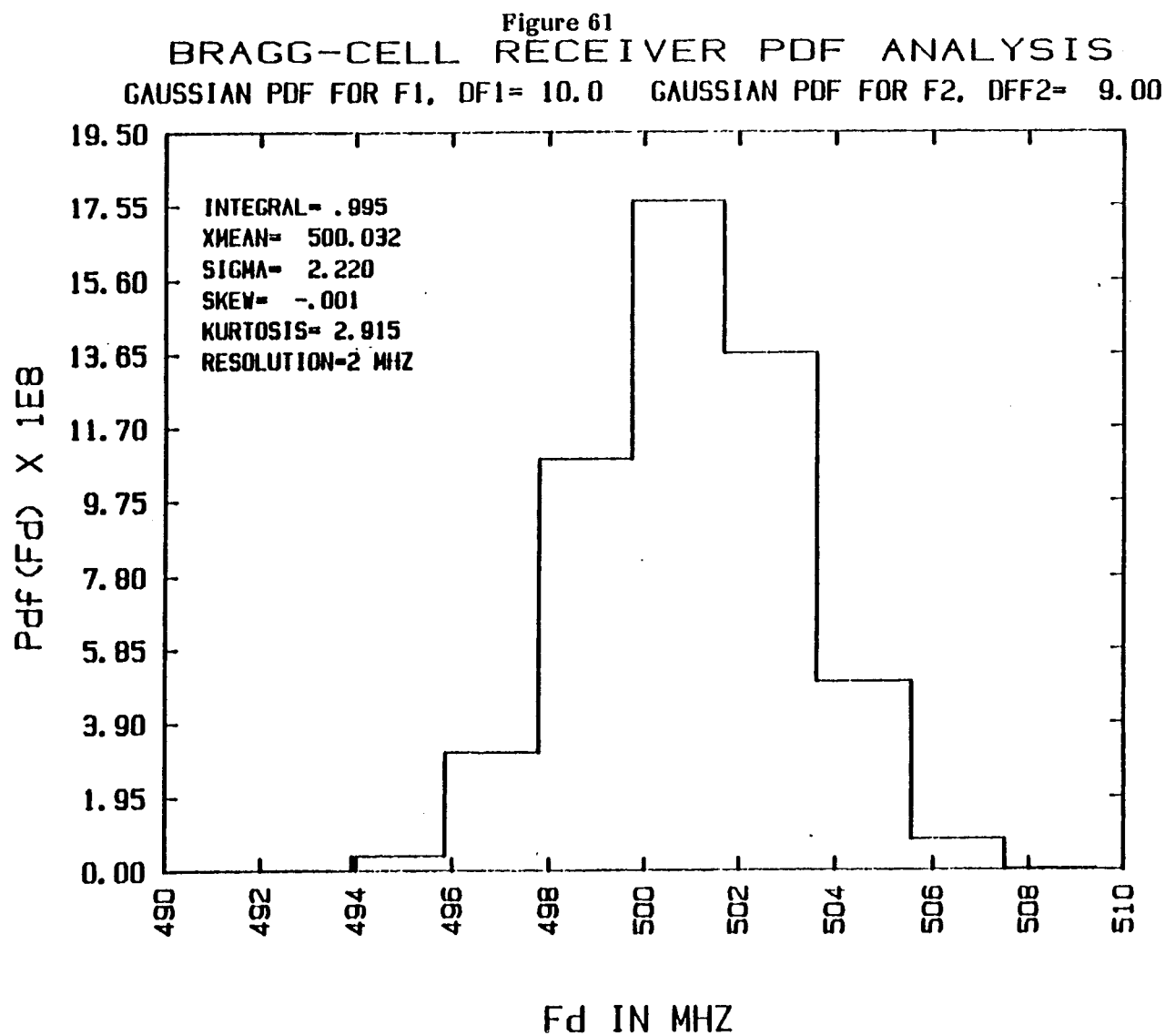


Figure 62

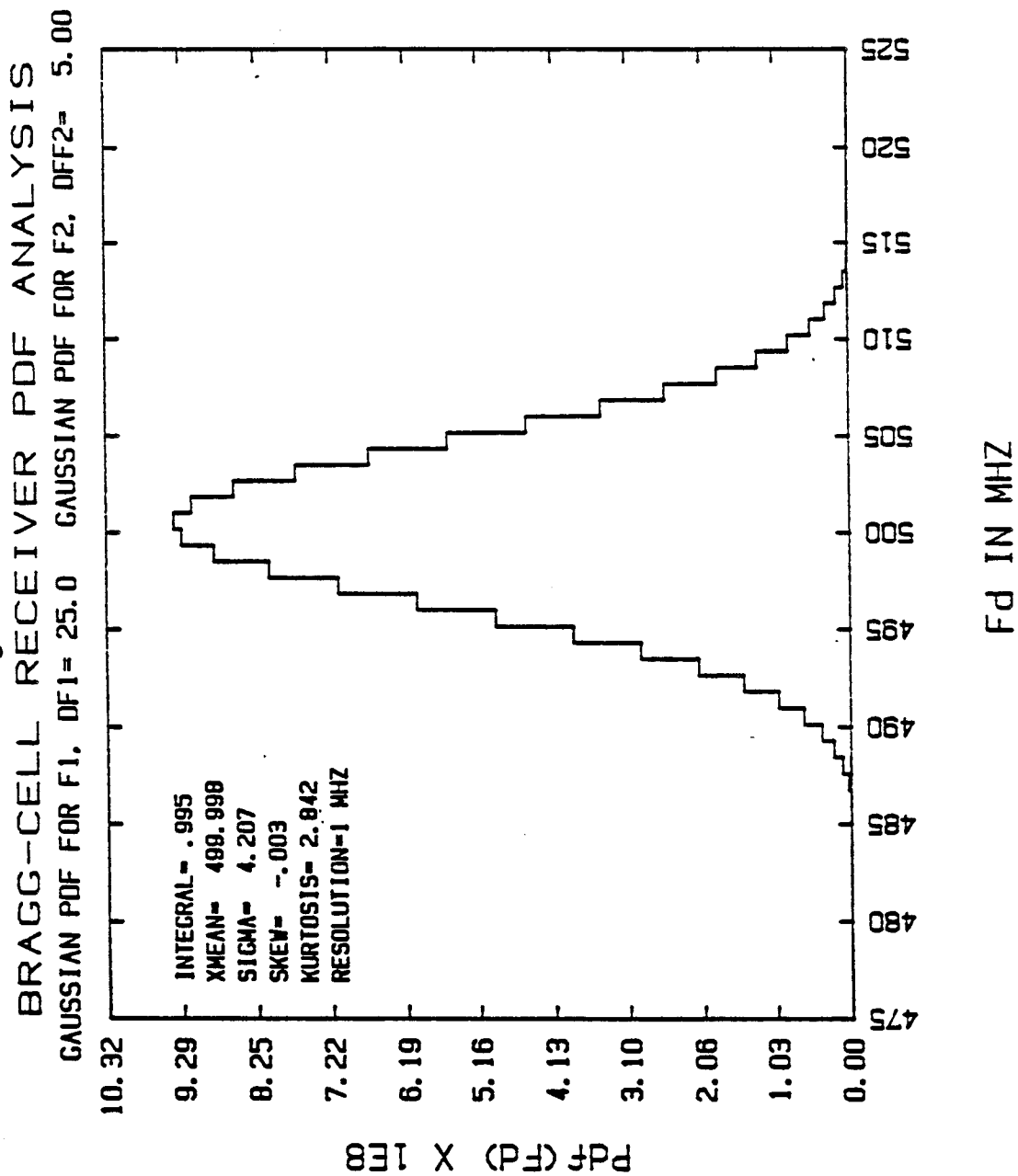


Figure 63

BRAGG-CELL RECEIVER PDF ANALYSIS

GAUSSIAN PDF FOR F1, DF1= 25.0 GAUSSIAN PDF FOR F2, DFF2= 5.00

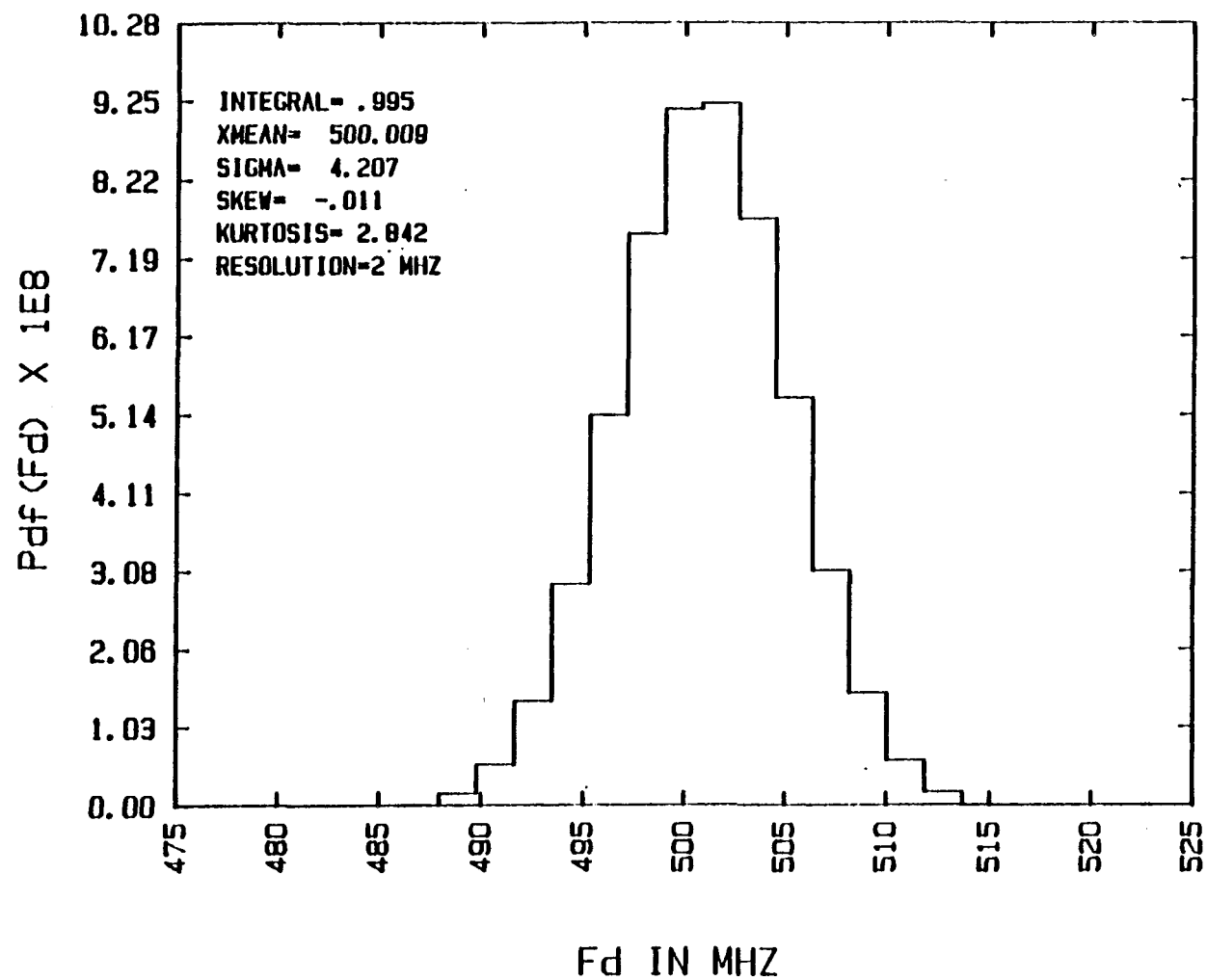


Figure 64

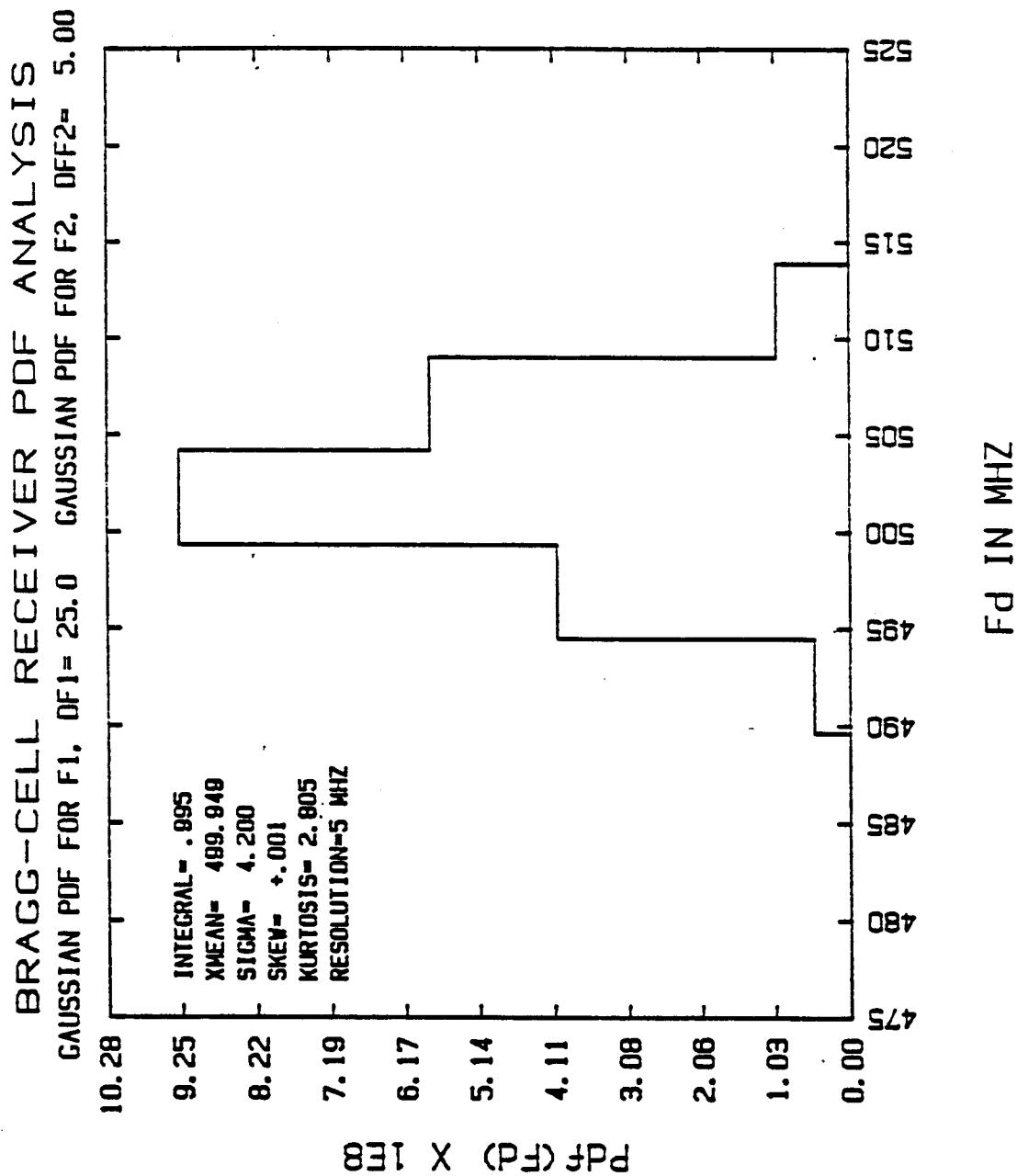


Figure 65

BRAGG-CELL RECEIVER PDF ANALYSIS
GAUSSIAN PDF FOR F1, DF1= 25.0 GAUSSIAN PDF FOR F2, DFF2= 15.00

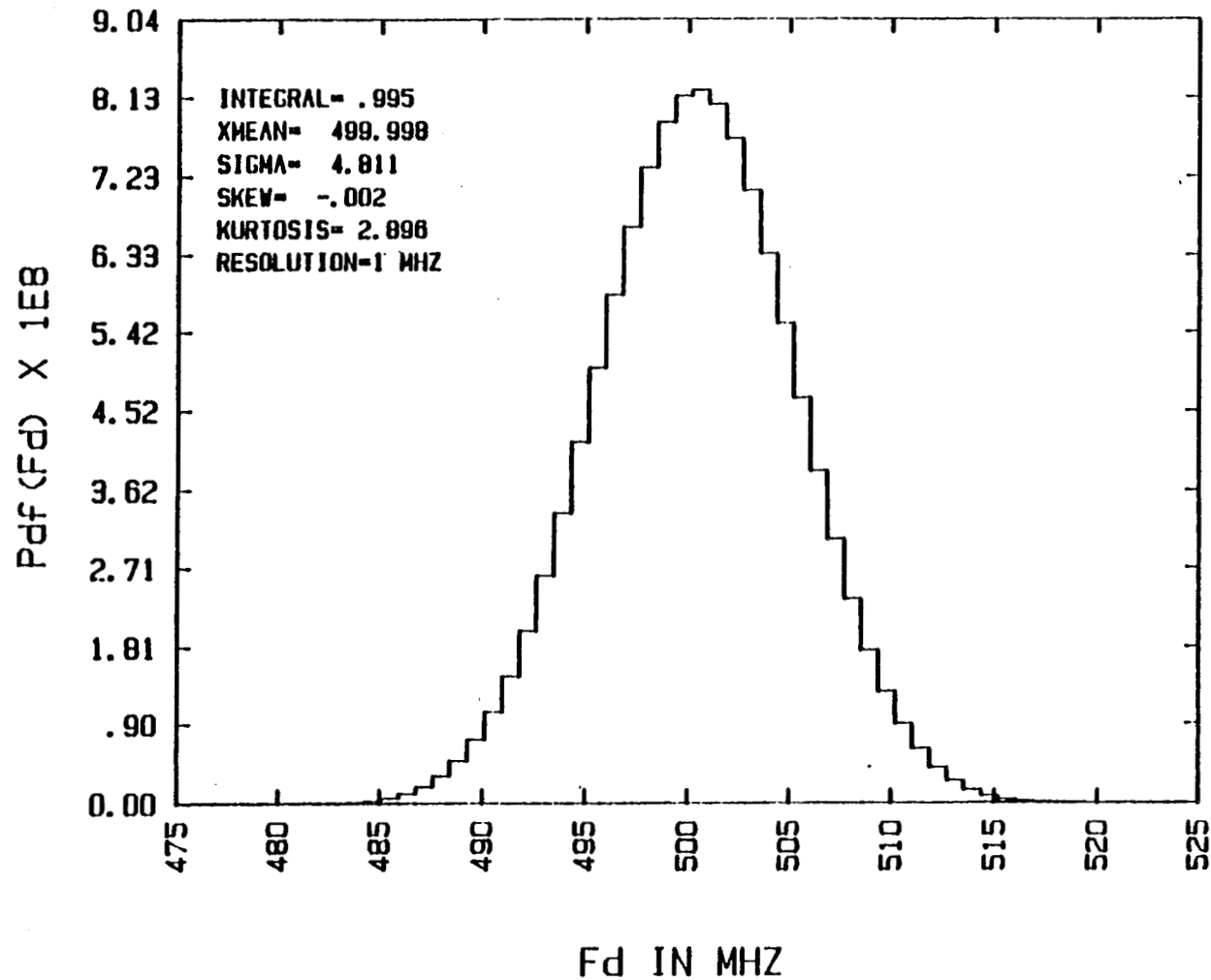


Figure 66
BRAGG-CELL RECEIVER PDF ANALYSIS
GAUSSIAN PDF FOR F1, DF1= 25.0 GAUSSIAN PDF FOR F2, DFF2= 15.00

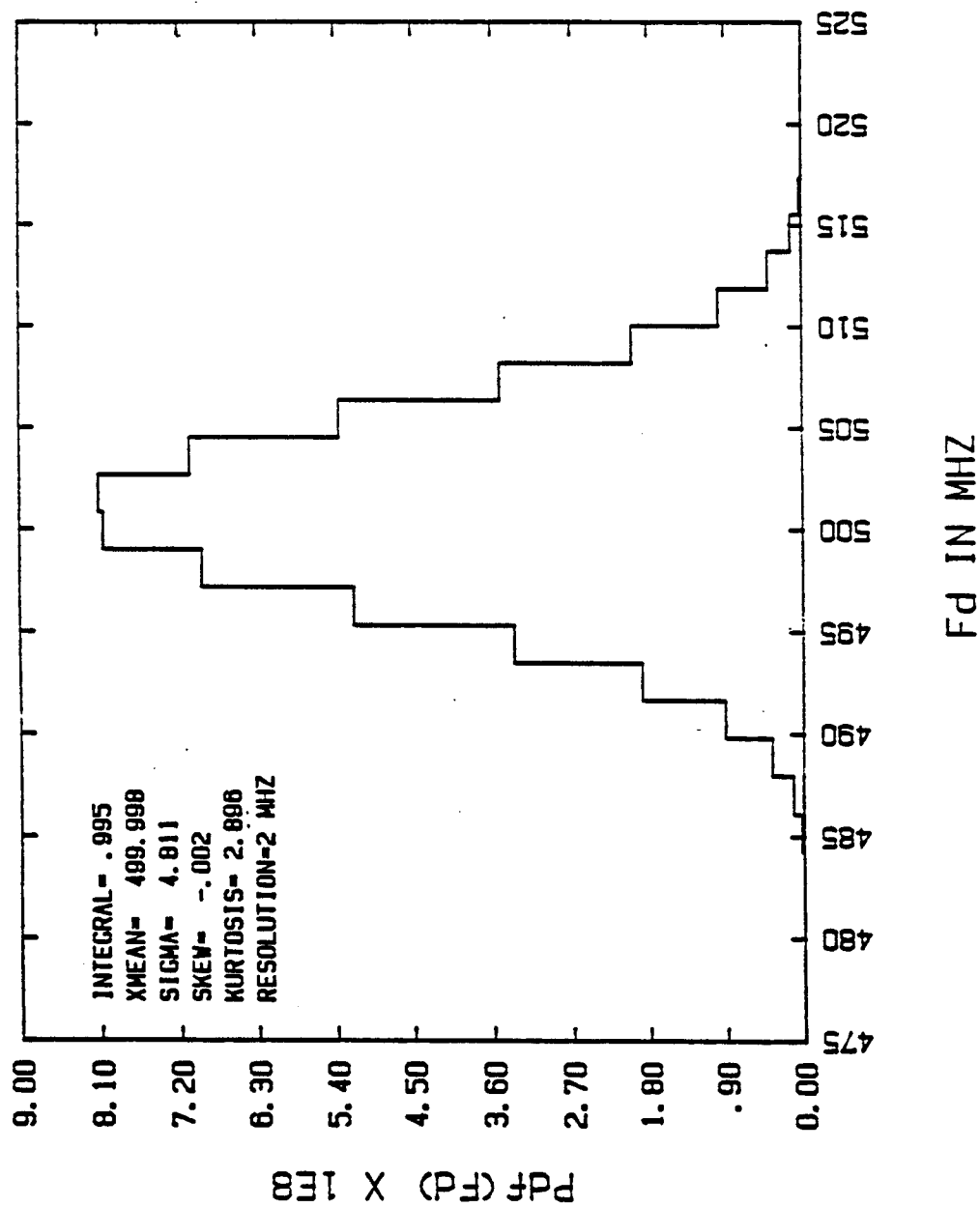


Figure 67

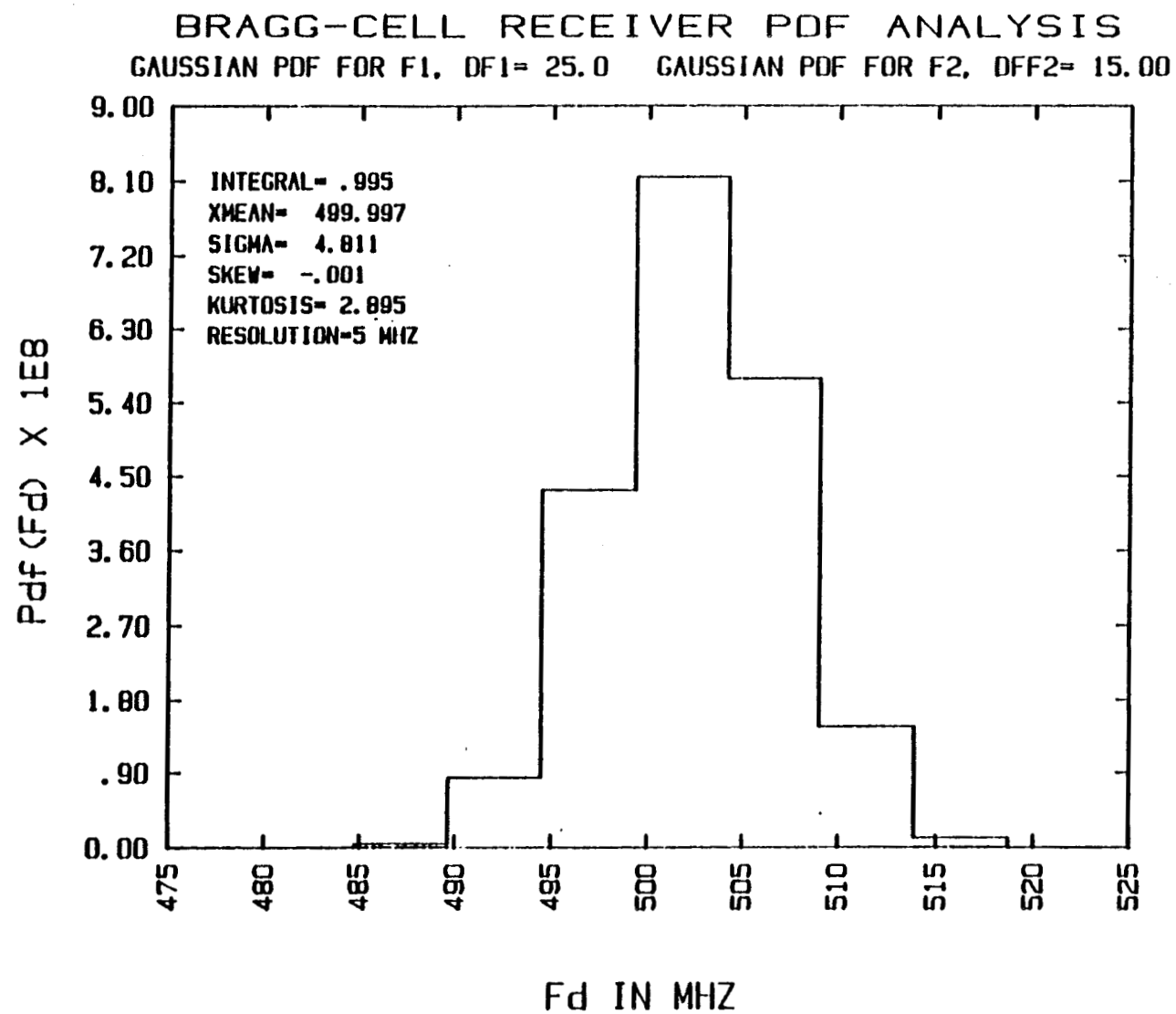


Figure 68

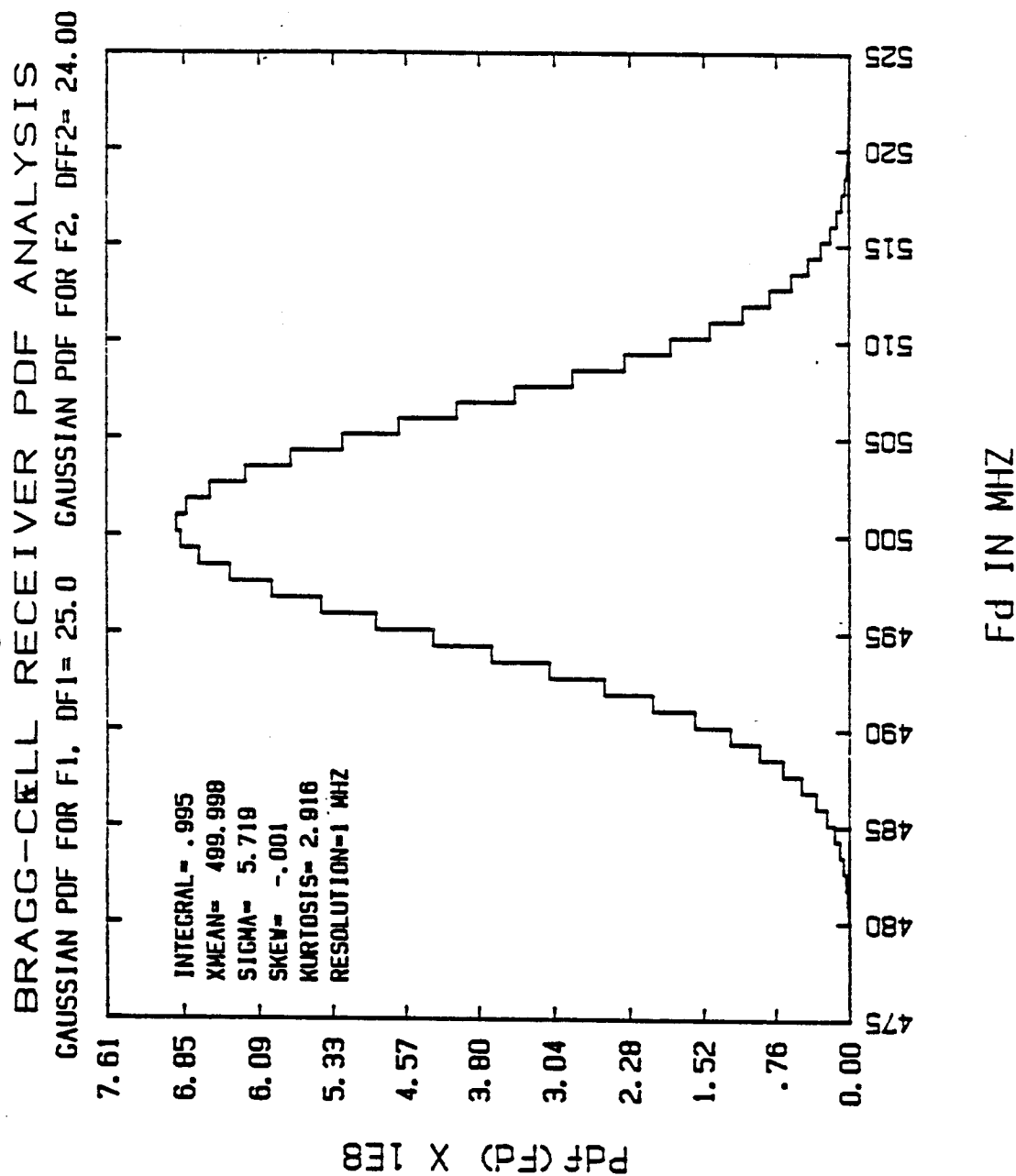


Figure 69

BRAGG-CELL RECEIVER PDF ANALYSIS
GAUSSIAN PDF FOR F1, DF1= 25.0 GAUSSIAN PDF FOR F2, DFF2= 24.00

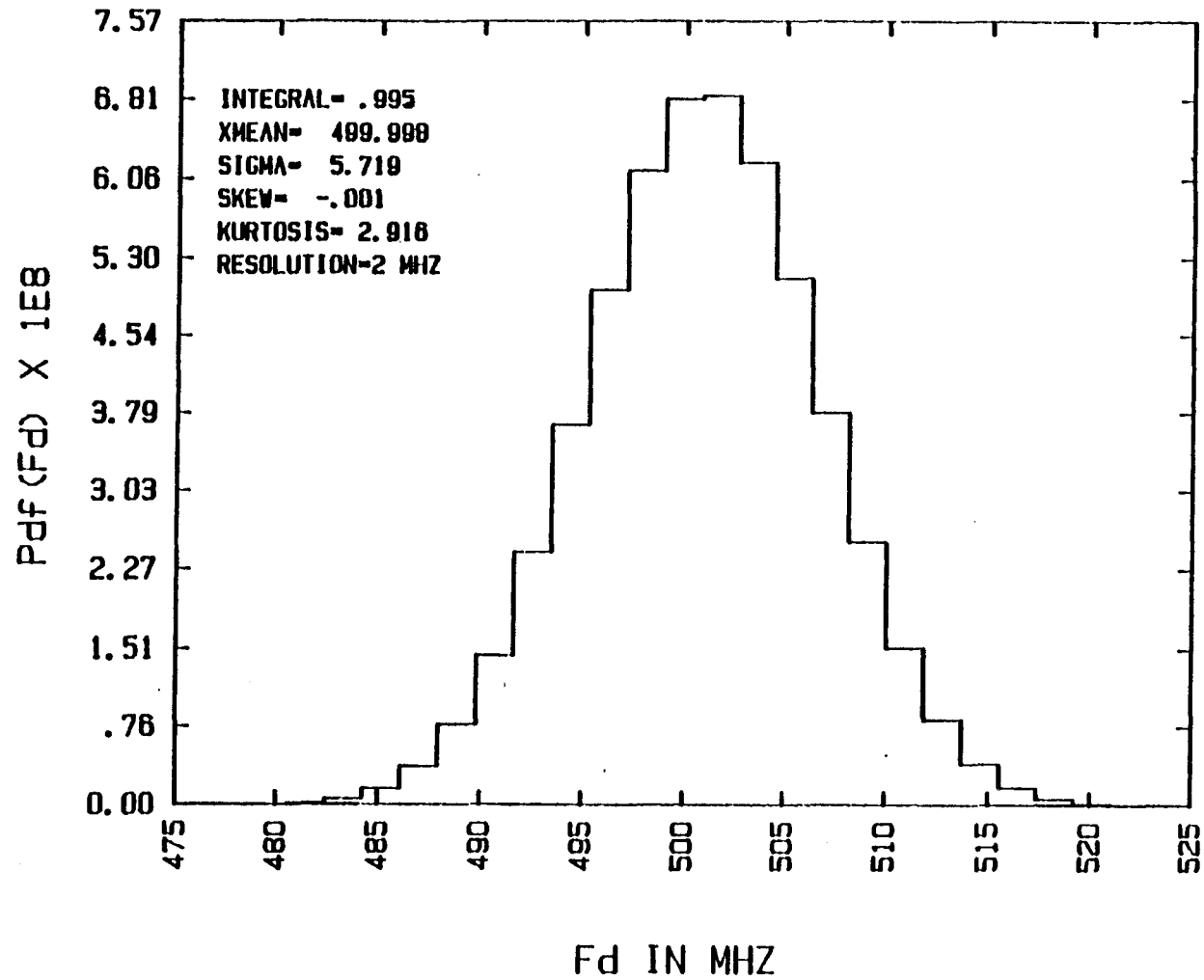
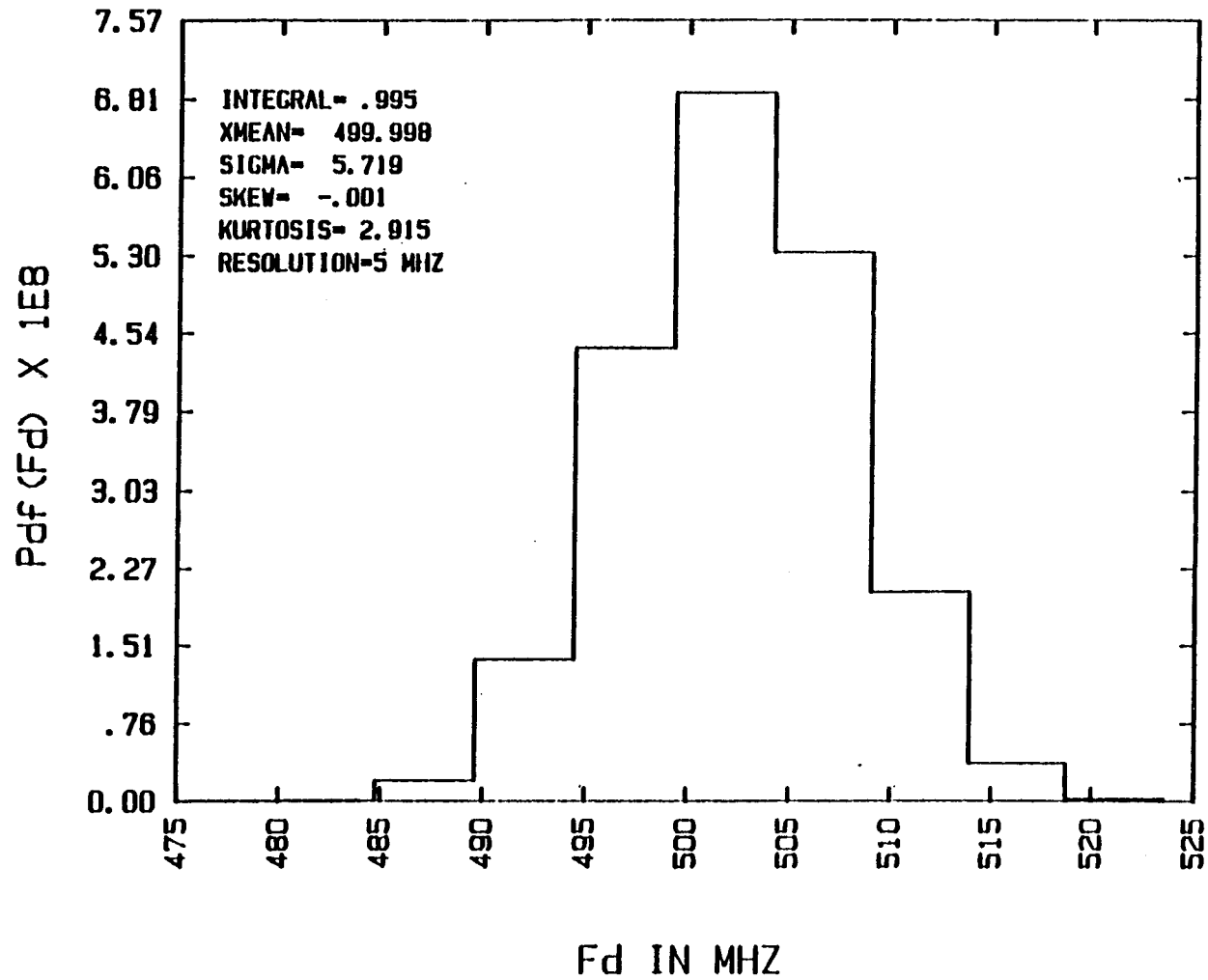


Figure 70

BRAGG-CELL RECEIVER PDF ANALYSIS
GAUSSIAN PDF FOR F1, DF1= 25.0 GAUSSIAN PDF FOR F2, DFF2= 24.00



CONCLUSIONS

Bragg-cell receivers can accurately measure frequencies of time coincident and time overlapped RF signals, which is a big advantage over other receiver types. Bragg-cell receivers are available with bandwidths to approximately 1 GHz, and frequency resolutions of 100 KHz to 10 MHz.

The Bragg-cell receiver's frequency parameter is analyzed and results are presented in this report. Probability density function analysis and statistical analysis results are presented for this receiver for selected frequency resolution capabilities.

The first order math model is developed for the Bragg-cell receiver. The input signal's frequency is assumed to be a constant pdf or Gaussian pdf characteristic. The primary distortion signal is generated by nonlinear acoustic transducer characteristics. The distortion signal is also assumed to have a constant pdf or Gaussian pdf characteristic.

Staircased pdf characteristics are observed for all pdf frequency characteristics. The staircased function is introduced by the frequency sampling of the photodiode detector array used in the Bragg-cell receiver. The output frequency pdf characteristic is observed to depart from the input signal's frequency pdf characteristic for many of the wideband RF signal cases and wideband distortion signals produced by the AO transducer. Distortion signals with large DF2 values can significantly change the output frequency's pdf characteristic. Also, the frequency sampling (or detector frequency resolution) at the detector can further distort the pdf characteristic. Low frequency resolution at the detector produces the most significant distortions. EW emitter classification and EW direction finding systems can be affected by Bragg-cell receiver distortions. These distortions are especially important for wideband radar emitters.

Math model validation is recommended for the Bragg-cell receiver. Model validations are readily performed using an actual Bragg-cell receiver and associated test equipment.

REFERENCES

1. "Instantaneous Frequency Measurement (IFM) Receiver Study - Final Report," SigPro Systems Inc., October 1986.
2. "Microwave Receivers and Related Components," James Tsui, NTIS PB84-108711, 1983.
3. "Acousto-Optic Processing Increase EW Capabilities," N. Berg, M. Caseday, and I. Abramovitz. Microwave System News, February 1982.
4. "Probability, Random Variable, and Stochastic Processes," A. Papoulis, McGraw-Hill, 1965.

APPENDIX A BRAGG-CELL RECEIVER CONVOLUTION PROGRAM

```

10 | "BRAGG" PROGRAM
20 | BRAGG-CELL RECEIVER ANALYSIS
30 | CONVOLUTION OF F1 ARRAY AND F2 ARRAY
40 | THIS VERSION PERMITS STORAGE OF CONVOLVED ARRAY WITH ITS FREQUENCY AXIS
50 | STORAGE TAKES PLACE PRIOR TO PLOTTING--A STRING NAMED INFO$ IS ALSO
60 | STORED--SHOULD CONTAIN MINIMUM INFORMATION ON STORED DATA
70 | PLOT BOTH INPUT ARRAYS ON K AXIS
80 | PLOT CONVOLUTION ON FREQUENCY AXIS
90 | LABEL TOTAL VALUES FOUND IN CONVOLUTION ARRAY
100 | ARRAYS MAY BE ANY COMBINATION OF FLAT/GAUSSIAN
110 |     DECEMBER 1986
120 | DISP "DO YOU WANT TO SAVE CONVOLVED ARRAYS?" @ LINPUT "ENTER Y/N",XP$
130 | IF KP$(1,1)="Y" THEN GOSUB KEEP
140 | DISP "ENTER INTEGER LENGTH OF LONG ARRAY" @ INPUT OF1
150 | DISP "ENTER LENGTH OF SHORT ARRAY" @ INPUT OF2
160 | DISP "MAKE THESE ENTRIES IN MHZ"
170 | DISP "ENTER DELTA FREQUENCY FOR THE LONG ARRAY" @ INPUT OFF1
180 | DISP "ENTER DELTA FREQUENCY FOR THE SHORT ARRAY" @ INPUT OFF2
190 | OF2=OF1/(OFF1/OFF2) @ N=OF1*2 @ SGF1=OFF1*1000000/6 @ SGFLO=OFF2*1000000/6
200 | DISP "OF1=";OF1;" OF2=";OF2;" N=";N @ NMR1=1/(SGF1*SQR(2*PI))
210 | OPTION BASE 1 @ RAD @ NMRLO=1/(SGFLO*SQR(2*PI)) @ MU=500000000
220 | DIM PX(500),PH(500),PY(499),TS(821),TIS(521),FX(500),X(500),Y(500),INFO$(80)
230 | LINPUT "ENTER <80 CHARACTERS DESCRIBING DATA",INFO$
240 | REDIM PY(N-1),FX(N-1),PX(N),PH(N)
250 | FOR K=1 TO N ! FILL INPUT ARRAYS WITH ZEROES
260 | PX(K)=0 @ PH(K)=0
270 | NEXT K
280 | DISP "      *****PICK COMBINATION*****"
290 | DISP "      1-BOTH ARRAYS FLAT"
300 | DISP "      2-SHORT FLAT, LONG GAUSSIAN"
310 | DISP "      3-LONG FLAT, SHORT GAUSSIAN"
320 | DISP "      4-BOTH GAUSSIAN"
330 | DISP "ENTER YOUR CHOICE" @ INPUT PIC
340 | IF PIC=2 THEN SHRT
350 | IF PIC=4 THEN GOSUB AR2
360 | LSTEP=1
370 | FOR K=1 TO N\2 !MAKES FLAT LONG ARRAY
380 | PH(K)=1/(OF1-1)
390 | NEXT K
400 | SHRT:      !MAKES FLAT SHORT ARRAY
410 | IF PIC=3 THEN GOSUB AR3
420 | SSTEP=1
430 | FOR K=N/4-OF2/2 TO N/4+OF2/2
440 | PX(K)=1/(OF2-1)
450 | NEXT K
460 | IF PIC=2 THEN GOSUB AR2
470 | CNVLV:
480 | YTOT=0
490 | FOR K=1 TO N-1

```

```

500 YSUM=0
510 STL=500-OFF1 @ STPL=500+OFF1 @ STZL=(STPL-STL)/(N-1) @ IVAL=STL+STZL/2
520 FOR J=1 TO K
530 YSUM=YSUM+PX(J)*PH(K-J+1)
540 PY(K)=YSUM/(STZL*1000000)
550 NEXT J
560 IF K MOD 50=0 THEN DISP "K=";K
570 NEXT K
580 FOR K=1 TO N-1 ! MAKE FREQ ARRAY FOR XAXIS
590 FX(K)=IVAL
600 IVAL=IVAL+STZL
610 NEXT K
620 SUMY=0
630 FOR K=1 TO N-2 ! INTEGRATE
640 XS=(FX(K+1)-FX(K))*1000000
650 YS=(PY(K)+PY(K+1))/2
660 SUMY=XS*YS+SUMY
670 NEXT K
680 DISP "SUM=";SUMY
690 !IF KP$(1,1)="Y" THEN GOSUB KP1
700 CHOICE: ! PICK PLOT
710 DISP " 1-PLOT BOTH ORIGINAL ARRAYS SAME AXIS"
720 DISP " 2-PLOT CONVOLUTION ON FREQUENCY AXIS"
730 DISP " 3-EXIT PROGRAM"
740 DISP " 4-STORE DATA"
750 DISP " ENTER YOUR CHOICE" @ INPUT CH
760 IF CH=4 THEN GOSUB KEEP
770 IF CH#1 THEN 790
780 LINPUT "EXTERNAL PLOTTER? Y/N",HP$
790 IF CH=3 THEN BEEP @ DISP "DONE" @ STOP
800 IF CH=1 THEN GOSUB PLT1
810 IF CH=2 THEN GOSUB PLT3
820 PLOTTER IS 1 @ PEN -1 @ GCLEAR @ LOCATE 30,170,25,80
830 Y1=0 @ Y2=AMAX(Y)*1.1 @ X1=STL @ X2=STPL
840 START:
850 SCALE X1,X2,Y1,Y2
860 FXD 2 @ LAXES (X2-X1)/10,(Y2-Y1)/10,X1,Y1
870 XAXIS Y2,(X2-X1)/10,X1,X2
880 YAXIS X2,(Y2-Y1)/10,Y1,Y2
890 MORDAT: ! ADD MORE DATA SAME SCALE
900 IF CH=1 THEN 950
910 IF CH=4 THEN 950
920 DISP "ENTER BRAGG-RECEIVER FREQUENCY RESOLUTION"
930 INPUT RES
940 KRES=INT(RES/(2*OFF1/N))
950 FOR K=1 TO TOP
960 PLOT X(K),Y(K) @ IF CH=1 THEN 1040
970 IF CH=4 THEN 1040
980 FOR L=1 TO KRES
990 IF K+L>=TOP THEN 1050
1000 PLOT X(K+L),Y(K)
1010 NEXT L
1020 K=K+L-2
1030 L=1
1040 NEXT K
1050 IF HP$="Y" THEN EPLT
1060 IF CH=1 THEN GOSUB PLT2
1070 IF CH=4 THEN PLOUT

```

```

1080 IMAGE "CONSTANT PDF FOR F1, DF1=",DD.D," CONSTANT PDF FOR F2 , OFF2=",DD.D
"
1090 IMAGE "CONSTANT PDF FOR F1, DF1=",DD.D," GAUSSIAN PDF FOR F2 , OFF2=",DD.D
"
1100 IMAGE "GAUSSIAN PDF FOR F1, DF1=",DD.D," CONSTANT PDF FOR F2 , OFF2=",DD.
D,"
1110 IMAGE "GAUSSIAN PDF FOR F1, DF1=",DD.D," GAUSSIAN PDF FOR F2 , OFF2=",DD.
D,"
1120 TS="BRAGG-CELL RECEIVER PDF ANALYSIS" @ CSIZE 3.3,1
1130 LONG 5 @ MOVE X2-(X2-X1)/2,Y2+(Y2-Y1)/9 @ LABEL USING "K" ; TS
1140 CSIZE 3
1150 MOVE X2-(X2-X1)/2,Y2+(Y2-Y1)/18 @ IF PIC=1 THEN LABEL USING 1080 ; OFF1,OFF
2 @ CSIZE 3
1160 IF PIC=3 THEN LABEL USING 1090 ; OFF1,OFF2 @ CSIZE 4
1170 IF PIC=2 THEN LABEL USING 1100 ; OFF1,OFF2 @ CSIZE 4
1180 IF PIC=4 THEN LABEL USING 1110 ; OFF1,OFF2 @ CSIZE 4
1190 MOVE X2-(X2-X1)/2,Y1-(Y2-Y1)/5 @ LABEL USING "K" ; "FD IN MHZ"
1200 MOVE X1-(X2-X1)/7,Y2-(Y2-Y1)/2 @ DEG @ LDIR 30 @ LABEL USING "K" ; "Pdf(FD)
X 1E8"
1210 IMAGE "TOTAL=",DD.DDD
1220 MOVE X1,Y1-(Y2-Y1)/5 @ LDIR 0 @ LONG 2 @ LABEL USING 1210 ; SUMY
1230 PLOUT:
1240 LINPUT "DUMP GRAPHICS? Y/N",DG$
1250 IF DG$="Y" THEN DUMP GRAPHICS
1260 EPLT:
1270 HP$="N"
1280 LINPUT "PLOT ON EXTERNAL DEVICE? Y/N",PLE$
1290 IF PLE$="Y" THEN PLOTTER IS 705 @ PEN 1 @ LOCATE 30,110,29,89 @ GOTO START
1300 IF CH=4 OR CH=2 THEN CHOICE
1310 BEEP 150,300 @ DISP "DONE"
1320 END
1330 PLT1: 1 PLOT SHORT ARRAY
1340 REDIM X(N),Y(N)
1350 IF CH=1 THEN MULT=1 ELSE MULT=1000000000
1360 FOR K=1 TO N IFILL X AND Y ARRAYS
1370 X(K)=K @ Y(K)=PX(K)*MULT
1380 NEXT K
1390 X1=1 @ X2=N @ Y1=0 @ Y2=AMAX(Y)*1.1 @ TOP=N @ LINE TYPE 1
1400 PLOTTER IS 1 @ PEN -1 @ GCLEAR @ LOCATE 30,170,25,80
1410 GOTO START
1420 RETURN
1430 PLT2: 1 PLOT LONG ARRAY SAME SCALE
1440 TS="INPUT ARRAYS"
1450 IMAGE "CONSTANT ARRAY FOR F1, DF1=",DD.D," CONSTANT ARRAY FOR F2 , OFF2=",
DD.DD
1460 IMAGE "CONSTANT ARRAY FOR F1, DF1=",DD.D," GAUSSIAN ARRAY FOR F2 , OFF2=",
DD.DD
1470 IMAGE "GAUSSIAN ARRAY FOR F1, DF1=",DD.D," CONSTANT ARRAY FOR F2 , OFF2=",
DD.DD
1480 IMAGE "GAUSSIAN ARRAY FOR F1, DF1=",DD.D," GAUSSIAN ARRAY FOR F2 , OFF2=",
DD.DD
1490 LONG 5
1500 MOVE X2-(X2-X1)/2,Y2+(Y2-Y1)/20 @ IF PIC=2 THEN LABEL USING 1470 ; OFF1,OFF
2 @ CSIZE 4
1510 MOVE X2-(X2-X1)/2,Y2+(Y2-Y1)/20 @ IF PIC=1 THEN LABEL USING 1450 ; OFF1,OFF
2 @ CSIZE 4
1520 MOVE X2-(X2-X1)/2,Y2+(Y2-Y1)/20 @ IF PIC=3 THEN LABEL USING 1460 ; OFF1,OFF
2 @ CSIZE 4

```

```

1530 MOVE X2-(X2-X1)/2,Y2+(Y2-Y1)/2 @ IF PIC=4 THEN LABEL USING 1480 ; OFF1,OFF
2 @ CSIZE 4
1540 LONG 5 @ MOVE X2-(X2-X1)/2,Y2+(Y2-Y1)/9 @ LABEL USING "K" ; T3
1550 IF CH=1 THEN MULT=1 ELSE MULT=1000000000
1560 MOVE X1-(X2-X1)/7,Y2-(Y2-Y1)/2 @ DEG @ LDIR 90 @ LABEL USING "K" ; "VALUE X
";MULT
1570 FOR K=1 TO N
1580 Y(K)=PH(K)*MULT
1590 NEXT K
1600 CH=4 @ LINE TYPE 4 @ TOP=N
1610 GOTO MORDAT
1620 RETURN
1630 PLT3: ! FILL CONVOLUTION ARRAY
1640 REDIM X(N-1),Y(N-1)
1650 MULT=1000000000
1660 FOR K=1 TO N-1
1670 X(K)=FX(K) @ Y(K)=PY(K)*MULT
1680 NEXT K
1690 TOP=N-1
1700 RETURN
1710 AR2: !SUB-GENERATE GAUSSIAN FOR THE LONG ARRAY
1720 Stt=MU-3*SGF1 @ Stp=MU+3*SGF1 @ STZ=(Stp-Stt)/(N\2) @ IVL=Stt
1730 FOR K=1 TO N\2
1740 PH(K)=NMR1*EXP((- (IVL-MU)^2)/(2*SGF1^2)) @ PH(K)=PH(K)*STZ
1750 IVL=IVL+STZ
1760 NEXT K
1770 IF PIC=4 THEN AR3
1780 IF PIC=2 THEN CNVLV
1790 RETURN
1800 AR3: !SUB-GENERATE GAUSSIAN FOR THE SHORT ARRAY
1810 Stt=MU-3*SGFLO @ Stp=MU+3*SGFLO @ STZ=(Stp-Stt)/(N/4+DF2/2-(N/4-DF2/2)) @ I
VL=Stt
1820 FOR K=N/4-DF2/2 TO N/4+DF2/2
1830 PX(K)=NMRLO*EXP((- (IVL-MU)^2)/(2*SGFLO^2)) @ PX(K)=PX(K)*STZ
1840 IVL=IVL+STZ
1850 NEXT K
1860 IF PIC=3 OR PIC=4 THEN CNVLV
1870 RETURN
1880 KEEP: ! FILENAME ENTRY
1890 DISP "FILENAME MUST BE ENTERED IN UNIX PATH FORM /DISCNAME/FILENAME"
1900 LINPUT "ENTER DESCRIPTIVE FILENAME",F3
1910 CREATE F3,1,299*2+89
1920 ASSIGN# 1 TO F3
1930 PRINT# 1 ; N,INFO3,FX(),PY()
1940 ASSIGN# 1 TO *
1950 GOTO CHOICE
1960 RETURN

```

APPENDIX A
BRAGG-CELL RECEIVER
PDF GENERATION & STATISTICAL ANALYSIS PROGRAM

```

5  !BRAGGPDF      THIS PROGRAM COMPUTES BRAGG-CELL RCVR. PDF AND STATISTICS
10 !             THIS PROGRAM GETS DATA FROM A CONVOLUTION FILE-DOES CEN MOMS
20 !DATA IS THEN PLOTTED WITH LABELLED CENTRAL MOMENTS, INT, ETC....
30 OPTION BASE 1
40 DIM FX(500),PH(500),INFO$(80),TS(75)
50 DISP "PLEASE USE FILENAMES WITH 2 DIGITS FOR DF1"
60 INPUT "FILENAME?",FS
70 ASSIGN# 1 TO FS
80 READ# 1 : N = N-1
90 REDIM FX(N),PH(N)
100 READ# 1 : INFO$,FX(),PH()
110 FOR K=1 TO N
120 FX(K)=FX(K)+100
130 NEXT K
140 ASSIGN# 1 TO *
150 DISP @ DISP INFO$ @ DISP
160 FIS=REVS(FS) @ PS=FIS(1,1)
170 IF PS="A" THEN PIC=1
180 IF PS="B" THEN PIC=2
190 IF PS="C" THEN PIC=3
200 IF PS="D" THEN PIC=4
210 DF1=VAL(FS(3,4)) @ DFLO=VAL(FS(6,7))
220 DISP "ENTER RESOLUTION IN MHZ" @ INPUT RES
230 XST=INT(RES/(2*DF1/N))
240 OFM=AMAX(FX)-AMIN(FX) @ FSTPM=OFM/(N-1)*XST @ OF=FSTPM+1000000 @ SUMZ=0
250 SUMY=0 @ SUMS=0 @ SUM3=0 @ SUM4=0
260 FOR K=1 TO N-1
270 XS=(FX(K+1)-FX(K))*1000000 @ YS=(PH(K)+PH(K+1))/2
280 SUMZ=SUMZ+XS+YS
290 NEXT K
300 FOR K=1 TO N STEP XST
310 FX(K)=FX(K)*1000000
320 PH(K)=PH(K)/SUMZ
330 SUMY=SUMY+PH(K)*FX(K)*OF
340 NEXT K
350 XMEAN=SUMY
360 FOR K=1 TO N STEP XST
370 SUMS=SUMS+(FX(K)-XMEAN)^2*PH(K)*OF
380 NEXT K
390 UNC=SUMS @ SIGMA=SQR(UNC)
400 FOR K=1 TO N STEP XST
410 SUM3=SUM3+(FX(K)-XMEAN)^3*PH(K)*OF
420 SUM4=SUM4+(FX(K)-XMEAN)^4*PH(K)*OF
430 NEXT K
440 CM3=SUM3 @ CM4=SUM4
450 SKEW=CM3/UNC^1.5 @ KURT=CM4/UNC^2
460 PLOTTER IS 1 @ PEN -1 @ GCLEAR @ LOCATE 30,170,25,80
470 Y1=0 @ Y2=AMAX(PH)*100000000*1.1 @ X1=FX(1)/1000000 @ X2=XS*N/1000000/2+500
480 START:

```

```

490 SCALE X1,X2,Y1,Y2
500 FXD 0,2 @ LAXES (X2-X1)/10,(Y2-Y1)/10,X1,Y1
510 XAXIS Y2,(X2-X1)/10,X1,X2
520 YAXIS X2,(Y2-Y1)/10,Y1,Y2
530 MORDAT: ! ADD MORE DATA SAME SCALE
540 FOR K=1 TO N STEP XST
550 IF K+XST>N THEN S60
560 PLOT FX(K)/1000000,PH(K)*100000000 @ PLOT FX(K+XST)/1000000,PH(K)*100000000
570 NEXT K
580 IMAGE "CONSTANT PDF FOR F1, DF1=",000.0," CONSTANT PDF FOR F2, OFF2=",000.0
590 IMAGE "CONSTANT PDF FOR F1, DF1=",000.0," GAUSSIAN PDF FOR F2, OFF2=",000.0
600 IMAGE "GAUSSIAN PDF FOR F1, DF1=",000.0," CONSTANT PDF FOR F2, OFF2=",000.0
610 IMAGE "GAUSSIAN PDF FOR F1, DF1=",000.0," GAUSSIAN PDF FOR F2, OFF2=",000.0
620 TS="BRAGG-CELL RECEIVER PDF ANALYSIS" @ CSIZE 3.3,1
630 LONG S @ MOVE X2-(X2-X1)/2,Y2+(Y2-Y1)/9 @ LABEL USING "K" ; TS
640 CSIZE 3
650 MOVE X2-(X2-X1)/2,Y2+(Y2-Y1)/18 @ IF PIC=1 THEN LABEL USING 580 ; DF1,DFLO @
- CSIZE 4
660 IF PIC=3 THEN LABEL USING 590 ; DF1,DFLO @ CSIZE 4
670 IF PIC=2 THEN LABEL USING 600 ; DF1,DFLO @ CSIZE 4
680 IF PIC=4 THEN LABEL USING 610 ; DF1,DFLO @ CSIZE 4
690 MOVE X2-(X2-X1)/2,Y1-(Y2-Y1)/5 @ LONG S @ LABEL USING "K" ; "Fd IN MHZ"
700 LONG S @ CSIZE 4 @ LONG S
710 MOVE X1-(X2-X1)/7,Y2-(Y2-Y1)/2 @ DEG @ LDIR 90 @ LABEL USING "K" ; "Pdf(Fd)
X 1E3"
720 LDIR 0 @ RAD
730 IMAGE "INTEGRAL=",0.000
740 IMAGE "XMEAN=",00000.000
750 IMAGE "SIGMA=",000.000
760 IMAGE "SKEW=",000.000
770 IMAGE "KURTOSIS=",00.000
780 CSIZE 2.5 @ LONG 2
790 MOVE X1+(X2-X1)/25,Y2-(Y2-Y1)/10 @ LABEL USING 730 ; SUMZ
800 LABEL USING 740 ; XMEAN/1000000
810 LABEL USING 750 ; SIGMA/1000000
820 LABEL USING 760 ; SKEW
830 LABEL USING 770 ; KURT
840 LABEL USING "K" ; "RESOLUTION=",RES," MHZ"
850 LINPUT "DUMP GRAPHICS? Y/N",GDMS
860 IF GDMS[1,1]="Y" THEN DUMP GRAPHICS
870 IF EPL3="Y" THEN 900
880 LINPUT "PLOT ON EXTERNAL DEVICE? Y/N",EPL3
890 IF EPL3="Y" THEN PLOTTER IS 705 @ PEN 1 @ LOCATE 30,110,29,89 @ GOTO START
900 BEEP 300,400 @ DISP "DONE"
910 END

```

